DISSERTATION

DIFFERENT DOMAINS OF AMPA RECEPTORS DIRECT STARGAZIN-MEDIATED TRAFFICKING AND STARGAZIN-MEDIATED MODULATION OF KINETICS

Submitted by

Matthew A. Bedoukian

Department of Biomedical Sciences

In partial fulfillment of the requirements

For the Degree of Doctor of Philosophy

Colorado State University

Fort Collins, CO

Summer 2006

COLORADO STATE UNIVERSITY

July 6, 2006

WE HEREBY RECOMMEND THAT THE DISSERTATION PREPARED UNDER OUR SUPERVISION BY MATTHEW ARAM BEDOUKIAN ENTITILED: DIFFERENT DOMAINS OF THE AMPA RECEPTOR DIRECT STARGAZIN-MEDIATED TRAFFICKING AND STARGAZIN-MEDIATED MODULATION OF KINETICS BE ACCEPTED AS FULFILLING IN PART REQUIREMENTS FOR THE DEGREE OF DOCTOR OF PHILOSOPHY.

Committee on Graduate Work

Advisor

Co-Advisor

Department Head

ABSTRACT OF DISSERTATION

DIFFERENT DOMAINS OF AMPA RECEPTORS DIRECT STARGAZIN-MEDIATED TRAFFICKING AND STARGAZIN-MEDIATED MODULATION OF KINETICS

Transmembrane AMPA Receptor Regulatory Proteins (TARPs) are the first transmembrane proteins known to associate with AMPA receptors. There are four known TARPs: γ-2, γ-3, γ-4, and γ-8. TARPs are expressed differentially in the brain but there is some overlap. Of these, γ-2, or stargazin is the most extensively studied. There is significant homology between the TARPs and all four have been shown to increase the relative amount of AMPA receptor surface expression in HEK293 cells as well as in several other recombinant expression systems. Additionally, stargazin slows both AMPA receptor desensitization and deactivation kinetics. The major purpose of this work was to determine the nature of the stargazin-AMPA receptor interaction. This work provides strong evidence that the AMPA receptor domains required for stargazin-modulation of gating and trafficking are separable. An intracellular interaction between the cytoplasmic tails of the two proteins is necessary for an enhancement of surface expression while this same site is not necessary for stargazin-mediated modulation of desensitization kinetics. This interaction appears to occur early in the biosynthetic pathway.

Matthew Aram Bedoukian
Department of Biomedical Sciences
Colorado State University
Fort Collins, CO 80523
Summer 2006

DISSERTATION OUTLINE

Chapter I provides a literature review of AMPA receptor plasticity and trafficking with and without TARPs. Here the mechanisms of AMPA receptor desensitization are briefly discussed as well as stargazin's ability to modulate AMPA receptor kinetics. I also discuss some possible mechanisms for stargazin-mediated AMPA receptor trafficking.

Chapter II contains a published manuscript that provides evidence that the extracellular domain of AMPA receptors is required for stargazin-mediated modulation of desensitization while the intracellular domain is required for stargazin-mediated trafficking. This paper proposes that stargazin mediates trafficking by blocking one or multiple ER retention signals per AMPA receptor subunit.

Chapter III contains a manuscript in preparation that correlates the degree of AMPA receptor ligand-binding domain closure to current amplitude.

Chapter IV is a discussion section focusing on the potential mechanism of AMPA receptor trafficking. Here I provide my view of how stargazin-mediated AMPA receptor trafficking works and discuss future experiments to answer some remaining questions.

ACKNOWLEDGEMENTS

My advisor Kathy has been great. I am thankful for her giving me a place in her lab and allowing me the opportunity to be creative and figure out how to do experiments that actually are designed to answer questions. I am very grateful for her support and patience. I would also like to thank my committee members Kurt Beam, Mike Tamkun, and Karolin Luger for taking time to listen to many frustrating presentations with scattered ideas. I would also like to thank them for scientific discussions and helping me with technical aspects of experiments. Many thanks to people I have worked with in the lab especially Autumn Weeks for being super cool and also helping me so much with electrophysiology recordings. I want to thank Bridget Mortell for being supportive and nice and someone I could always talk to even though I was sometimes mean when things weren't going well. I thank John Gieser for his artwork and making my figures look nice and Suzanne Clark for believing in me and always being willing to help. I would like to thank my roommate Chi Pak for tons of scientific discussions and listening to me rambling about stuff and also Rod Tompkins for being an awesome friend and someone to go on outdoor adventures with to keep my sanity and lower the risk of a mountain lion attack. Finally I'd like to thank my entire family but especially my mom and dad for everything they've done and sacrificed to make it possible for me to pursue an academic career. Maybe I'm ready to listen to them now and take their advice. Thanks again to everyone, I owe you a lot!

CREDITS

For this project I made all of the DNA constructs that were not gifts (see methods section of paper in chapter 2) and did all confocal imaging and analysis. I did the electrophysiology experiments for GluR4i-ATD with and without stargazin, while Autumn Weeks performed all other electrophysiology for the remaining HEK293 cell data. In chapter 3, I made all of the constructs and did all of the Xenopus oocyte recordings. John Gieser harvested the eggs used for injection with the aid of Autumn Weeks.

LIST OF ABBREVIATIONS

Abbreviations used: AMPA, a-amino-3-hydroxy-5-methylisoxazole-4-propionate; NMDA, *N*-methyl-D-aspartic acid; cMEM complete minimal essential medium; FRET, fluorescence resonance energy transfer; ECFP, enhanced cyan fluorescent protein; EYFP, enhanced yellow fluorescent protein; EGFP, enhanced green fluorescent protein; PCR, polymerase chain reaction; GluR, glutamate receptor; HEK, human embryonic kidney; ATD, amino terminal domain; stg, stargazin; i, flip; o, flop; R1, GluR1; R2, GluR2; LTP, long term potentiation; LTD, long term depression; AD, Alzheimer's disease; BDNF, brain derived neurotrophic factor; CaMKII, calmodulin kinase II; PKC, protein kinase C; PKA, protein kinase A; LBC, ligand-binding core; CTZ, cyclothiazide; TARP, transmembrane AMPA receptor regulatory protein; PDZ, Postsynaptic-density protein of 95 kDa, Discs large, Zona occludens-1; SAP97, synapse associated protein 97; ER, endoplasmic reticulum; GRIP1/ABP, Glutamate Receptor Interacting Protein 1/AMPA receptor Binding Protein; PICK1, Protein Interacting with C-Kinase; NSF, N-ethyl maleimide sensitive factor; AP-2, activating factor 2; GTP, guanosine triphosphate; VDCC, Voltage dependent calcium channels; UPR, unfolded protein response.

TABLE OF CONTENTS

Chapter I: Introduction

Significance

AMPA receptors and NMDA receptors are the two major classes of postsynaptic glutamate receptors. AMPA receptors are ionotropic, ligand-gated membrane proteins in the mammalian nervous system opened by glutamate released from presynaptic vesicles. AMPA receptors are the major determinant of postsynaptic excitability and act to induce neuronal firing by depolarizing the postsynaptic cell (Esteban, 2003). This depolarization allows NMDA receptors to flux a large amount of calcium into the neuron, which may lead to synaptic plasticity. NMDA receptor-dependent plasticity is thought to be important for learning and memory (Kandel, 2001). This plasticity includes an increase in AMPA receptors at synapses (Zamanillo et al., 1999; Daw et al., 2000; Kennedy, 2000; Malinow et al., 2000). It is no surprise then that AMPA receptors are very dynamic and highly regulated components of excitatory synapses.

AMPA receptor dysfunction is implicated in multiple illnesses including schizophrenia (Konradi and Heckers, 2003), epilepsy (Raol et al., 2001), and Alzheimer's disease (AD) (Walsh et al., 2002). Positive allosteric modulators of these channels have been studied and used in clinical trials as an attempt to alleviate the memory loss associated with dementia and AD but to date have not had notable success. A recent experiment using a double knock-in mouse carrying mutations in the human genes for amyloid precursor protein and presenilin-1 suggests that the onset of AD is related to the malfunction of synapses, notably the loss of AMPA receptor currents. These mice show age-related decreases in long term depression (LTD) and long term potentiation (LTP), which correlates with the loss of synaptic AMPA receptors (Chang et al., 2006). LTP is considered to be a long lasting change in the synaptic strength of a synapse, which

involves the regulated trafficking of AMPA receptors to the postsynaptic membrane. In contrast, LTD requires the regulated loss of AMPA receptors from the membrane. Like LTP, LTD may also be an important requirement of learning.

Certain defects in memory and learning are thought to be related to dendritic deterioration and the resultant decrease in AMPA receptor number. One idea to alleviate impaired excitatory transmission would be to enhance the transmission of the remaining population of excitatory synapses. The use of certain AMPA receptor allosteric modulators would presumably help induce LTP and also have the positive effect of enhancing neurotrophin expression (Lynch, 2004). Neurotrophins such as BDNF have been shown to increase expression levels of AMPA receptors in the central nervous system (Narisawa-Saito et al., 1999). Endogenous neurotrophins secreted during enhanced synaptic activity may be what induces morphological changes including the formation of new spines (Poo, 2001). Additionally, BDNF has been shown to selectively increase the surface expression of GluR2 in neurons (Narisawa-Saito et al., 2002). It would seem, however, due to a lack of positive clinical results that enhancement of synaptic plasticity using this approach is limited. Perhaps the levels of BDNF induction are insufficient or the receptors are not dynamically regulated. A better strategy may be to devise drug therapies meant to enhance both the number of synaptic receptors and the dynamics of AMPA receptor trafficking. This of course is easier said than done, but the discovery of a new AMPA receptor accessory protein promises to further our understanding of synaptic plasticity.

In the past several years it has become clear that stargazin, an AMPA receptor auxiliary protein (Vandenberghe et al., 2005b) is essential for trafficking AMPA receptors to both synapses and extrasynaptic sites (Fukata et al., 2005; Tomita et al., 2005a; Nicoll et al., 2006). Stargazin phosphorylation is required for hippocampal LTP and promotes synaptic trafficking of AMPA receptors. Both LTP and LTD require NMDA receptor mediated phosphorylation and dephosphorylation, respectively (Tomita et al., 2005a). Two proteins necessary for LTP, CaMKII

and PKC, have been previously implicated in synaptic plasticity (Sanes and Lichtman, 1999; Bredt and Nicoll, 2003) and we now have a more complete understanding of why this is the case.

Background

AMPA receptor composition

AMPA receptors are believed to be tetramers (Rosenmund et al., 1998; Matsuda et al., 2005) composed of a dimer of dimers, based on crystal structure data (Sun et al., 2002a). There are four AMPA receptor genes (GluR1-4) and native channels are believed to be composed of homomers and heteromers of these subunits. Each subunit contains an ~400 amino acid extracellular amino terminal domain, a ligand binding core (LBC), three transmembrane domains, a pore loop, and a variable intracellular cytoplasmic tail (**Figure 1.1**)(Gouaux, 2003). Homomeric receptors besides GluR2 are inward rectifiers and calcium permeable. The reason for this difference in GluR2 was mapped to a single site - an arginine at position 586 in the mature receptor (Hume et al., 1991) that is a glutamine in the other three channel subunits. It was revealed that this difference was due to deamination of the glutamine residue by posttranscriptional mRNA editing in >99% of channels (Kask et al., 1998). The second extracellular domain of all AMPA receptors is alternatively spliced and contains a 38 amino acid region that defines the receptor as being either the flip or flop isoform. This flip and flop splicing is regulated developmentally and regionally and influences pharmacologic and kinetic properties of the channel (Sommer et al., 1990). GluR1/2 or GluR2/3 heteromers constitute the majority of channels in the mature hippocampus (Wenthold et al., 1996). Factors influencing receptor composition include perhaps the preferential assembly of heteromers versus homomers (Mansour et al., 2001; Brorson and Suzuki, 2004), or to the presumed excess of GluR2 subunits that reside in the ER (Greger et al., 2002).

AMPA receptor gating and desensitization

AMPA receptors open in response to glutamate and subsequently close on the order of several milliseconds, upon which they may either desensitize or agonist may dissociate.

Desensitization plays a substantial role in shaping the time course of a postsynaptic response at some synapses (Jones and Westbrook, 1996). Glutamate binds to what is known as the ligand binding core (LBC) (Stern-Bach et al., 1994). Desensitization is defined as the closing of the pore while agonist is still present. No crystal structure is available for a full AMPA receptor subunit, although the LBC has been crystallized with glutamate as well as many other partial agonists and allosteric modulators (Armstrong et al., 1998; Armstrong and Gouaux, 2000; Sun et al., 2002b; Jin et al., 2003; Jin et al., 2005). Glutamate receptor membrane domains may share homology with the distantly related bacterial K^+ channels that have been crystallized (Doyle et al., 1998; Tikhonov et al., 2002). The AMPA receptor crystal structure data illustrates that the LBC can be thought of as a clamshell constituted from domains 1 (the upper shell) and 2 (the lower shell). The comparison of crystal structures with ligand and without suggests that agonist binding translates into pore opening by movement of domain 2 up toward domain 1 (which initially binds glutamate). Because a dimer is formed from two clamshells that are in a "back-to back" orientation, the movement of domain 2 in each subunit of the dimer increases the intra-dimer separation distance (**Figure 1.2**)(Jin et al., 2003). An allosteric modulator, cyclothiazide (CTZ) that blocks receptor desensitization was found to bind at the dimer interface; in the absence of such manipulation the LBC forms only monomers. This result led to the hypothesis that desensitization of the AMPA receptor is due to a rearrangement of an unstable dimer interface (Sun et al., 2002a). This is supported by the fact that a GluR2 mutation L483Y that prevents desensitization resides along the dimer interface makes an additional contact with the neighboring subunit, and also promotes dimerization in an equilibrium sedimentation analysis.

AMPA Receptor Trafficking B.S. (before stargazin)

To understand how AMPA receptor insertion into synapses and extrasynaptic sites is regulated it is useful to have an understanding of the proteins known to interact with the different subunits of AMPA receptors. There appear to be numerous associations that direct targeting and clustering to different subcellular compartments, as well as stabilizing channels at cell surface and

intracellular pools (Malenka, 2003). These interactions are complex and can be subunit specific. Below is a brief review of the major proteins thought to play important roles in the trafficking of AMPA receptors before the discovery of TARPs.

The cytoplasmic tail of GluR1 interacts with the PDZ protein SAP97 (synapse associated protein 97) early in the biosynthetic pathway while in the ER or cis-Golgi, but not at the membrane (Nagarajan et al., 2001; Sans et al., 2001). GluR2 and GluR3 interact with the PDZ proteins GRIP1/ABP (Glutamate Receptor Interacting Protein 1/AMPA receptor Binding Protein) and PICK1 (Protein Interacting with C-Kinase). GRIP/ABP may limit receptor endocytosis since mutating GluR2 to prevent association with this protein resulted in a receptor that was only transiently associated at synapses and could not accumulate on the plasma membrane (Osten et al., 2000). In contrast, PICK is known to reduce surface expression of GluR2 and it is hypothesized that there is a GRIP/PICK control mechanism of synaptic expression (Liu and Cull-Candy, 2005). GluR2 also associates with NSF, a multimeric ATPase, that helps vesicles fuse to the plasma membrane (Nishimune et al., 1998; Osten et al., 1998; Song et al., 1998) and also seems to be important for recycling AMPA receptors back into the plasma membrane (Lee et al., 2002). The NSF binding site overlaps with the AP2 site, a clathrin adaptor complex that binds to all four subunits and is important for receptor endocytosis (Lee et al., 2002). Protein 4.1 has a known association with GluR1 and GluR4 and is important for linking the channels via the cytoplasmic tail to the actin cytoskeletal netweork (Shen et al., 2000; Coleman et al., 2003). GluR4 containing channels are expressed mostly early in postnatal development (Zhu et al., 2000) and as a result have not been as well classified. Narp (neuronal activity-regulated pentraxin) and the related NP1 protein bind to the amino terminal domain (ATD) of all AMPA receptors. Narp has been shown to cluster AMPA receptors in large aggregates (O'Brien et al., 1999; O'Brien et al., 2002) and is regulated by synaptic activity while NP1 is constitutively active and also binds to the ATD with similar effect (Xu et al., 2003).

There are also a number of phosphorylation sites along the AMPA receptor cytoplasmic tail. Protein Kinase A (PKA), for example, has been shown to phosphorylate the C-terminus of GluR1 (at serine 845), (Ehlers, 2000) and controls synaptic incorporation (Esteban, 2003). In contrast, the removal of AMPA receptors from the plasma membrane involves phosphorylation of GluR2 by PKC (Protein Kinase C) There is evidence that this causes GRIP/ABP dissociation, favoring the PICK1 association which keeps GluR2 and associated subunits in the tetramer from synapses (Hanley et al., 2002).

The proteins that associate with AMPA receptors have important consequences for trafficking AMPA receptors from the cytosol to the plasma membrane or synapse. GluR1/2 heteromers have been shown to exit the ER more rapidly than GluR2/3 heteromers (Greger et al., 2002; Greger et al., 2003). There are several proteins thought to be necessary to chaperone AMPA receptors from the ER. Once out of the ER, GluR2/3 containing heteromers are constitutive while GluR1 or GluR4 containing tetramers are delivered in an activity-dependent manner upon NMDA activation (Hayashi et al., 2000; Zhu et al., 2000; Shi et al., 2001).

The transport to the dendrites is likely to depend on the microtubular cytoskeleton that runs along dendritic shafts mediated through liprin-α, a mutant of which prevents synaptic targeting. Liprin-α interacts with KIF1, a kinesin family motor, and GIT1 also is involved in trafficking (Esteban, 2003). Another protein, Rab8, a small GTPase, is required for both the constitutive and regulated delivery of AMPA receptors into synapses (Gerges et al., 2004) and is necessary for synaptic plasticity.

Stargazin and AMPA Receptor Association

The Stargazer Mouse and the identification of the stargazin gene

In the 1980's a mouse (now known as the stargazer mouse) was detected at the Jackson laboratories. This mouse made repeated head elevations, had an unsteady gait, and had absence

seizures (Letts, 2005). This mouse was found to have an insertion in the second intron of Cacng2 (the stargazin gene), a mutation that drastically reduced expression of the gene product.

Voltage dependent calcium channels (VDCC) and low-voltage T-type channels are altered in the stargazer mouse (Zhang et al., 2002). Calcium channel mutations reflect many human and mouse models of epilepsy. These channels are thought to be responsible for helping to keep balance in the excitatory and inhibitory network activities between the cortex and thalamus, and dysfunction in these channels is one explanation for the absence seizures (Letts, 2005). Defects in the cerebellum would explain the ataxic phenotype and these mice were subsequently found to be missing functional AMPA receptors in this brain region.

It was soon found that stargazin was necessary for effective trafficking of AMPA receptors from the ER and Golgi to the plasma membrane. Stargazin is proposed to target AMPA receptors to the synapse via a two-step mechanism. Stargazin first traffics AMPA receptors to the extrasynaptic membrane and then subsequently traffics them to the postsynaptic membrane in conjunction with a protein that interacts with the last four amino acids of its carboxyl tail. These residues have been shown to interact with PSD-95 (Chen et al., 2000).

Stargazin shares great homology with γ-3, γ-4, and γ-8, each having four transmembrane domains, and together are known as transmembrane AMPA-receptor regulatory proteins (TARPs). These proteins are expressed in different brain regions, yet their expression pattern largely overlaps. For example, γ-8 dominates expression in the hippocampus but the other TARPs are also expressed there in fair number (Tomita et al., 2003). Only stargazin is expressed in cerebellar granule cells, however, and this explains the lack of rescue of the AMPA receptor trafficking defect by endogenous TARPs. Stargazin is known to be related to the Claudin family of proteins by its ability to mediate cell-cell-adhesion (Price et al., 2005). To date, no human diseases have been found to involve mutations of the TARP family genes in this family (Black, 2003) but research in the TARP field is relatively recent.

Mechanism of stargazin-mediated surface expression

Stargazin was the first transmembrane protein discovered to associate with AMPA receptors (Chen et al., 2000). Biochemical copurification of stargazin with AMPA receptors has been shown with numerous studies (Tomita et al., 2003; Tomita et al., 2004; Nakagawa et al., 2005; Vandenberghe et al., 2005b; Nakagawa et al., 2006). AMPA receptors are notorious for their lack of surface expression in both HEK293 cells (Turetsky et al., 2005) and Xenopus oocytes (Priel et al., 2005). The most recent literature suggests that stargazin traffics AMPA receptors by blocking ER retention signals (Vandenberghe et al., 2005a, b).

Insight into the mechanism of stargazin-mediated trafficking of AMPA receptors was found by occluding its effect. It has been shown that the accumulation of unassembled or unfolded proteins induces the unfolded protein response (UPR). The UPR leads to increased transcription of ER chaperone proteins such as BiP (Ma and Hendershot, 2001; Zhang and Kaufman, 2004) and helps proteins exit from the ER. In a recent study, proteasome inhibitors, lactacystin and MG-132, were used to induce the UPR because they have been shown not to hinder protein folding (Sitia and Braakman, 2003; Zhang and Kaufman, 2004). Both inhibitors increased BiP levels, and co-expression of stargazin did not produce an additive effect for AMPA receptor surface expression (Vandenberghe et al., 2005a). Thus, stargazin shows a direct chaperone-like effect on AMPA receptor folding and assembly, suggesting that stargazin has a role in the ER processing of these receptors. More evidence that the primary effect of stargazin-mediated trafficking occurs in the ER comes from the finding that the stargazer mouse has AMPA receptors with an immature glycosylation pattern compared to normal mice (Tomita et al., 2003).

The possibility that stargazin enhances AMPA receptor surface expression by reducing AMPA receptor endocytosis has also been explored. Stargazin is a membrane protein and association in the plasma membrane with AMPA receptors would presumably increase relative AMPA receptor surface expression by reducing endocytosis. However, the stargazin trafficking

effect in COS7 cells was additive when co-expressed with a dominant-negative dynamin mutant (Vandenberghe et al., 2005a) that prevents endocytosis of membrane proteins (Damke et al., 1994). Thus, stargazin does not inhibit receptor endocytosis. Stargazin actually can dissociate from AMPA receptors during agonist binding, as AMPA-stimulated AMPA receptor endocytosis did not reduce the amount of stargazin at the surface membrane (Tomita et al., 2004).

Although it has been suggested that stargazin blocks an AMPA receptor ER retention signal, there are still other possibilities. Stargazin could also act by associating with AMPA receptors and providing the complex with an ER exit site, perhaps only present on stargazin. ER exit sites are implicated in enhanced transport from the ER to Golgi via targeting to COPII vesicles (Klumperman, 2000). Another possibility is that stargazin could merely pull AMPA receptors out of the ER by virtue of their own targeting for the surface membrane. Single particle electron microscopy studies suggest that multiple stargazin molecules bind to native AMPA receptors (Nakagawa et al., 2005; Nakagawa et al., 2006). Despite this study as well as another (Vandenberghe et al., 2005b) that suggests that multiple stargazin molecules bind to AMPA receptor tetramers, it is unclear if stargazin molecules associate at the dimer interface as has been suggested (Vandenberghe et al., 2005b). That there are four stargazin binding sites per tetramer seems equally likely. Independent of how stargazin enhances AMPA receptor maturation and surface expression, it would be predicted that multiple stargazin molecules would increase the probability of AMPA receptor exit from the ER.

Stargazin domains necessary for AMPA receptor trafficking

Stargazin differentially traffics individual AMPA receptor subunits, only slightly increasing surface expression of GluR3, while significantly increasing GluR1, 2, and 4 (Turetsky et al., 2005). The cytoplasmic tail of stargazin has been shown to be critical for trafficking AMPA receptors. The first extracellular loop of stargazin has also been implicated as having some role in trafficking, although this region is not as critical as the cytoplasmic tail (Tomita et al., 2004; Turetsky et al., 2005). Interestingly, the length of the cytoplasmic tail of stargazin produces a

graded response of AMPA receptor current density, with ~ 35 amino acids of the most distal tail not being at all essential in HEK293 cells (Turetsky et al., 2005).

Stargazin-mediated modulation of AMPA receptor kinetics

In addition to increasing relative AMPA receptor surface expression, stargazin also slows AMPA receptor desensitization (Priel et al., 2005; Tomita et al., 2005b; Turetsky et al., 2005). Stargazin also increases the efficacy of the partial agonist kainate relative to glutamate (Tomita et al., 2005b; Turetsky et al., 2005). The domain responsible for both of these effects has been linked to the first extracellular loop of stargazin (Tomita et al., 2005b; Turetsky et al., 2005), but the proximal tail of stargazin has also been implicated in its modulation of desensitization and kainate efficacy. Like its effects on trafficking, stargazin has also been shown to differentially effect AMPA receptor desensitization depending on the subunit and isoform composition of the tetramer (Turetsky et al., 2005).

PSD-95 has also been shown to alter glutamate receptor kinetics. PSD-95 association with kainate receptors decreases desensitization (Garcia et al., 1998) and PSD-95 association with NMDA receptors increases open probability (Lin et al., 2004).

The proteins involved in trafficking AMPA receptors to synapses (other than TARPs)

It is still debatable whether AMPA receptors are brought to the synapse from intracellular pools or from first being inserted into extrasynaptic regions. Perhaps a combination of the two is possible. Studies of the stargazer mouse suggest that AMPA receptors are first inserted into nonsynaptic regions before getting transferred to the synapse. A stargazin molecule lacking the distal cytoplasmic tail cannot restore synaptic targeting of AMPA receptors but can still enhance total surface expression (Chen et al., 2000).

Since the discovery of stargazin and its association with AMPA receptors, the importance of the previously characterized accessory proteins is in question. AMPA receptors in mouse brain extracts have recently been found to pull down little or no protein 4.1N, GRIP, AP-2, NSF, PICK1, or SAP97, especially compared to that of the amount of TARPs that are pulled down

(Fukata et al., 2005). This discrepancy is troubling, as are studies that show, for example, that expression of the GluR1 cytoplasmic tail prevents LTP (Shi et al., 2001). It has also been shown that the SAP97 binding site on GluR1 is necessary for activity dependent trafficking to spines (Piccini and Malinow, 2002) and synapses (Hayashi et al., 2000). In addition, surface expression and inducible exocytosis of GluR1 is impaired with a mutated C-terminus (Passafaro et al., 2001). How can TARP data be reconciled with this? It seem clear that other proteins besides TARPs play a role in trafficking and plasticity - the question is their relative importance. It is clear, however, that TARP protein knockouts have severe effects on LTP.

It is known that γ-8 deficient mice have impaired synaptic plasticity. LTP in these knockout (KO) mice was reduced by 75%. γ-8 is the predominant TARP in the hippocampus, although the other three related TARPs are also present and could provide some rescue. Extrasynaptic sites in this mouse were impaired more than synaptic pools. Synaptic AMPA receptors were reduced by only 35% while extrasynaptic receptors were reduced by 90%. Although total AMPA receptor expression was reduced by 85%, the number of extrasynaptic AMPA receptors is clearly related to the number of γ-8 molecules (Rouach et al., 2005). This data is in accord with the most important role of stargazin being to get AMPA receptors out of the ER.

The severity of knocking out individual AMPA receptor subunits is less clear than the knockout of TARPs. Interestingly, the young GluR1 knockout mouse has normal LTP in the CA1 area of the hippocampus but not during adulthood. This knockout has the same number of synaptic AMPA receptors but has a great decrease in extrasynaptic AMPA receptors, which is not consistent with SAP97 being necessary for LTP. The GluR2/3 double knockout mouse has normal amplitude miniature EPSCs which is an indication that there are the same number of synaptic AMPA receptors as the normal mouse (Meng et al., 2003; Nicoll, 2003). Thus, basal transmission at the synapse seems to be the same even with defects in plasticity. There is an

increasing amount of data to suggest that AMPA receptor number is mostly controlled by TARPs and not subunit composition.

Knockouts of other AMPA receptor accessory proteins will be needed to know the importance of each protein.

Summary

The dynamic regulation of AMPA receptors mediated by the growing list of known accessory proteins still remains to be clarified. Whereas many of the proteins that bind AMPA receptors are subunit specific, TARPs such as stargazin appear to associate with all subunits and isoforms. The study of knockout mice illustrates the great importance of TARPs in both LTP and trafficking. The domains of stargazin necessary for modulation of kinetics (mostly extracellular) and trafficking (mostly intracellular) have already been dissected. The aim of this work was to define regions of the AMPA receptor that stargazin associates with and to determine if an extracellular interaction between the two proteins mediates modulation of desensitization while an intracellular interaction mediates modulation of trafficking.

Experimental Design

The approach used for this study was to make functional deletions and mutations of several AMPA receptor subunits and isoforms and then test the ability of stargazin to slow receptor desensitization kinetics and increase current amplitude by expressing the cDNA in HEK293 cells. Stargazin's ability to enhance receptor trafficking could be conveniently assayed by using a CFP or YFP tagged AMPA receptor in conjunction with confocal imaging. AMPA receptors have notoriously poor surface expression in recombinant systems and are largely ER retained. Fluorescent AMPA receptors expressed in HEK293 cells show a uniform distribution throughout the cytosol. Co-expression of functional AMPA receptors with stargazin, however, resulted in a population of cells that had reduced cytosolic expression and increased amounts of channel located at the surface membrane.

Figure 1.1:

Illustration taken from (Gouaux 2003)(Gouaux, 2003): Image shows a cartoon of an AMPA receptor subunit. The amino terminal domain (ATD) is shown in green. Domains 1 and 2 comprise the ligand-binding core for glutamate (shown bound in yellow). There are 3 transmembrane domains (1,2, and 3) and a pore loop (P). The crystallized ligand-binding core was constructed by removing the transmembrane domains and ATD (shown cut with scissors) and linking S1 and S2. The 38 amino acid flip/flop region (not shown) would be after domain 1 and before the last transmembrane domain.

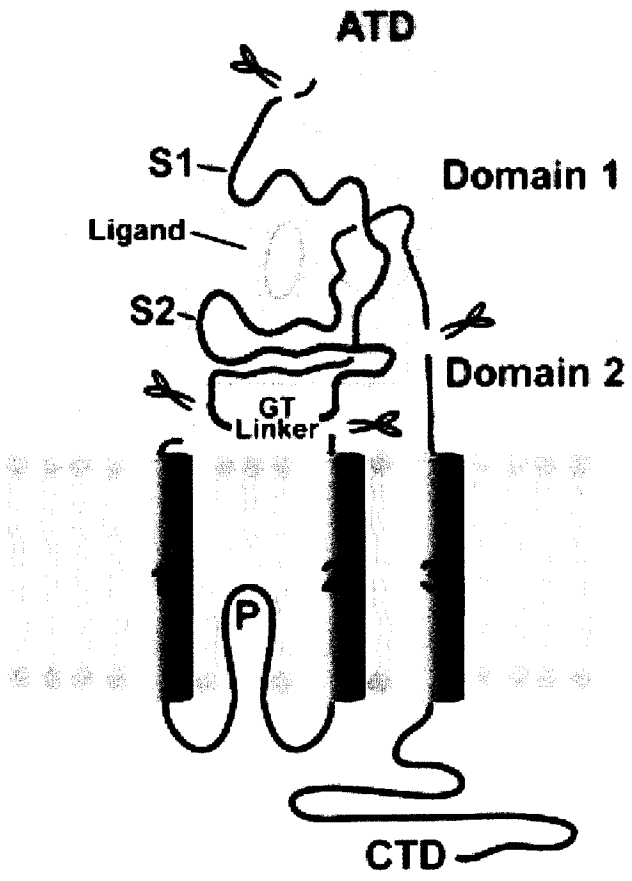

Figure 1.2:

Illustration and figure legend taken from (Jin et al., 2003). This figure shows that the degree of LBC closure dictates the degree of channel opening. Smaller AMPA receptor agonists can allow for greater domain closure than larger ones.

The 5-substituted willardiines produce greater domain closure and separation of residue Pro632 as the size of the 5-substituent decreases.

(**a**) Superposition of the structures of the GluR2 ligand-binding core in complexes with glutamate (yellow), HW (green), FW (red), BrW (cyan) and IW (purple) using main-chain atoms in domain 1. Glutamate and IW are shown in ball-and-stick representation. (**b**) Close-up view of domain 2 derived from the superimposed structures in **a**. Note the spectrum of conformational states from the glutamate-bound form to the IW bound state. (**c**) The dimer of the ligand-binding core in the activated, non desensitized state illustrating how the increase in domain closure of individual subunits, with the glutamate and IW complexes as examples, results in a corresponding increase in the separation between the linker regions of each subunit. The outlines of the glutamate and IW dimers are in green and pink, respectively. (**d**) Illustration of how greater domain closure is correlated to greater separation between Pro632 residues in the ligand-binding core dimer. (**e**) Graphical representation of the correlation between the separation of Pro632 in the dimer in the HW, FW, BrW and IW structures and the corresponding maximum current response and extent of desensitization. I ss is the current amplitude for the steady state response on the wild-type receptor and I pk is the peak current for the wild-type receptor in the presence of cyclothiazide.

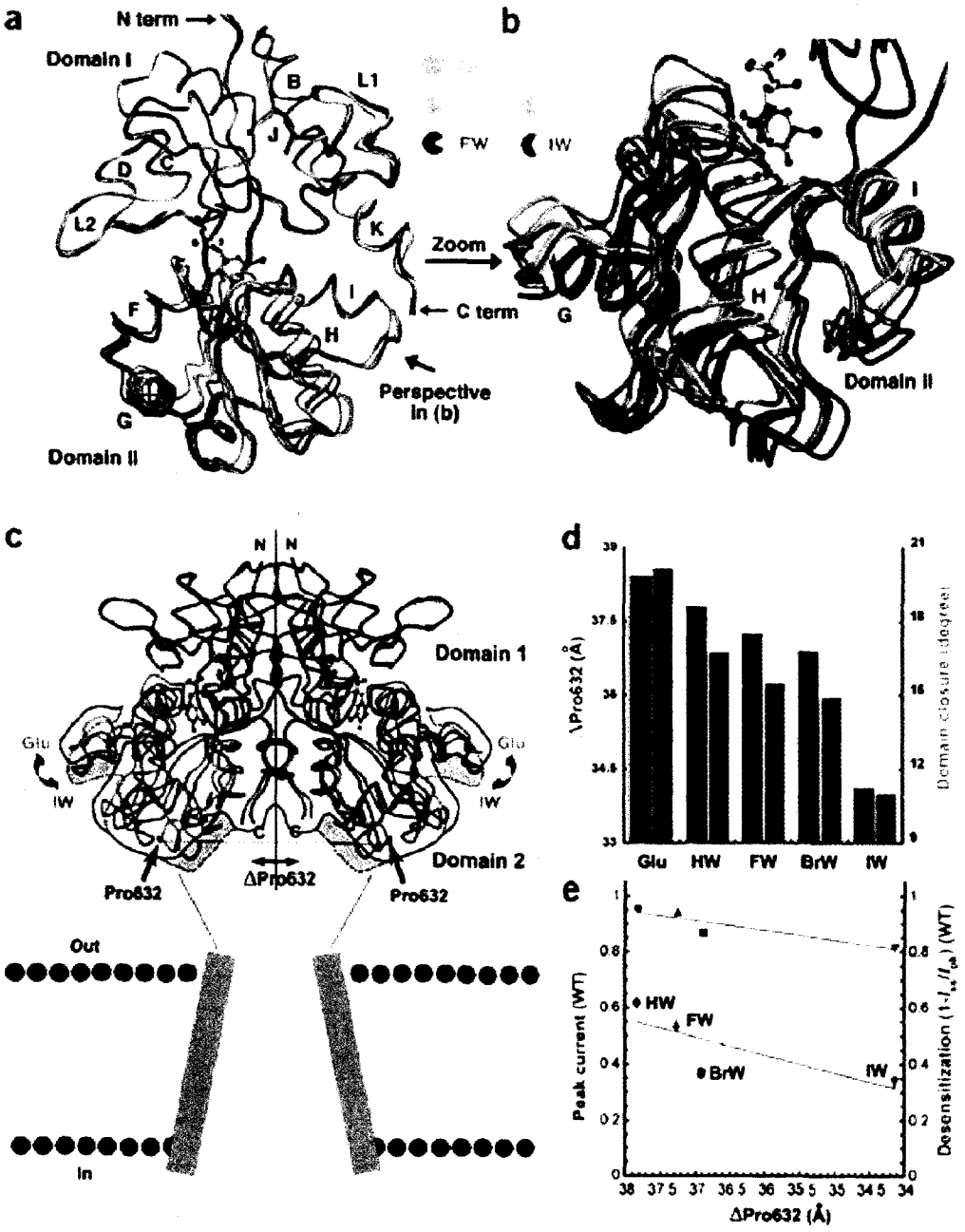

Chapter II: DIFFERENT DOMAINS OF THE AMPA RECEPTOR DIRECT STARGAZIN-MEDIATED TRAFFICKING AND STARGAZIN-MEDIATED MODULATION OF KINETICS

Matthew A. Bedoukian, Autumn M. Weeks and Kathryn M. Partin

Dept. of Biomedical Sciences, Colorado State University, Fort Collins, CO 80521

Stargazin is an accessory protein of AMPA receptors that enhances surface expression and also affects the biophysical properties of the receptor. AMPA receptor domains necessary for either of these two processes have not yet been identified. Here, we used confocal imaging and electrophysiology of heterologously expressed, fluorophore-tagged GluR1, GluR2 and stargazin to study surface expression and desensitization kinetics. Stargazin-mediated trafficking was sensitive to the nature of the AMPA receptor cytoplasmic domain. The insertion of YFP after residue 15 of the truncated cytoplasmic tail of GluR1i perturbed stargazin-mediated trafficking of the receptor but not its modulation of desensitization kinetics. This construct also failed to permit fluorescence resonance energy transfer (FRET) with stargazin in the ER, whereas FRET between fluorophore-tagged stargazin and non-truncated AMPA receptors demonstrated a specific interaction between these proteins, both in the ER and the plasma membrane. Rather than encoding a specific binding site, the fluorophore-tagged C-terminus may restrict access to one or more endoplasmic reticulum (ER) retention sites. Although perturbations of the C-terminus impeded stargazin-mediated trafficking to the plasma membrane, the effects of stargazin on the biophysical properties of AMPA receptors (i.e., modulation of desensitization) remained intact. These data provide

strong evidence that the AMPA receptor domains required for stargazin-modulation of gating and trafficking are separable.

INTRODUCTION

AMPA (a-amino-3-hydroxy-5-methyl-isoxazole-4-propionate) receptors, a subtype of ionotropic glutamate receptors, are expressed at the postsynaptic membrane of neurons where they mediate rapid excitatory synaptic transmission (Dingledine et al., 1999; Gouaux, 2003; Mayer, 2005; Palmer et al., 2005). Native AMPA receptors are hetero-oligomers composed of four subunits (GluR1-4) that are either a flip (i) or flop (o) isoform (Sommer et al., 1991). AMPA receptors play a critical role in neuronal signal transduction that is necessary for memory and learning. AMPA receptors cycle rapidly in and out of the plasma membrane in an activity-dependent manner (Barry and Ziff, 2002; Malenka, 2003; Malinow, 2003; Kim and Sheng, 2004) that requires assembly with auxiliary proteins such as stargazin (Vandenberghe et al., 2005b).

Stargazin, also known as g-2 or CACNG2, is a member of the transmembrane AMPA receptor regulatory protein (TARP) family (Bredt and Nicoll, 2003; Tomita et al., 2003; Letts, 2005; Nicoll et al., 2006). It was initially identified from the stargazer mouse, an inbred mouse strain with a phenotype of an unsteady gait, persistent head-raising ("star-gazing"), and frequent spike-wave discharges (Letts et al., 1998; Letts, 2005). Granule cells from the cerebellum of stargazer mice are missing functional AMPA receptors. A biochemical interaction between stargazin and both AMPA receptors and PSD-95 exists (Chen et al., 2000). The interaction between stargazin and AMPA receptors is essential for efficient delivery of receptors to the surface of cerebellar granule cells, whereas its interaction with PSD-95 is essential for clustering receptors to the postsynaptic membrane.

Stargazin enhances the total current of AMPA receptors, consistent with its ability to traffic more receptors to the plasma membrane where current is measured (Chen et al., 2003; Yamazaki et al., 2004; Priel et al., 2005; Tomita et al., 2005b; Turetsky et al., 2005). Recombinant AMPA receptors are poorly trafficked to the cell surface in the absence of stargazin

and remain trapped in intracellular pools (Hall et al., 1997). Stargazin may facilitate AMPA receptor export from the ER (Tomita et al., 2003) by masking ER retention signals of the tetrameric receptor in vivo (Vandenberghe et al., 2005b). In addition to enhancing AMPA receptor trafficking, stargazin also slows AMPA receptor desensitization and deactivation (Priel et al., 2005; Tomita et al., 2005b; Turetsky et al., 2005) and increases channel opening (Tomita et al., 2005b). The domains of stargazin essential for modulating trafficking versus biophysical properties are partially separable. Stargazin is a four-pass transmembrane protein: the cytoplasmic C-terminal domain is required for receptor trafficking but the first extracellular domain controls stargazin's modulation of AMPA receptor biophysical properties (Tomita et al., 2005b; Turetsky et al., 2005). The stargazin extracellular domain may allosterically modulate the AMPA receptor's extracellular ligand-binding core, altering AMPA receptor subunit interactions (14). Single-particle electron microscopy indicates that stargazin associates primarily with the AMPA receptor transmembrane domains (Nakagawa et al., 2005; Nakagawa et al., 2006). However, there is little information about AMPA receptor domains involved in stargazin-mediated trafficking or modulation.

The present study uses functional deletions of AMPA receptors to identify domains necessary for effective trafficking and modulation of desensitization by stargazin. Because the intracellular C-terminus of stargazin is necessary for targeting AMPA receptors, we hypothesized that an intracellular region of the AMPA receptor such as the C-terminus might directly interact with stargazin. Consistent with this idea, the C-termini of AMPA receptors are known to bind a number of different proteins that effect trafficking and the stabilization of the channel at synapses (**Figure S1**). Our data suggest that stargazin requires access to a cytoplasmic binding site for effective trafficking to the surface membrane but does not require this same interaction for modulation of desensitization.

METHODS

Transient transfections for electrophysiology. Human embryonic kidney 293 (HEK 293) fibroblasts (CRL 1573; American Type Culture Collection, Rockville, MD) were cultured as described previously (Leever et al., 2003). Cells were transiently transfected using FuGene 6 reagent (Roche Products, Indianapolis, IN) or Lipofectamine 2000 (Invitrogen, Carlsbad, CA) with AMPA receptor cDNA (0.5–2 μg/35 mm dish) and if channel was not tagged, soluble yellow fluorescent protein cDNA (0.1– 0.15 μg/35 mm dish). When used, stargazin was always added in a 1:2 stargazin ratio (with total amounts of cDNA transfected ranging from 0.1-3 μg). After transfection, 10-40 μM NBQX was added to the media to prevent cell toxicity.

Transfections for confocal microscopy. Collagen or poly-d-lysine coated 14 mm glass bottom culture dishes (MatTek Corporation, Ashland, MA) were incubated with ECL Attachment Matrix (Upstate Cell Signaling Solutions, Lake Placid, NY) for 1hr at 37°C then washed with cMEM before plating cells. Cells were transfected using Lipofectamine 2000 (Invitrogen, Carlsbad, CA) when 60-90% confluent and incubated under identical conditions as cells used for standard electrophysiology. For each transfection 70 μl of MEM was incubated with 3 μl of Lipofectamine and in another tube 30 μl of MEM was incubated with 0.1 to 3 μg of total cDNA and thoroughly mixed. Contents of the tubes were combined, and after 20-30 minutes the solution was added to the cells along with 0-10 μM NBQX. 4.5-24 hours later, the solution was exchanged with fresh cMEM with 20-40 μM NBQX. All cells were imaged at room temperature 2-3 days after transfection. Immediately before imaging the solution was exchanged with cMEM containing no phenol red.

Outside-out patch recordings. Currents were recorded 2–3 days after transfection, as described previously (Leever et al., 2003). Extracellular solutions (ECS) contained the following: 20 mM sucrose, 145 mM NaCl, 5.4 mM KCl, 5 mM HEPES, 1 mM $MgCl_2$, 1.8 mM $CaCl_2 \cdot H_2O$, and 0.01 mg/ml phenol red, pH 7.3. Outside-out membrane patches were voltage clamped at -60 mV using an Axopatch 200B amplifier (Molecular Devices, Union City, CA). Synapse (version 3.6d;

Synergy Research, Silver Spring, MD) controlled piezoelectric movement, data acquisition, and trace analysis. Responses were filtered at 5 kHz, digitized at 10–500 μs/point, and stored on a Power Macintosh computer (Apple Computers, Cupertino, CA) using an ITC-16 interface (InstruTech, Port Washington, NY). Micropipettes (TW150F; 2–5 MΩ; World Precision Instruments, Sarasota, FL) contained the following (in mM): 135 CsCl, 10 CsF, 10 HEPES, 5 Cs-BAPTA, 1 $MgCl_2$, and 0.5 $CaCl_2$, pH 7.2 (292 mOsm). Patches were perfused at 0.2 ml/min with solutions emitted from a two-barrel flow pipe made with θ tubing (BT150–10; Sutter Instruments, Novato, CA). One barrel contained vehicle (control) composed of the following: 145 mM NaCl, 5.4 mM KCl, 5 mM HEPES, 1 mM $MgCl_2$, 1.8 mM $CaCl_2 \cdot H_2O$, with 0.01 mg/ml phenol red, pH7.3. The other barrel had this solution plus L-glutamate (10 mM). After going into voltage clamp, an outside-out patch was pulled, lifted up to the flow pipe, positioned near the interface between the glutamate-free and glutamate-containing solution and jumped rapidly from the vehicle control into glutamate. Rapid solution exchanges of 1 or 500 ms were driven by a piezoelectric device (Burleigh Instruments, Fishers, NY). Solution exchange rates were determined at the end of each experiment by open-tip junction currents and excluded if rise times exceeded 0.5 ms.

Analysis of rapid responses. Desensitization rates were estimated by fitting a single-exponential function (τ_{des}) to the 500 ms response decay (from 95% of peak to steady state). Deactivation rates were estimated by fitting a single-exponential function (τ_{deact}) to the 1 ms response decay (from 95% of peak to steady state). Three to 20 responses per patch were averaged for analysis. Current traces and graphs were plotted using KaleidaGraph 3.5 (Synergy Software, Reading, PA).

Generation of constructs. The CMV expression plasmids (pRK) for GluR1, GluR2 ($R_{607}Q$) and GluR6 ($R_{621}Q$) were provided by Dr. Peter Seeburg (Max Planck Institute for Medical Research, Heidelberg, Germany). $R1_{81}$YFP was generated using overlapping PCR to make an in-frame fusion protein with CFP or YFP, using pECFP or pEYFP (Clontech, Palo Alto, CA) as templates.

The first residue from the fluorescent protein followed immediately after the last amino acid in the sequence ATGL. $R1_{46}$YFP was made by inserting the restriction site MluI (ACGCGT) between amino acids GGG and SGE of the C-terminal domain using QuikChange II XL Site-Directed Mutagenesis Kit (Stratagene, La Jolla, CA). The final sequence at the fusion was GGGTR(YFP). $R1_{36}$YFP, $R1_{15}$YFP, $R1_{7}$YFP, $R1_{2}$YFP, $R2_{46}$YFP, and $R2_{16}$YFP were generated similarly (see **Figure S1** for the locations of insertion sites). All point mutations were made using the QuikChange II XL Site-Directed Mutagenesis Kit as was the insertion of a stop codon for $R1i_{14}$ after amino acids KRMK of the cytoplasmic tail. The insertion sequence of the $R1i_{15+38}$YFP, $R1i_{7+38}$YFP, and $R1i_{2+38}$YFP constructs had a 38 amino acid linker before fluorophore attachment with the sequence: TRGGSEQKLISEEDLSQFRVSPLDRTWNLGETVELKTR. GluR2i and GluR2o DATD were constructed to delete 380 amino acids of the mature protein. The N-terminus thus began with LPS preceded by the Kozak sequence (ACC) and the GluR6 signal sequence. Stargazin constructs: StgEGFP/Gw1-CMV plasmid (British Biotechnology; (Tomita et al., 2004)) was a generous gift from Dr. David Bredt (UCSF, San Francisco), as was pcDNA3-stg. StgCFP and stgYFP were inserted in frame at the BglII site in pcDNA3 (Stratagene) homologous to stgGFP but truncated after amino acid 269. GluR4i DATD and FLAG-GluR4i were kind gifts from Dr. Kari Keinanen (University of Helsinki; Helsinki, Finland; (Pasternack et al., 2002)) FLAG-GluR4i DCTD was made by inserting a stop codon after EF, the first two amino acids of the cytoplasmic tail. Kv2.1 was a kind gift from Dr. Michael Tamkun (Colorado State University; Fort Collins, CO; (O'Connell and Tamkun, 2005)). The CD8 plasmid (MGC-34614) was purchased from American Type Culture Collection (Rockville, MD) and CD3CFP was a generous gift from Dr. Nicholas Gascoigne (The Scripps Research Institute; La Jolla, California (Yachi et al., 2005)).

DNA mutations were confirmed by sequencing (Macromolecular Resources, Fort Collins, CO).

Measurements of FRET. Transfected cells were imaged using an LSM 510 META laser scanning confocal microscope (Zeiss, Thornwood, NY) with a Plan-Achromat 63x/1.4 oil DIC objective

(Leuranguer et al., 2006). CFP and YFP were excited with separate sweeps of the 458 and 514 nm lines, respectively, of an argon laser operated at 6.3-6.7A, attenuated to 5% and 2% respectively, and directed to the cell via a 458/514 nm dual dichroic mirror. Airy units for imaging were between 1 and 2 for CFP and always 1 for YFP. The emitted cyan fluorescence was directed to a photomultiplier with a 460-500 nm bandpass filter and yellow fluorescence was directed to a photomultiplier equipped with a 530 nm long-pass filter. Confocal fluorescence intensity data (I_{CFPpre} and I_{YFPpre}) were recorded as planar line scans digitized at 8 or 12-bits. Repeated scans (20-50) with un-attenuated 514 nm illumination to photobleach YFP, which required ~15-45 s at maximal scan rates, were used to photobleach YFP. After completion of YFP bleaching, fluorescence intensity ($I_{CFPpost}$ and $I_{YFPpost}$) was measured using the identical parameters as before bleaching. FRET efficiency (E) was calculated as $1-(I_{CFPpre}/I_{CFPpost})$, where I_{CFPpre} and $I_{CFPpost}$ are the background-corrected CFP fluorescence intensities before and after photobleaching YFP, respectively. Membrane FRET measurements were taken from cells illustrating an obvious increase in fluorescence intensity around the cell perimeter relative to the cytosol. Whole cell measurements were taken from visible fluorescence from the entire cell (minus the nucleus), whereas cytosolic measurements included the whole cell without obvious plasma membrane.

Confocal imaging of GFP and fluorescent microspheres. Cells transfected with stgGFP were excited using the 488 nm line of an argon laser attenuated to 6%. Emission was collected using the meta filter set to capture between 508 and 551 nm. Yellow-green biotin labeled 0.04 μM beads (Fluospheres, Molecular Probes, Eugene, OR) were imaged at the bottom of an ECL coated cell dish at identical settings. Determination of protein at the cell surface was calculated as described previously (Sugiyama et al., 2005).

Immunofluorescence for confocal imaging. After transfection as described above for 3 days with 0.3 μg of FLAG-GluR4i cDNA with or without 0.6 μg stg, cells were rinsed with PBS then fixed with 4% paraformaldehyde for 15-20 minutes. Cells were blocked for 1 hour with 1% BSA and

3% normal goat serum in PBS. A 1:9000 dilution of ANTI-FLAG M2 Monoclonal Antibody (Sigma, Saint Louis, Missouri) was applied for 1 hour then washed 3 x 10 minutes in blocking solution before applying 1:700 goat anti-mouse Alexa Fluor 568 (Molecular Probes, Eugene, Oregon) for 1 hour. Cells were again washed 3 x 10 minutes in blocking solution then rinsed several times in PBS before imaging with an Olympus FV1000 confocal microscope. All staining and imaging were done at room temperature.

Quantitation of surface expression.

Transfected HEK 293 cells were visualized using a confocal microscope and divided into 3 categories (where a "ring" is defined as markedly enhanced surface expression, which if imaged as an optical slice with a confocal microscope, appears as enhanced fluorescent intensity co-localizing with the plasma membrane): definitely rings, definitely no rings, and unclassifiable. Unclassifiable cells represented were, for example, cells with very low expression or hints of enhanced surface expression in only a very small portion of the surface membrane. Only 4% of over a hundred cells co-transfected with $R1i_{15}$YFP and stargazin were deemed unclassifiable, whereas 14% of over two hundred cells co-transfected with $R1i_{81}$YFP and stargazin were not classifiable. To ensure non-biased quantification, a blind observer was trained to detect rings from non-rings and did not identify a single cell co-transfected with $R1i_{15}$YFP and stargazin that had a surface expression ring.

Statistical significance was determined with an unpaired Student's t-test. Data are reported as mean ± SEM.

RESULTS

1. Stargazin alters GluR1i distribution in the cytosol and the plasma membrane.

To assay stargazin-mediated trafficking of AMPA receptors, in-frame chimeric proteins were constructed by fusing a fluorescent protein (ECFP or EYFP) to the C-terminal domain of either GluR1 (R1) or GluR2 (R2). Functional channels were expressed heterologously in HEK293 cells then imaged using a confocal microscope. Effects on trafficking were assayed by

determining subcellular localization and, in particular, whether or not the protein could be detected at the plasma membrane surface. Confocal imaging through live cells that expressed fluorophore-tagged AMPA receptors allowed us to distinguish between accumulation of protein in reticular, perinuclear networks (presumably colocalized with the ER) or within the plasma membrane, such that the labeled protein formed prominent "surface rings".

Full length $GluR1_{flip}$ (R1i) with YFP ($R1i_{81}YFP$) fused to its C-terminus was heterologously expressed with and without stargazin. This construct yielded a fully functional ion channel (**Figure 2.1**). Although currents may be recorded from this construct, confocal imaging of $R1i_{81}YFP$ demonstrated uniformly distributed fluorescence, typical of ER-associated expression (**Figure 2.1b**). In contrast, expression of fluorophore-tagged stargazin (stgYFP) alone resulted in the formation of pronounced surface rings in virtually every cell. When $R1i_{81}YFP$ was co-transfected with stargazin, the plasma membrane intensity relative to the cytosolic intensity was markedly increased in a population of cells (**Figure 2.1b**, **Table 1**), due to decreased cytosolic expression of $R1i_{81}YFP$. The population of fluorescent cells with pronounced surface expression was quite variable (~5-35%) across more than ten independent transfections (using a 1:2 receptor:stg ratio in all cases). Nevertheless, increased amounts of stargazin always resulted in an increased percentage of $R1i_{81}YFP$-expressing cells with rings (**Figure 2.1c**, inset). However, in the absence of stargazin, surface rings of $R1i_{81}YFP$ were never observed at any cDNA concentration used (0.1 to 2 μg). The ability to generate pronounced surface rings in all cells was not due to poor transfection efficiencies, in that ≥96% of all cells (N>100) that contained $R1i_{81}YFP$ also expressed the fluorophore-tagged stargazin.

Stargazin has a dual effect on AMPA receptors: it traffics them to the surface and also alters their biophysical properties. Specifically, stargazin slows receptor deactivation and desensitization, as well as increasing open probability and current amplitude (Chen et al., 2003; Yamazaki et al., 2004; Priel et al., 2005; Turetsky et al., 2005). We therefore accessed whether stargazin could modulate the biophysical properties of both populations of co-transfected cells

(with and without ER retention). Outside-out membrane patches from cells co-transfected with $R1i_{81}$YFP and stargazin, either with or without pronounced surface expression, demonstrated a significant slowing of receptor desensitization compared with $R1i_{81}$YFP in the absence of stargazin (**Figure 2.1c**). As expected, cells co-transfected with $R1i_{81}$YFP and stargazin *with* surface rings had current amplitudes about 6-fold greater than without stargazin (1507± 426 pA).

In addition, the desensitization kinetics were significantly different between these two cell populations. In the absence of stargazin, GluR1i desensitized with a decay time constant of 3.7±0.4 ms, whereas stargazin-transfected cells *with* rings had desensitization kinetics (8.5±0.8 ms) that were only slightly slower than stargazin-transfected cells *without* rings (7.1±1.1 ms). Deactivation kinetics followed this same trend, with decay kinetics in the absence of stargazin (0.7±0.1 ms) slowed to 1.0±0.2 ms versus 2.6±0.3 ms in cells with pronounced stargazin-mediated surface expression (**Figure 2.1c**).

2. An intracellular interaction between stargazin and AMPA receptors is necessary for up-regulation of surface expression.

To map the domains of AMPA receptors essential for stargazin-mediated trafficking, a series of receptor deletion proteins (fused to fluorophores) was constructed. To determine the role of the AMPA receptor C-terminus, R1i and R2i C-terminal truncations were made (**Figure 2.2a, 2.4a**). As seen for $R1i_{81}$YFP, $R1i_{46}$YFP and $R1i_{36}$YFP expression was mostly cytosolic in the absence of stargazin. However, these receptors could form fluorescent membrane surface rings when co-expressed with stargazin. No decrease in the frequency of surface rings or differences in the ratio of membrane to cytosolic intensity were found for these truncated proteins compared with the wild type C-terminus. However, a third fusion protein that deleted all but the first 15 amino acids of the C-terminus, $R1i_{15}$YFP, resulted in a receptor that never formed surface rings (10 independent transfections with >1000 counted fluorescent cells). Rings also did not form when $R1i_{15}$YFP was co-expressed with stgCFP (**Figure 2.2b**). Rings were not seen even at a 1:8 stargazin ratio.

The homologous deletion made in GluR2 ($R2i_{16}$) tagged with CFP or YFP was also tested for stargazin-mediated trafficking. Similar to $R1i_{15}$YFP, the expression of this protein was cytosolic in either the absence or presence of stargazin. In contrast, the C-terminal deletion mutation $R2i_{46}$YFP also formed surface expression rings (**Figure 2.4a**). Thus, the cytoplasmic requirements for trafficking of GluR1 or GluR2 by stargazin appear to be similar. All flop isoforms tested followed the same trend.

3. The intracellular interaction necessary for effective stargazin-mediated trafficking is not necessary for stargazin-mediated modulation of desensitization.

The inability of stargazin to traffic $R1_{15}$YFP or $R2_{16}$YFP to the surface membrane suggests that stargazin cannot interact with these proteins. To determine whether trunctions that impair trafficking also impair modulation of AMPA receptor function, we examined the electrophysiological properties of the mutated receptors. Outside-out patches of cells transfected with the C-terminal trunctions, $R1i_{15}$YFP or $R1i_{36}$YFP, demonstrated no significant difference in stargazin-mediated slowing of desensitization compared to the non-truncated $R1i_{81}$YFP (**Figure 2.2c, 2.2e**). Stargazin slowed the kinetics of $R1i_{81}$YFP from 3.2±0.1 to 5.8±0.7 ms, $R1i_{36}$YFP from 3.4±0.5 to 4.8±0.3 ms, and $R1i_{15}$YFP from 2.9±0.1 to 5.8±0.3 ms. It is important to note that cells with surface expression rings were not selected for in these experiments and are not paired with the data used for **Figure 2.1**.

As expected if the formation of surface expression (and reduced ER retention) is related to overall current density, $R1i_{15}$YFP showed only a two-fold increase in current amplitude when co-expressed with stargazin (370±113 vs. 733±175 pA), whereas both $R1i_{81}$YFP (198±69 vs, 694±301 pA) and $R1i_{36}$YFP (172±82 vs, 630±140 pA) showed a ~3.5-fold increase in current amplitude (**Figure 2.2d**). $R1i_{14}$, which lacked a fluorophore and had one less amino acid than $R1i_{15}$YFP, produced currents that were significantly smaller 30±3 pA, but when co-transfected with stargazin the mean current increased ~11–fold to 364±118 pA. Together, the data presented

in Figures 1 and 2 suggest that the domains of AMPA receptors necessary for trafficking of or modulation by stargazin are separable.

4. The cytoplasmic tail of AMPA receptors does not contain a specific stargazin-binding site.

Stargazin did not traffic $R1_{15}$YFP to the surface. To determine if this was due to steric hindrance when the fluorophore was attached immediately after residue 15, we inserted a 38 amino acid linker between the last AMPA receptor residue of $R1i_{15}$YFP and the fluorophore ($R1i_{15+38}$YFP). Co-transfection of $R1i_{15+38}$YFP with stargazin permitted ring formation, demonstrating that no more than 15 amino acids of the cytoplasmic tail of AMPA receptors were necessary for stargazin mediated trafficking. To determine if there is a specific interaction between stargazin and any of the residues within the conserved proximal 14 amino acids in the tail of AMPA receptors, a series of point mutations was constructed. These mutations either disrupt a known protein-interacting site (**Figure S1**) or replace critical differences in the proximal cytoplasmic tail between AMPA receptors and GluR6 (**Figure 2.3a**), which does not associate with stargazin (Chen et al., 2003). All point mutants were constructed within $R1i_{81}$YFP or $R1i_{36}$YFP. Each of these mutant receptors permitted stargazin-mediated surface expression rings (**Figure 2.3a**) suggesting that specific C-terminal residues are not necessary for stargazin trafficking. Because previous studies have shown that an AMPA receptor without a C-terminus has virtually no surface expression (Coleman et al., 2003), we constructed an extreme C-terminal truncation, $R1i_2$YFP as a negative control. As expected, $R1i_2$YFP did not form surface expression rings either in the absence or presence of stargazin. However, when the same 38 amino acid linker was added between the receptor and the fluorophore ($R1i_{2+38}$YFP), surface expression rings formed for a small number of cells (<1%) co-transfected with stargazin (**Table 1**). The failure to see more surface expression rings may be due to the already diminished surface expression that results from this impaired receptor.

The experiments with fluorophore-tagged receptor mutants led us to question whether the cytoplasmic tail of AMPA receptors contains a specific stargazin-binding site or whether the tail can in some cases interfere with another stargazin-binding site present at the cytoplasmic face of the receptor. To demonstrate that stargazin does not require specific determinants on the cytoplasmic tail, we used another assay for surface expression, namely immunofluorescence of unpermeabilized cells transfected with an extracellularly FLAG-tagged receptor. FLAG-R4i$_2$ (with only the first 2 amino acids of the cytoplasmic tail of GluR4i (Coleman et al., 2003)) was co-transfected with stargazin. Although surface expression levels of this construct without stargazin were almost undetectable, stargazin did increase the surface expression (**Figure 2.3b**) but not to the levels of full-length FLAG-R4i (with or without stargazin). This experiment verified through an independent method that nearly all of the C-terminus is dispensable for stargazin-mediated trafficking of AMPA receptors, as long as there is no fluorophore attached.

5. Mutations of ER retention signal residues enhance trafficking without and with stargazin.

Stargazin may enhance AMPA receptor trafficking by masking an ER retention signal (Vandenberghe et al., 2005b). Although we found that stargazin could enhance the surface expression of both the R4i$_2$ and R1i$_{2+38}$YFP constructs, the fact that stargazin did not fully rescue surface expression is likely due to the importance of the proximal cytoplasmic tail residues for AMPA receptor expression. To rule out that this lack of complete rescue was not due to an impaired ability of stargazin association with specific residues of the cytoplasmic tail, we tested R1i$_{7+38}$YFP (with the third of seven amino acids being Leu instead of Cys, so all seven residues would be identical to the first seven amino acids of the untraffickable GluR6 tail) (**Figure 2.3a**). This construct has the 38 amino acid linker between the seventh amino acid and the fluorophore. Although this receptor should not interact with protein 4.1, shown to be important for AMPA receptor surface expression (Shen et al., 2000; Coleman et al., 2003), in one experiment we found that 28% of all fluorescent cells had pronounced stargazin-mediated surface expression rings,

comparable to "wild type" $R1i_{81}$YFP. In addition, residues 4-6 of the cytoplasmic tail (implicated in ER retention (Greger et al., 2002)) were mutated from YKS to FQA (**Figure 2.3a**), using $R1i_{81}$YFP as a template. Even without stargazin, surface expression rings were formed in ~2% of the cells, something we had never observed for $R1i_{81}$YFP. Additionally, 36% of fluorescent cells formed stargazin-mediated surface expression rings (**Table 1**).

Since stargazin may increase surface expression by blocking an intracellular ER retention signal in the pore, we tested $R2_{46}$YFP (R_{607}). Wild type GluR2 contains a residue that undergoes RNA editing, converting the glutamine for an arginine in the pore region (Higuchi et al., 1993). This channel would be expected to be retained largely in the ER (Greger et al., 2002), have difficulty forming tetramers (Greger et al., 2003), and presumably not get to the surface membrane even with stargazin unless stargazin could somehow block the ER retention signal. The number of cells co-transfected with stargazin and $R2_{46}$YFP that had rings was about the same regardless of whether residue 607 was an R or a Q (**Table 1**). Together, these data suggest that stargazin occludes one or more ER retention signals at the cytoplasmic face of the receptor.

6. Stargazin mediates trafficking of AMPA receptor N-terminal deletions with isoform differences related to differential protein stability.

The amino-terminal domain (ATD) of glutamate receptors has been implicated in assembly, trafficking and allosteric modulation (Ayalon and Stern-Bach, 2001; Zheng et al., 2001; Xu et al., 2003). To test whether or not the ATD plays a role in stargazin-mediated trafficking or modulation of the biophysical properties of AMPA receptors, the flip and flop isoforms of GluR2 (R2i and R2o) lacking the ATD, similar to $R4i_{DATD}$ (Pasternack et al., 2002), were made.

$R2o_{DATD}$ and $R2i_{DATD}$ were tagged with YFP at the C-terminus, after amino acid 46 of the cytoplasmic tail ($R2o_{DATD46}$YFP, $R2i_{DATD46}$YFP). Without stargazin, these proteins demonstrated a cytosolic expression pattern, and with stargazin, $R2o_{DATD46}$YFP formed pronounced surface expression rings (**Figure 2.4b**). In contrast to $R2o_{DATD46}$YFP, $R2i_{DATD46}$YFP did not form surface

expression rings. A large number of cells expressing $R2o_{DATD46}$YFP or $R2i_{DATD46}$YFP formed aggresomes (Corboy et al., 2005) with or without stargazin (**Table 2**), but this was most pronounced for $R2i_{DATD46}$YFP with stargazin (**Figure 2.4b** and **2.4d**). All R1 and R2 fluorescently tagged, C-terminal deletions with an intact ATD, however, were virtually free of aggresomes regardless of the length of the C-terminal tail (with the exception of GluR2 R_{607}, but not $R_{607}Q$). Differential aggresomal accumulation in the flip isoform may account for the inability of $R2i_{DATD46}$YFP to permit efficient stargazin-mediated surface expression. Aggresome formation may also explain the reduction in current amplitude seen for $R2i_{DATD}$ (382±129 vs. 166±67 pA with stargazin) as well as $R4i_{DATD}$ (166±43 vs. 23±4 pA with stargazin, $p<.01$). Consistent with this interpretation, stargazin increased the current amplitude of $R2o_{DATD46}$YFP (41±17 vs. 597±146 pA with stargazin).

7. The ATD is not necessary for stargazin modulation of AMPA receptor kinetics.

Whereas previous studies using $R4i_{DATD}$ showed only a modest change in desensitization from wild type R4i (32), $R2i_{DATD}$ desensitization kinetics (t_{des}=13.7±0.6 ms) were much slower than wild type R2i (t_{des}=6.9±0.5 ms). t_{des} for $R2o_{DATD46}$YFP was 2.9±0.3 vs. 1.4±0.1 ms for wild type R2o. Stargazin also modulated desensitization of $R4i_{DATD}$ (t_{des}=5.6±0.4 vs. 8.4±0.7 ms with stargazin) and $R2i_{DATD}$ (t_{des}=13.7±0.6 vs. 32.3±4.1 ms with stargazin) (**Figure 2.4c**). In contrast, the effects of stargazin on modulation of $R2o_{DATD46}$YFP were more modest (t_{des}=2.9±0.3 vs. 4.1±0.9 ms with stargazin). This flip/flop difference has been previously reported for full length GluR2 (Turetsky et al., 2005) and suggests that the ATD does not play a significant role in stargazin-mediated modulation of desensitization.

We next looked at deactivation kinetics and found no detectable slowing of deactivation for $R2i_{DATD}$ (t_{deact}=1.9±0.6 vs. 1.4±0.3 ms with stargazin), or for $R2o_{DATD46}$YFP (1.8±0.3 vs. 2.4±0.8 ms with stargazin). The rate of deactivation, however, was slower without an ATD for

both $R2i_{DATD}$ (t_{deact}=1.9±0.6 ms compared to wt R2i = 0.9±0.1 ms (Jin et al., 2005) and $R2o_{DATD46}$YFP (t_{deact} = 1.8±0.3 vs. 0.7±0.1 ms for wild type R2o).

8. Fluorescence resonance energy transfer (FRET) suggests stargazin self-assembly.

Our results from the amino- and carboxyl-termini deletions strongly suggest that stargazin acts upon an AMPA receptor intracellular site to direct trafficking to the surface. Whereas biochemical methods such as "pull-down assays" would not distinguish between a direct protein-protein interaction or participation in a protein complex, FRET between fluorophores on two proteins is strong evidence for a tight (≤100 Å) intermolecular interaction. Therefore, we studied the interaction using FRET between the fluorophore-tagged GluR1 and stargazin proteins. Initially, we measured the ability of stargazin molecules to undergo FRET in the absence of receptor. Varying ratios and total concentrations of stgCFP and stgYFP were transfected, and FRET in the membrane was measured using a photobleaching protocol (**Figure 2.5a** and **2.5c**). At all DNA concentrations and ratios tested, FRET between two stargazin molecules (7.8-16.2% efficiency) was significantly greater than a membrane control, Kv2.1CFP: $R1i_{81}$YFP: stargazin at a 1:2:2 ratio (0.2±0.1% FRET efficiency, $p<.005$). Due to the profound stargazin-stargazin membrane fluorescence compared to that of cells co-transfected with fluorescent AMPA receptors and stargazin (see below), it was necessary to rule out that FRET occurred from overcrowding of the plasma membrane.

Yellow-green fluorescent beads were used to estimate how much stargazin protein was in the membrane (Sugiyama et al., 2005). A confocal image of stgGFP-transfected cells is shown in **Figure 2.5b**, with a fluorescent bead in a different dish taken at an identical setting. Analysis of the comparative intensity of the bead and the cell (see figure legend) suggests that the membrane density of stargazin was ~820 molecules per μm^2, and therefore overcrowding by fluorophore-tagged stargazin could not explain the FRET data shown in **Figure 2.5c**, unless certain regions of the membrane have greatly increased protein density. These data are consistent with an

interpretation that stargazin:stargazin FRET arises from specific homo-oligomerization rather than nonspecific membrane crowding.

9. FRET occurs between stargazin and GluR1.

To determine whether stargazin and AMPA receptors interact closely enough to permit energy transfer that can be measured by FRET, we used a competition assay. The first goal was to determine whether the stargazin complex known to FRET (stgCFP:stgYFP) could be disrupted by co-expression with a non-fluorescent AMPA receptor. The FRET efficiency of a 1:1 ratio of stgCFP and stgYFP (0.2 μg total cDNA) was 10.6±1.4%, which was competed by over-expressing R1i (2 μg of cDNA), reducing the FRET efficiency to 3.9±1.1%, p=.003 (**Figure 2.6a** and **6c**). However, neither 2.0 μg of cDNA encoding CD8 (11.8±2.6%), Kv2.1 (8.0±0.9%) nor R6 (8.5±1.6%) significantly decreased membrane FRET (**Figure 2.6a**). A dose-dependency of R1i competition was determined, in that concentrations of 0.5, 1.0 and 2.0 μg cDNA significantly reduced membrane FRET efficiency from the basal level of 16.2±2.8% to 7.7±1.4, 9.1±1.6, and 5.8±1.1%, respectively (**Figure 2.6b** and **2.6d**). The reduction of FRET between stargazin molecules suggests that when there is an excess amount of R1i, but not other membrane proteins, the stargazin homo-oligomer population declines.

Based upon the mutational analysis of the C-terminus of GluR1, one would predict that co-expression of $R1i_{81}$CFP with stgYFP would permit FRET, whereas co-expression of $R1i_{15}$CFP with stgYFP would not. Indeed, $R1i_{81}$CFP:stgYFP produced robust FRET (20.2±2.1%) in the plasma membrane, but also produced FRET (7.6±1.0%) in the cytosolic, reticular network of cells with AMPA receptor rings (**Figure 2.6e**, left). However, cells that did not contain $R1i_{81}$CFP rings had a cytosolic FRET efficiency (3.4±1.0%) that was significantly lower and not significantly different than the negative soluble CFP and YFP control (2.4±0.5%). As predicted, co-expression of $R1i_{15}$CFP with stgYFP showed no membrane fluorescence (**Figure 2.6e**, right) and no significant FRET efficiency in the cytosol (4.1±1.0%).

As a putative negative control for membrane FRET, the T cell receptor CD3CFP (Yachi et al., 2005) was co-expressed with stgYFP (0.3 μg: 1 μg stgYFP), but also showed robust membrane FRET efficiency (30.4±2.1%) that was competed to 15.4±2.0% by stargazin. Thus, we cannot rule out that the high expression levels of stargazin may contribute to some background FRET from overcrowding. The FRET between stargazin and both negative controls, CD3 and Kv2.1CFP (~20%), was much higher than would be expected of a negative control. Nevertheless, a control FRET experiment using Kv2.1CFP with excess $R1_{81}$YFP and non-fluorescent stargazin (to get $R1_{81}$YFP to the membrane) demonstrated ~0% membrane FRET efficiency.

10. AMPA receptor hetero-oligomerization can rescue C-terminal deletions with trafficking defects.

The previous experiments focused on AMPA receptor homo-oligomer trafficking by stargazin. Because our data support the idea that stargazin and AMPA receptors associate in the ER where subunit assembly is also occurring, we tested whether stargazin-mediated trafficking requires access to each of the subunits in the tetrad. $R1_{15}$- and $R2_{16}$-tagged channels ("shorter" C-termini) that did not form surface expression rings with stargazin were co-transfected with both stargazin and an R1 or R2 channel that did form surface expression rings when co-transfected with stargazin ("medium" or "longer" C-termini). $R1i_{81}$YFP, $R1i_{46}$CFP, and $R1i_{36}$YFP could rescue $R1i_{15}$CFP trafficking (**Figure 2.7a**). $R1i_{46}$CFP was able to rescue $R2o_{16}$YFP as well as $R2o_{DATD16}$YFP, suggesting that stargazin does not need to bind all four subunits in a tetramer.

We further analyzed the data to assess the trafficking of subunits with different C-termini within a tetramer. Two channels that could be trafficked independently by stargazin had virtually the same membrane to cytosolic fluorescence intensity ratio, $(I_{membrane}/I_{cytosol})_A/(I_{membrane}/I_{cytosol})_B$, where A=$R1i_{46}$CFP and B=$R2o_{46}$YFP (.99±.06) or A=$R1i_{46}$YFP and B=$R1i_{81}$CFP (0.94±.06). In contrast, short channels co-expressed with long channels had significantly reduced membrane to cytosolic ratios compared to the long forms, for example, where A=$R2o_{16}$YFP and B= $R1i_{46}$CFP

(0.78±.06); where A=R1i$_{15}$YFP and B=R1i$_{46}$CFP (0.77±.04); and, where A=R1i$_{15}$CFP and B=R1i$_{36}$YFP (0.71±.08) (**Figure 2.7b**).

Shorter forms are rescued to the point that they are only ~25% less effectively trafficked than the longer forms. This suggests that perhaps only 1 long form per tetramer is needed for stargazin-mediated trafficking. We therefore compared the membrane FRET, in the presence of stargazin, between tetramers composed of short and medium length subunits, R1i$_{15}$ and R1i$_{46}$, at different ratios of co-expression (**Figure 2.7c**). As a control for differences in expression levels we compared the FRET between R1i$_{15}$CFP and R1i$_{46}$YFP (1:1; 0.5 CFP: 0.5 YFP: 2 stg) or (1:4; 0.2 CFP:0.8 YFP: 2 stg) and R1i$_{46}$CFP and R1i$_{15}$YFP (1:1) or (1:4) in the cytosol. We found equal FRET between both combinations of subunits at 1:1 (~7%) and 1:4 (~11%). As expected the FRET efficiency was greater at the 1CFP:4YFP ratio because more tetramers would be composed of excess YFP subunits. We next measured the FRET efficiency at the membrane for R1i$_{15}$CFP and R1i$_{46}$YFP at 1:4 (18.5±2.9%) to determine the maximum FRET efficiency and what value we could expect if stargazin was trafficking tetramers predominantly in a 1R1i$_{15}$:3R1i$_{46}$ ratio. The membrane FRET efficiency of the 1:1 ratio (16.5±2.8%) was significantly greater than the 1:1 cytosolic ratio, but not different from the 1:4 cytosolic or membrane FRET. This suggests that the preferred heteromeric stoichiometry for stargazin mediated trafficking was 1R1i$_{15}$: 3R1i$_{46}$. In support of this conclusion, membrane FRET efficiency between R1i$_{46}$CFP and R1i$_{15}$YFP at 1:1 was significantly less (6.5±1.8%), and no greater than the cytosolic 1:1 ratio, suggesting that tetramers composed of fewer R1i$_{15}$YFP and more R1i$_{46}$CFP were preferentially trafficked.

As an attempt to rule out that other combinations of heteromeric receptors besides 1R1i$_{15}$:3R1i$_{46}$ could not be trafficked by stargazin we looked at membrane FRET using a 1R1i$_{46}$CFP:4R1i$_{15}$YFP ratio, to force the majority of tetramers with a CFP subunit into a 3R1i$_{15}$:1R1i$_{46}$ ratio. The membrane FRET efficiency (13.3±1.6%) was significantly greater than the 1:1 membrane FRET efficiency ($p<.03$). This suggests that stargazin can traffic hetero-

oligomers containing two short subunits, and does not rule out the possibility that stargazin may traffic tetramers containing a single long subunit.

DISCUSSION

In this study, we found that stargazin-mediated trafficking of GluR1 and GluR2 is hindered when CFP or YFP is inserted at the proximal cytoplasmic tail. We also determined that the first 380 amino acids of AMPA receptors (the ATD) are not necessary for stargazin trafficking but this domain has an important role in tetrameric stability of AMPA receptors. FRET analysis demonstrated that a homo-oligomeric population of stargazin exists in the plasma membrane, which could be specifically out-competed by GluR1 protein, but not by high concentrations of CD8, GluR6 or Kv2.1. AMPA receptors with traffickable C-termini interact with stargazin in a close association that permits FRET in both the plasma membrane and the ER network of transfected cells.

The AMPA receptor-stargazin binding site. We propose that stargazin interacts with AMPA receptors via a binding site that is comprised of the AMPA receptor "domain 2" of the ligand-binding core (including the flip/flop region), the transmembrane domains, and the cytoplasmic face including access to the pore. An extracellular interaction with the flip/flop domain is consistent with single-particle electron microscopy experiments that show the primary interaction being near the transmembrane domains (Nakagawa et al., 2005; Nakagawa et al., 2006). Swapping experiments using γ-5 (an inactive, structurally similar protein to stargazin) suggest that only the second stargazin transmembrane domain is an important AMPA receptor contact, and was necessary for maintaining kainate responses (Tomita et al., 2005b). Consistent with our results, it was not a required domain for trafficking. Since our experiments suggest that the primary, specific, intracellular site of interaction with stargazin is not the C-terminus of AMPA receptors, other intracellular sites are implicated. The part of the cytoplasmic tail of stargazin that was found to be essential for AMPA receptor trafficking (up to residue 269, (Tomita et al., 2004))

contains 16 basic residues (and 4 negative residues). Interestingly, the 26 amino acid intracellular domain after M1 of GluR1 contains 8 acidic residues (and 3 positive residues). This cytoplasmic region between M1 and the pore loop may contribute to the stargazin-AMPA receptor interaction necessary for trafficking receptors to the surface. A stargazin interaction with this site may explain how GluR2 R_{607} homo-oligomers, typically retained in the ER (Greger et al., 2002), can form surface expression rings when co-transfected with stargazin.

Our results are consistent with previous studies suggesting that the first extracellular domain of stargazin plays a role in AMPA receptor trafficking (Tomita et al., 2004; Turetsky et al., 2005). The swap of γ-5 in this region still results in a stargazin hybrid that enhances AMPA receptor surface expression, though not as robustly (Tomita et al., 2004). If there are at least two distinct sites of interaction between stargazin and AMPA receptors (one extracellular, and one intracellular) the removal of an extracellular interaction, though not intrinsically necessary for trafficking, would reduce association between the two proteins.

Stargazin enhances trafficking by blocking ER retention. Our data suggest that in order for GluR1 and GluR2 to be trafficked by stargazin, it must have intracellular access to the cytoplasmic face of AMPA receptors (**Figure 2.8**). In contrast, no such cytoplasmic interaction is necessary for subsequent stargazin-mediated modulation of desensitization. The intracellular interaction responsible for stargazin-mediated trafficking may block one or multiple ER retention signals; multiple ER retention signals are consistent with the graded response in current density seen with progressive C-terminal deletions of stargazin (21). The receptor mutant that exemplifies the different moieties of the stargazin-receptor interaction is $R1i_{15}$CFP. Although the kinetics of this channel were modulated by stargazin as well as the kinetics of $R1i_{81}$CFP, stargazin was unable to force the channel to form surface rings. This difference could be explained if $R1i_{81}$CFP interacts with stargazin in the ER while $R1i_{15}$CFP does not (or has a reduced affinity of interaction), or if

association of stargazin in the ER with $R1i_{15}$CFP homo-oligomers does occur, but fails to block any ER retention signals.

Support for the hypothesis that there is an initial interaction between AMPA receptors and stargazin in the ER is lent not only by measuring FRET between stargazin and AMPA receptors in the cytosol but also by experiments in which different glutamate receptor constructs were over-expressed in the presence of stargazin. If there were an initial protein-protein interaction in the ER, we should be able to sequester stargazin in the ER and prevent it from forming surface expression rings. An interpretation of results of this experiment (**Table 3**) is that stargazin can be sequestered in the ER by over-expression of $R1_{81}$CFP but not $R1_{15}$CFP, suggesting not only that association between stargazin and $R1_{15}$CFP occurs preferentially at the surface membrane, but also that multiple stargazin molecules per tetramer traffic AMPA receptors more efficiently. Stargazin is found primarily in the surface membrane and could forego its interaction with AMPA receptors until both proteins reached the plasma membrane. The lower-affinity association may be similar to stargazin's association with calcium channels, which alters the biophysical properties of this voltage-gated channel without influencing its trafficking (Black, 2003). Our hypothesis would predict that stargazin over-expression would result in more association with $R1_{15}$YFP in the ER. The failure of $R1_{15}$YFP to form surface expression rings even when co-expressed with a 1:8 stg ratio is consistent with there being a transmembrane/extracellular association between the two proteins in the ER that does not associate intracellulary to block any retention sites.

Stargazin modulation demonstrates flip/flop isoform differences in channels without the ATD. Although this study did not focus on splice-isoform differences in stargazin trafficking and/or modulation of AMPA receptors, there is evidence that stargazin affects AMPA receptors in an isoform-selective manner (Turetsky et al., 2005). Flip and flop isoforms differ in their kinetic properties and allosteric modulation (Mosbacher et al., 1994; Partin et al., 1996; Koike et al., 2000), so if stargazin is modulating deactivation and/or desensitization through the ligand-binding

core, one might predict that there could be splice isoform differences. Isoform differences may also explain the discrepancy between our data and those of Arai and co-workers, who found that C-terminal deletions of GluR1o resulted in increased rates of deactivation and desensitization (Suzuki et al., 2005). The desensitization kinetics of the GluR1i C-terminal deletions we studied were not significantly different from wild type. Additionally, deletion of 52 amino acids of the C-terminus (equivalent to $R1_{29}$) for GluR1o was shown to prevent stargazin-mediated effects on desensitization and deactivation (Arai and Suzuki, 2005), which is significantly different than what we found with GluR1i.

Our results indicate that the ATD is not necessary for stargazin modulation of desensitization for either the flip or flop isoform. However, stargazin association may alter the stability of the both $GluR2i_{DATD}$ and $GluR4i_{DATD}$ homo-tetramers. $GluR2o_{DATD}$ was not only trafficked effectively to the surface membrane by stargazin, aggresome frequency was decreased with stargazin (**Table 2**). In contrast, the aggresomes increased in size for $GluR2i_{DATD}$ co-transfected with stargazin (**Fig 2.4d**) without changing significantly in frequency. Since GluR2 modulation of desensitization by stargazin is strongly influenced by the flip-flop isoform, this suggests that there could be an interaction between stargazin and the flip/flop region.

Aggresome formation and density may be related to the amount of monomeric and dimeric subunits in the ER. This correlation is in agreement with the aggresome formation observed when we expressed wt GluR2 R_{607} homomers but not $R_{607}Q$ homomers (**Table 2**). R_{607} homomers are mostly in the monomeric or dimeric state in the ER while $R_{607}Q$ homomers have an enhanced proclivity to form tetramers (Greger et al., 2003). It is interesting that stargazin did not alter the number of aggresomes for R_{607}. This result is in agreement with previous work that provides evidence that stargazin binds only to tetramers in the ER and would not affect the dimer-dimer interaction.

Insight into the stoichiometry of the stargazin-AMPA receptor interaction. The finding that GluR1 subunits with differing C-termini could form hetero-oligomers but were different in their

ability to be trafficked by stargazin enabled us to rule out that four stargazin binding sites (1 per subunit) were necessary for stargazin-mediated trafficking. The ability of multiple stargazin molecules to associate with a receptor was confirmed by different stoichiometry-dependent FRET efficiencies (**Figure S2**). Our study of hetero-oligomers leaves open the possibility that stargazin binds to a dimer interface composed of two "sufficient" subunits (2 short: 2 long) or binds to a single "sufficient" subunit (3 short: 1 long). We hypothesize that only one stargazin per tetramer needs to bind to enhance trafficking of the AMPA receptor although more than one association leads to the blockade of more ER retention signals and thus more effective trafficking. The question still remains as to whether there are two stargazin binding sites per tetramer or one for each subunit.

Summary. Our studies bring a new level of resolution to investigate the nature of the interaction between AMPA receptors and stargazin. However, stargazin's contribution to the synapse is complex, in part because of the many unpredicted activities of this protein (see for example, (Price et al., 2005)), and the fact that its actions are activity-dependent (Rouch et al., 2005). An intriguing property of stargazin is that it interacts with both calcium channels and AMPA receptors at the plasma membrane (Kang et al., 2006). It is unclear whether stargazin's trafficking of AMPA receptors from the ER, modulation of AMPA receptor biophysical properties in the plasma membrane, complex-formation with AMPA receptors and calcium channels, or ability to mediate cell-cell adhesion are all regulated by activity and contribute to synaptic plasticity. Additional experiments will be needed to address these important issues.

Acknowledgements: This work was supported by an NIH predoctoral training grant to MAB (NS43115-02) and by R01MH64700 (KMP). The authors thank John Gieser for his help in the production of this manuscript. We thank Drs. Kurt Beam, Nancy Lorenzon and Michael Tamkun for useful discussions and their critique of an earlier version of the paper.

FIGURE LEGENDS

Fig 2.1. Stargazin traffics fluorophore-tagged GluR1 to the plasma membrane. (a) Topology of the AMPA receptor and stargazin (stg) proteins showing the site of fluorophore insertions at the carboxyl termini. Dashed line indicates C-terminal truncation of fluorophore-tagged stargazin. (b) Confocal images of yellow fluorescence in HEK293 cells expressing ($R1i_{81}$YFP, *left*), (stgYFP, *center*) and $R1i_{81}$YFP co-expressed with stg, *right*. Profile intensities (in arbitrary units) along the red line demonstrate that surface expression of GluR1 is markedly enhanced by stargazin. (c) Time constants of desensitization (black bars) measured as the decay in response to a 500 ms pulse of 10 mM glutamate, or deactivation (gray bars) measured as the decay in response to a 1 ms pulse of 10 mM glutamate, for $R1i_{81}$YFP in the absence or presence of stargazin, *left*. Cells co-expressing $R1i_{81}$YFP and stargazin were visually scored as either not having pronounced surface expression (- rings) or having pronounced surface expression (+ rings). Mean current amplitude measured in response to a 500 ms pulse of 10 mM glutamate in the absence or presence of stargazin, with and without surface expression rings, *right*. (*, $p<.05$;**, $p<.01$ comparing stargazin + or – rings to without stargazin; ##, $p<.02$ comparing $R1i_{81}$YFP deactivation with stargazin + or – visible surface expression rings). Inset shows ring formation as a function of increasing concentrations of stargazin cDNA (filled circles), co-transfected with a constant amount (0.2 μg) of $R1i_{81}$YFP. The solid line represents a curve fit with to a logarithmic function extrapolated to 0, $R^2 = .91$.

Fig 2.2. A cytoplasmic interaction between stargazin and GluR1 promotes stargazin modulation of trafficking but is not essential for stargazin modulation of desensitization. (a) Fluorophore-tagged C-terminal deletions of GluR1 (*left*); + or – indicate whether co-expression with stargazin increased surface expression (*right*). Two constructs ($R1i_{2+38}$YFP and $R1i_{15+38}$YFP) have an insertion of a 38 amino acid linker between the receptor and the fluorophore (*thin line*). Note that $R1i_{14}$ does not contain a fluorophore tag. (b) Confocal images and corresponding profile intensities of yellow fluorescence from R1i truncations co-expressed with stgCFP. (c)

Electrophysiological response of R1i truncations to a 500 ms pulse of 10 mM glutamate (black line is response without stargazin, gray line is response with stargazin. Mean current amplitudes plotted on a log scale (d) and desensitization rates (e) of tagged $R1i_{81}$YFP, $R1i_{36}$YFP and $R1i_{15}$YFP, and $R1i_{14}$ expressed with (gray bars) and without (black bars) stargazin. (*, $p< .05$; **, $p<.01$; ***, $p<.005$)

Fig 2.3. The GluR1 cytoplasmic tail does not contain a specific stargazin-binding site. (a) Alignment of the first 14 amino acids of the cytoplasmic tails of the AMPA receptors GluR1-4, and the kainate receptor GluR6, *top*. Shaded areas show identity to GluR1. Below are a series of mutant $R1i_{81}$YFP constructs with the mutations as indicated by the unshaded residues. All constructs formed stargazin-mediated surface expression rings, as indicated with by the +. (b) Confocal images of fixed, unpermeabilized HEK293 cells expressing FLAG-R4i or FLAG-$R4i_{DCTD}$ without or with stargazin. Cells were labeled with a FLAG antibody and visualized with Alexa Fluor 568. All fluorescent images were acquired at the same gain; red pseudo-color represents intensity saturation. A smaller DIC image is shown for each field of cells.

Fig 2.4. The amino-terminal domain (ATD) is not essential for stargazin modulation of trafficking or desensitization. (a) Fluorophore-tagged N- and/or C-terminal deletions of GluR2 (*left*); + or – indicate whether co-expression with stargazin increased surface expression as determined by confocal microscopy (*right*). (b) Confocal images of $R2i_{DATD46}$YFP/stg (*left)* and $R2o_{DATD46}$YFP/stg (*right)* demonstrating the formation of surface rings and aggresomes (arrows). (c) Bar graphs show mean time constant of desensitization (*left)* and mean current amplitudes on a log scale (*right)* of $R2o_{DATD46}$YFP and $R2i_{DATD}$ without (black) or with (gray) stargazin. Inset showing glutamate-evoked currents; red line is without stargazin and black line is with, vertical scale bar is 200 pA, horizontal scale bar is 60 ms. (***, $p<.001$) (d) Representative images of cells co-transfected with ATD-deleted receptors and stargazin. Panels 1, 3, and 5 are confocal images acquired at a 652 amplifier gain setting and 2, 4, and 6 are the same field acquired at a 237 amplifier gain setting to permit visualization of only the aggresomes. Images 1 and 2 are cells

transfected with GluR2i$_{DATD46}$YFP (no aggresomes), images 3 and 4 are cells co-transfected with R2i$_{DATD46}$YFP/stg (large aggresomes), and images 5 and 6 are cells co-transfected R2o$_{DATD46}$YFP/stg (no aggresomes). Red pseudo-color represents intensity saturation.

Fig 2.5. Fluorescence resonance energy transfer (FRET) suggests stargazin self-assembly. (a) Photobleaching of stgCFP and stgYFP co-transfected into HEK293 cells (1CFP:4YFP). Upper two panels demonstrate CFP and YFP emission prior to photobleaching; lower two panels show that after selective YFP photobleaching, stgCFP emission is enhanced. (b) Confocal images of green fluorescence from 1 μg stgGFP transfected into HEK293 cells (*left*) and green fluorescence arising from a 0.4 μm fluorescent bead (*right*) measured by the same settings as the cells (the image of the bead was then digitally magnified for clarity). CFP and YFP have a Forster radius of about 50 Å, so the maximum distance these fluorophores could be apart and still transfer energy is 100 Å. By this reasoning, 10^4 molecules/μm^2 would be necessary to get FRET from overcrowding of the membrane. Imaging the beads at the lowest setting possible yielded a maximum detection limit before saturation of 820 stargazin molecules per μm^2. Approximately 50% of the imaged cells were not saturated. If the brightest cells were even twice the detection limit at 1640/μm^2, this would still fall short of the 10,000/μm^2 needed. (c) Mean membrane FRET efficiencies (E)=1-($I_{CFPpre}/I_{CFPpost}$) arising from stargazin self-assembly in HEK293 cells with varying input ratios and total DNA concentrations (0.1 -1.0 μg); in all cases, the FRET interaction between stargazin molecules is significantly greater than control ($p<.03$).

Fig 2.6. Stargazin assembly with GluR1i is a specific interaction. (a) The FRET efficiency of self-assembled stargazin molecules at the membrane (1 stgCFP:1 stgYFP) is competed when co-transfected with excess R1i in HEK293 cells (1:1:20 or 0.1:0.1:2 in μg), but not by CD8, Kv2.1 or GluR6 (1:1:20 or 0.1:0.1:2). (b) Membrane FRET efficiency between stargazin molecules (.07 μg stgCFP:0.13 μg stgYFP) co-transfected with 0.5, 1.0, or 2.0 μg of R1i. (c) Confocal images of (.07 μg stgCFP:0.13 μg stgYFP) before (red) and after stgYFP photobleach (blue) with corresponding profile intensities. (d) Same interaction as (c) but competed with 2 μg of R1i. (*,

p< .05; **, p<.005; ***, p <.001). (e) Confocal images of a HEK293 cell co-transfected with $R1i_{81}$CFP and stgYFP, pre and post photobleaching of YFP (*left*). Confocal images of HEK293 cells co-transfected with $R1i_{15}$CFP and stgYFP pre and post photobleaching of YFP (*right*).

Fig 2.7. Hetero-oligomerization can rescue C-terminal deletions with trafficking defects. (a) Confocal images of cyan and yellow fluorescence from HEK293 cells expressing $R1i_{15}$ or $R2o_{16}$, with either longer form of R1i or R2o (1 shorter:1 longer:2 stg). In all cases, $R1_{15}$ and $R2_{16}$ co-transfected with stargazin without a longer form had failed to form surface expression rings (Figure 2 and data not shown). (b) The ratio of mean membrane fluorescence intensity/ mean cytosol fluorescence intensity was compared between two different constructs ("A", constructs in the left column; or "B", constructs in the right column) that could either be independently trafficked by stargazin or required co-expression of a longer form to form rings. Two constructs that could independently form surface expression rings with stargazin had approximately equal amounts of membrane:cytosolic intensity, whereas short forms co-expressed with long forms were significantly less and were trafficked ~75% as well as the long forms. (*, p< .05 for both controls; ■, p< .05 compared to $R1i_{46}$C + $R2o_{46}$Y). (c) Membrane FRET efficiency between $R1i_{15}$ and $R1i_{46}$ was compared to cytosolic FRET efficiency using a 1CFP:1YFP:2stg or 0.2CFP:0.8YFP:2stg ratio between tagged $R1i_{15}$ and $R1i_{46}$.

Fig 2.8. Model of stargazin modulation of trafficking versus desensitization of $R1i_{15}$YFP and $R1i_{81}$YFP. Shown is a model that assumes that stargazin binding occurs at both dimer interfaces of the tetrameric channel; our data would also be consistent with a model in which stargazin binds individual subunits within the tetramer. In the ER stargazin (red) associates with higher affinity to the dimer interface of the $R1i_{81}$YFP AMPA receptor tetramer (magenta, with an extended tail showing the yellow YFP attachment) than to the dimer interface of the $R1i_{15}$YFP AMPA receptor (magenta, with a minimal tail showing the yellow YFP). The thickness of the magenta arrows correlates with the hypothesized relative affinities; the lower affinity arises due to some steric hindrance by the fluorophore. Known ER retention signals are shown in black; one is located in

the proximal cytoplasmic tail and the other within the pore loop. Association between stargazin and $R1i_{81}$YFP in the ER blocks at least one retention signal, hypothesized to be the pore loop. When more than one stargazin associates with AMPA receptors in the ER more retention signals are blocked, permitting greater exodus from the ER to the surface membrane (blue). This pathway represents stargazin modulation of trafficking, which is sensitive to the C-terminus. The few $R1i_{15}$YFP channels that reach the surface membrane without the aid of stargazin can associate with stargazin (red arrow) despite the lowered affinity because of the excess amount of stargazin in the surface membrane. This pathway represents stargazin modulation of desensitization and deactivation, which is relatively independent of the nature of the C-terminus.

SUPPLEMENTAL FIGURE LEGENDS

Fig S1. Similarity of the C-termini of AMPA receptors and the kainate receptor GluR6. Alignment of amino acid sequences between the M4 domain and the C-terminus are shown. Sites of deletions are indicated with arrows ($R1_{15}$, $R1_{36}$, $R1_{46}$, $R2_{16}$, and $R2_{46}$). Known protein-interacting sites (4.1, SAP97/RIL, NSF, GRIP, ABP and PICK1) are boxed and shown in blue (Malenka, 2003; Malinow, 2003). An ER retention sequence is shown in green (Greger et al., 2002). Serine residues phosphorylated by PKC or PKA are shown in red (Malinow and Malenka, 2002). A palmitoylated cysteine is shown in orange (Hayashi et al., 2005).

Fig S2. Multiple stargazin molecules can bind to GluR1i in the plasma membrane. (a) FRET between stargazin molecules bound to GluR1i increases significantly (from 3.9±1.1% to 9.1±2.0%, p=.01) as the relative concentration of acceptor (stgYFP) is increased from 1:1 to 1:4 respectively while keeping the total stargazin concentration the same. Ratios used in μg for 1:1 and excess channel (0.1 stgCFP: 0.1 stgYFP: 2 R1i) and 1:4 and excess channel (0.04 stgCFP: 0.16 stgYFP: 2 R1i). The ratio of 1:2 had an intermediate value of 5.8±1.1%. This is consistent with the interpretation that multiple stargazin molecules can bind to each GluR1i receptor complex, and there are at least two stargazin binding sites per tetrameric complex. Although there was a trend, no significant differences were seen between FRET efficiencies with stargazin alone

at 1:1 (10.6±1.4%), 1:2 (16.2±2.8%), 1:4 (14.3±2.3%) or with GluR6 at 1:1 (8.5±1.6%), or 1:4 (12.0±3.0%). (b) A model of different stgCFP and stgYFP ratios with or without excess AMPA receptor. At a 1:1 stgCFP/stgYFP ratio with no channel (*top*) it is expected that if stargazin (red) can form a dimer, some dimers will be composed of 1 CFP and 1 YFP stargazin and thus FRET (an interaction denoted by a black arrow from CFP to YFP), but some dimers will consist of 1 CFP and 1 YFP stargazin which would not FRET. We also suggest that there are some CFP and YFP stargazin monomers in the membrane. If the ratio is changed to 1:4 stgCFP to stgYFP almost all CFP molecules bound in a dimer or multimer would be in a complex with at least another YFP and thus the FRET efficiency measurement would increase. Our interpretation of the data is that a hetero-oligomeric population of 1 and 2 stargazin molecules per AMPA receptor tetramer (green), as well as stargazin monomers that did not bind to R1i on their way to the plasma membrane, may be found (*middle, bottom*). Changing the ratio of stgCFP: stgYFP to 1:4 while keeping the total stargazin concentration the same should drive the majority of channels that have 2 stargazin molecules bound to be either CFP and YFP or YFP and YFP; the latter would not affect FRET measurements.

TABLES

Table 1. C-terminal mutations of GluR1 and GluR2 alter stargazin-mediated trafficking. The constructs imaged with confocal microscopy after co-expression with excess stargazin are shown in the left column, the corresponding percentage of cells forming stargazin-mediated rings is shown in the right column. The raw data (actual number of cells with rings/total cells counted) for each construct is shown in parentheses.

C-terminal truncation	*Cells with surface expression (%)*
GluR1	
$R1i_{81}$YFP	12 (26/218)
$R1o_{81}$YFP	4 (7/178)
$R1i_{36}$YFP	9 (22/241)
$R1i_{15}$YFP	0 (0/1000)
$R1i_{15+38}$YFP	2 (3/129)
$R1i_{2}$YFP	0 (0/200)
$R1i_{2+38}$YFP	<1 (2/243)
$R1i_{7}$(C to L)	0 (0/200)
$R1i_{7+38}$(C to L)	28 (36/130)
$R1i_{81}$(YKS to FQA)YFP	36 (48/133)
GluR2	
$R2i_{46}$YFP (R607Q)	7 (6/90)
$R2i_{46}$YFP (R607)	9 (9/101)
$R2i_{16}$YFP (R607Q)	0 (0/200)
$R2o_{16}$YFP (R607Q)	0 (0/200)

Table 2. ATD deletions promote aggresome formation in the absence or presence of stargazin. The constructs tested are indicated in the left column, and the percentage of cells forming aggresomes in the right column. The raw data (actual number of cells with aggresomes/total cells counted) for each condition is shown in parentheses. Stargazin was co-expressed in a 1:2 stg ratio (in μg) and the total concentration of AMPA receptor DNA was not changed.

Receptor Constructs	*Cells with aggresomes (%)*
$R2i_{46}$YFP (R607Q)	~ 0
$R2i_{46}$YFP (R607Q)+stg	~ 0
$R2i_{46}$YFP (R607)	17 *(25/148)*
$R2i_{46}$YFP (R607)+stg	15 *(15/101)*
$R2i_{46DATD}$YFP (R607Q)	70 *(97/139)*
$R2i_{46DATD}$YFP (R607Q)+stg	74 *(105/142)*
R2oDATD $_{46}$YFP (R607Q)	62 *(110/178)*
R2oDATD $_{46}$YFP (R607Q)+stg	40 *(51/126)*
$R1i_{2+38}$YFP+stg	2 *(6/243)*

Table 3. Stargazin surface expression is reduced by $R1i_{81}CFP$. Quantification of the cells forming stgYFP expression rings when stgYFP was expressed alone or in the presence of channel (0.15 stg: 2 μg channel). Channel combinations are indicated in the left column, with the percentage of cells with pronounced stgYFP rings in the right column. The raw data (actual number of cells with rings/total cells counted) for each condition is shown in parentheses.

Co-expressed proteins	*Cells with stgYFP surface expression (%)*
stgYFP	82 *(97/119)*
+ GluR6	76 *(41/54)*
+ $R1i_{15}CFP$	73 *(24/33)*
+ $R1i_{81}CFP$	44 *(25/57)*

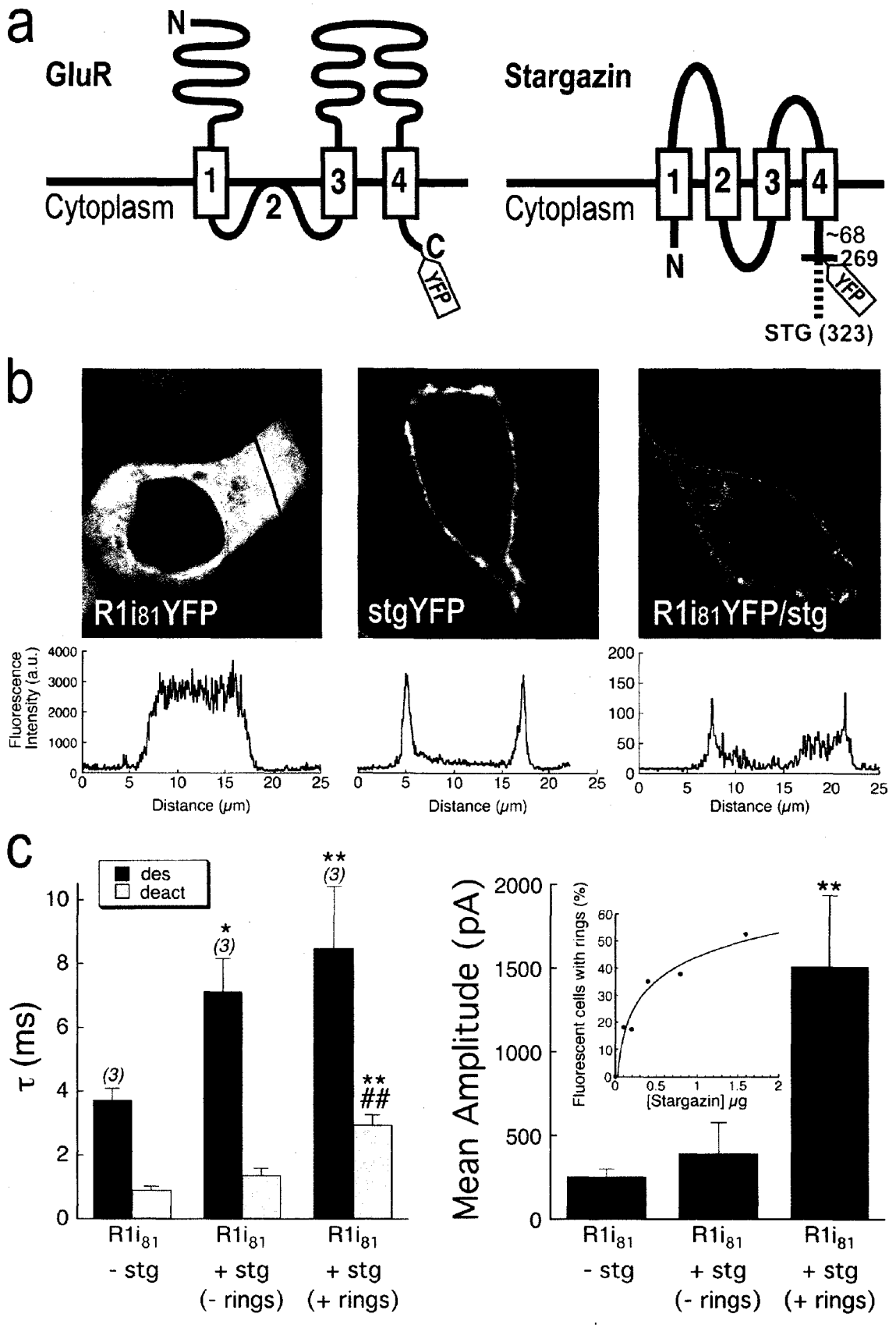

Figure 2.1

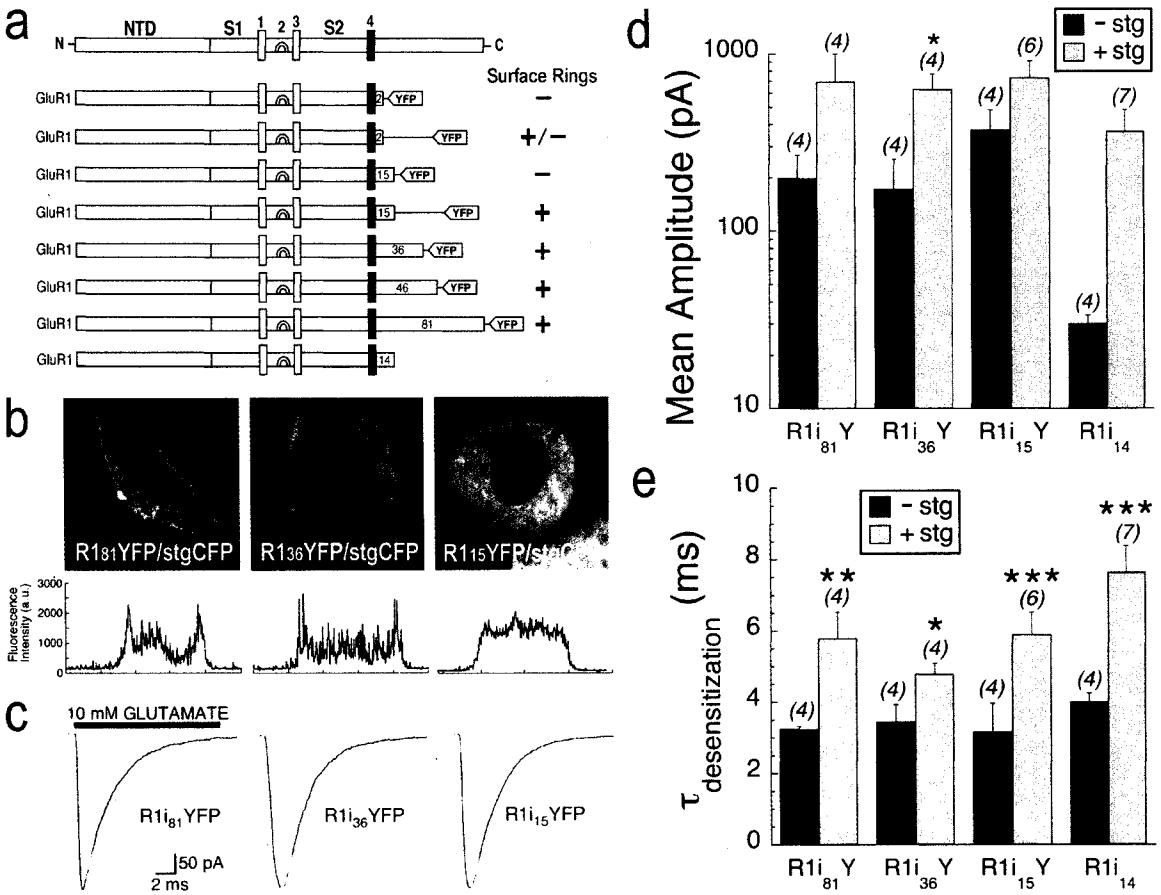

Figure 2.2

a

															Surface Rings
GluR1	**E**	**F**	**C**	**Y**	**K**	**S**	**R**	**S**	**E**	**S**	**K**	**R**	**M**	**K**	
GluR2	**E**	**F**	**C**	**Y**	**K**	**S**	**R**	A	**E**	A	**K**	**R**	**M**	**K**	
GluR3	**E**	**F**	**C**	**Y**	**K**	**S**	**R**	A	**E**	**S**	**K**	**R**	**M**	**K**	
GluR4	**E**	**F**	**C**	**Y**	**K**	**S**	**R**	A	**E**	A	**K**	**R**	**M**	**K**	
GluR6	**E**	**F**	L	**Y**	**K**	**S**	**R**	K	N	N	D	V	E	Q	
R1i$_{36}$4.1 mut	**E**	**F**	**C**	**Y**	**K**	**S**	S	**S**	**E**	**S**	S	S	**M**	**K**	+
R1i$_{813}$C➔L	**E**	**F**	L	**Y**	**K**	**S**	**R**	**S**	**E**	**S**	**K**	**R**	**M**	**K**	+
R1i$_{819}$E➔A	**E**	**F**	**C**	**Y**	**K**	**S**	**R**	**S**	A	**S**	**K**	**R**	**M**	**K**	+
R1i$_{8113}$M➔A	**E**	**F**	**C**	**Y**	**K**	**S**	**R**	**S**	**E**	**S**	**K**	**R**	A	**K**	+
R1i$_{8114}$K➔A	**E**	**F**	**C**	**Y**	**K**	**S**	**R**	**S**	**E**	**S**	**K**	**R**	**M**	A	+
R1i$_{7Linker}$3C➔L	**E**	**F**	L	**Y**	**K**	**S**	**R**								+
R1i$_{81}$FQA mut	**E**	**F**	**C**	F	Q	A	**R**	**S**	**E**	**S**	**K**	**R**	**M**	**K**	+

b

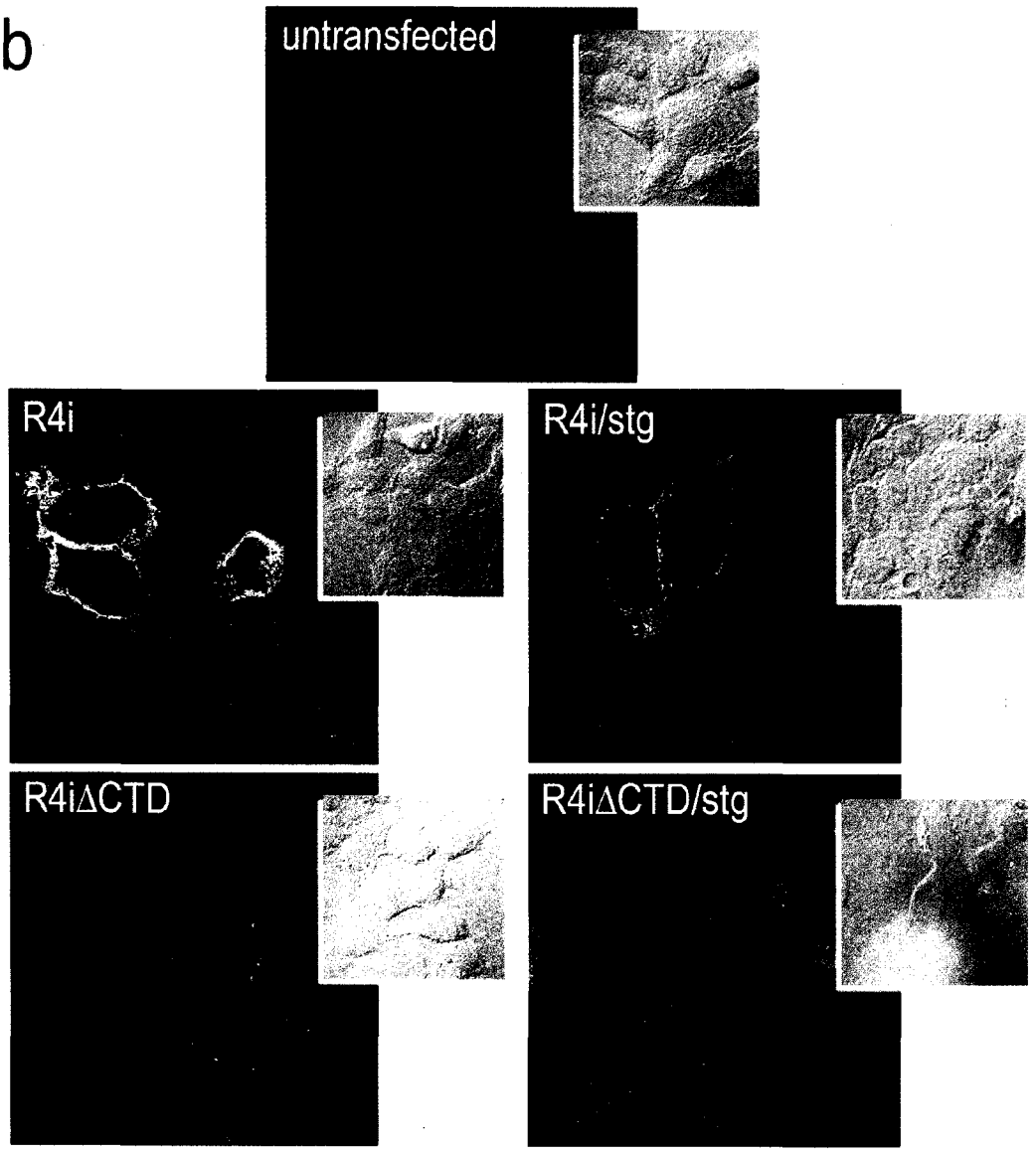

Figure 2.3

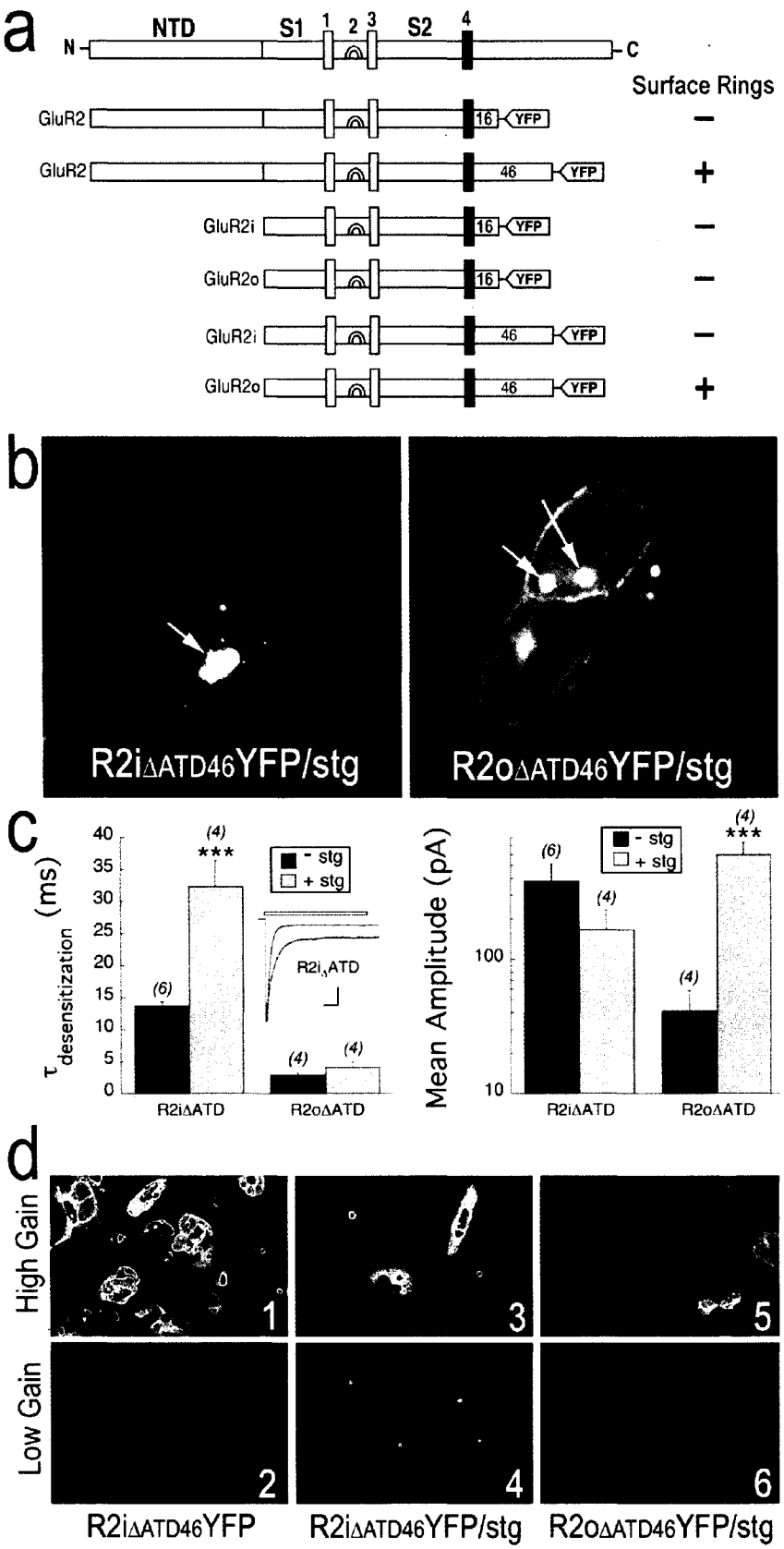

Figure 2.4

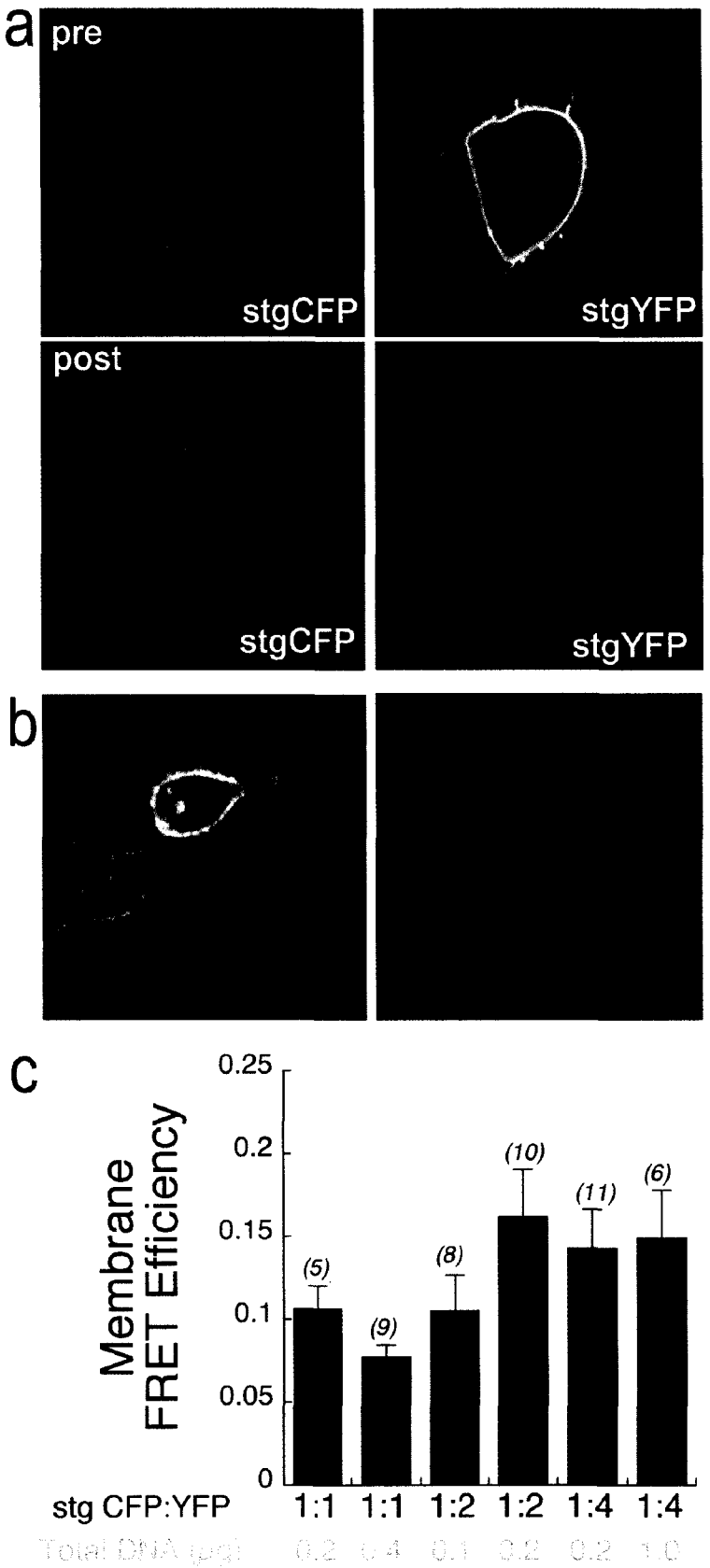

Figure 2.5

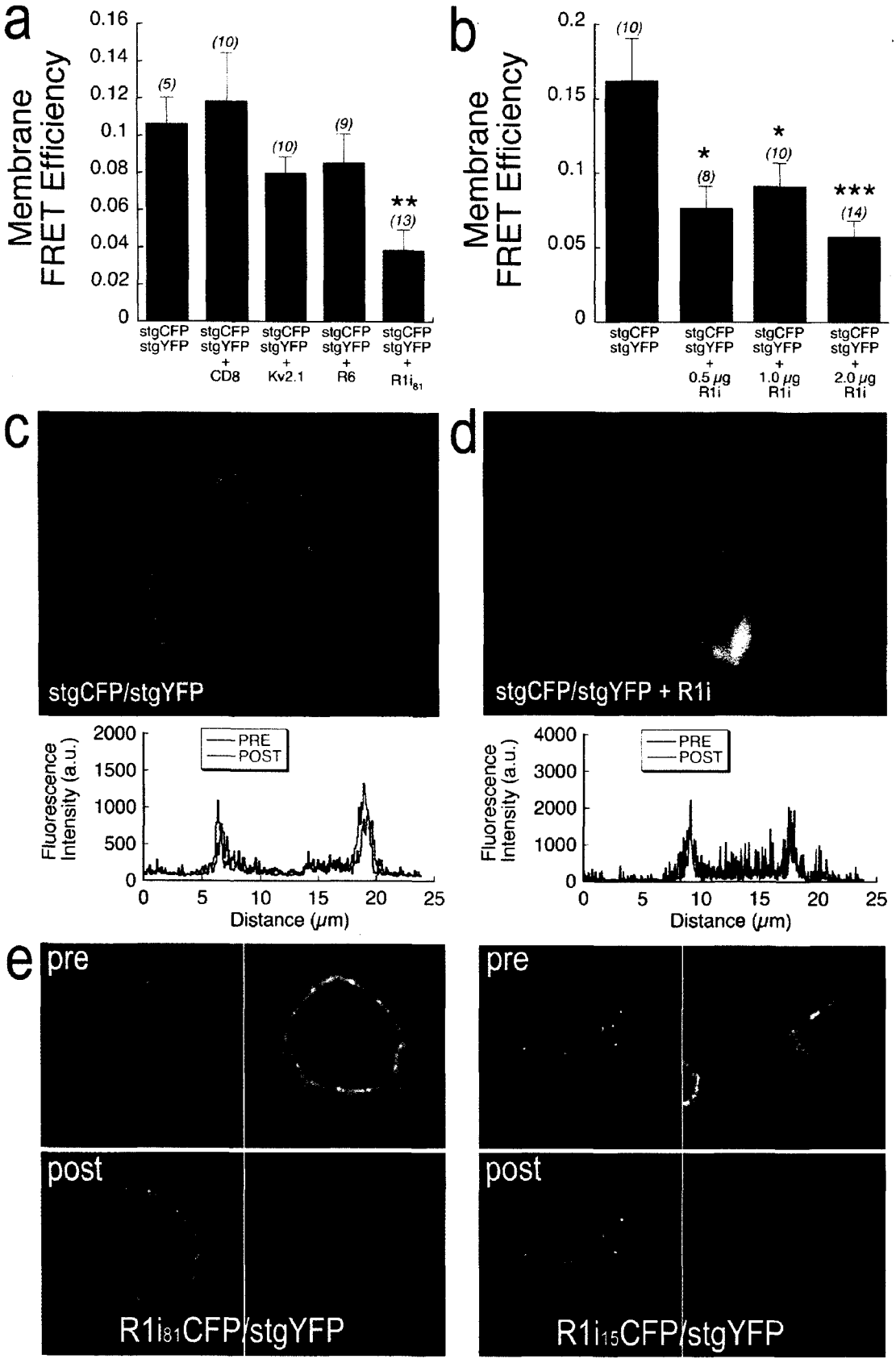

Figure 2.6

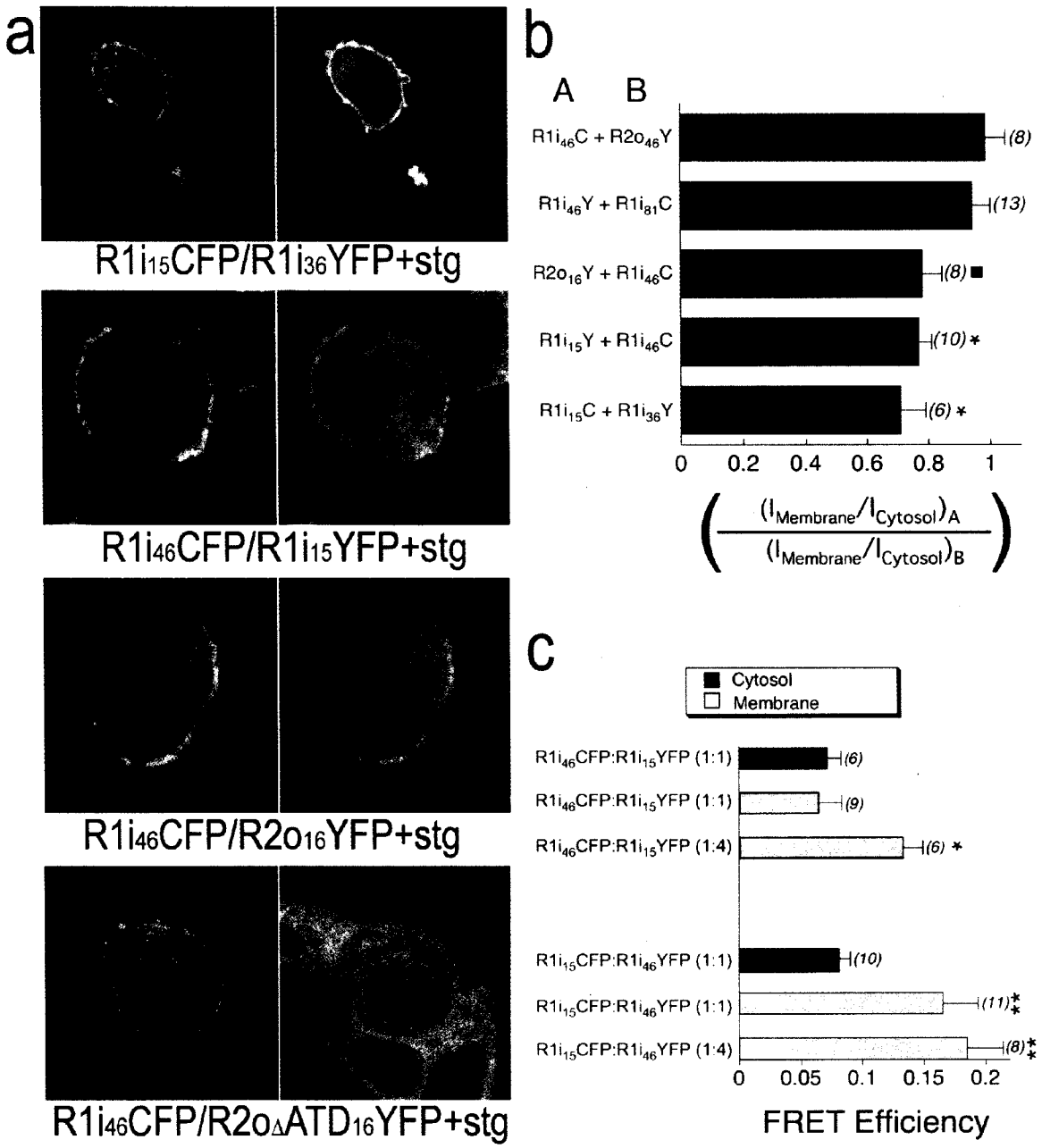

Figure 2.7

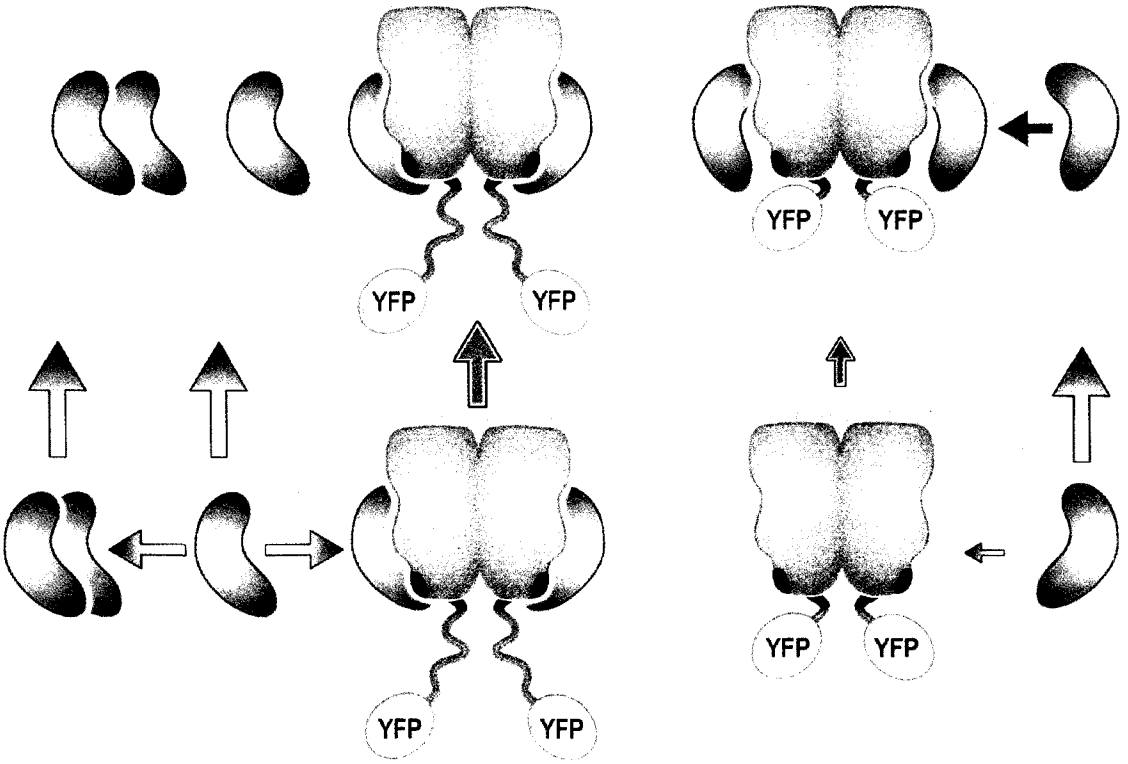

Figure 2.8

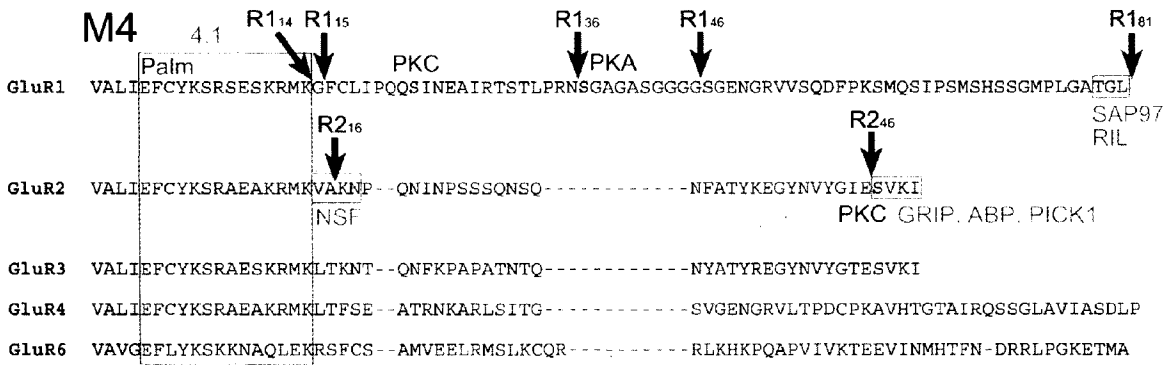

Figure 2.S1

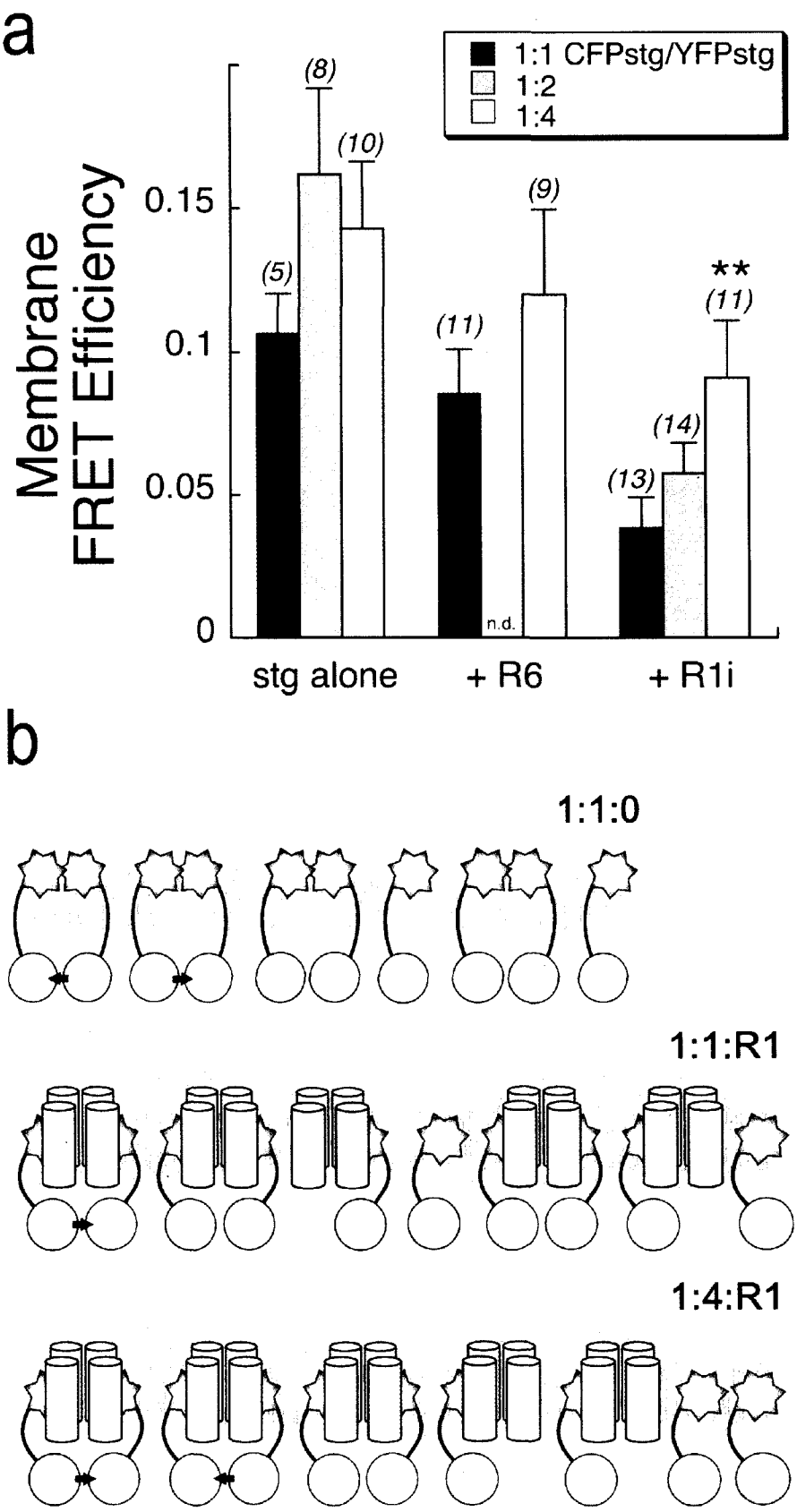

Figure 2.S2

Chapter III: THE RELATIONSHIP BETWEEN CLEFT-CLOSURE AND GATING OF THE AMPA RECEPTOR BINDING DOMAIN

MATTHEW A. BEDOUKIAN AND KATHRYN M. PARTIN

Dept. of Biomedical Sciences, Colorado State University, Fort Collins, CO 80521

ABSTRACT

AMPA receptors bind glutamate extracellularly to gate an ion channel pore in the plasma membrane. Insight into the structure and function of the AMPA receptor ligand-binding core (LBC) has led to a model that relates structure to function: full agonists permit complete closure of the LBC and this translates to a relatively high probability of channel opening, whereas partial agonists do not permit full LBC-closure and concomitantly result in a lower probability of channel opening. Here we test this model using two different length homobifunctional crosslinkers on a functional ion channel, GluR2o. The longer crosslinker reduced current amplitude to a greater extent than did the shorter crosslinker, consistent with the positive correlation between extent of cleft closure and gating. In addition, these crosslinked channels were modulated more efficaciously than uncrosslinked channels by CX546, a modulator that slows both desensitization and deactivation.

INTRODUCTION

AMPA (alpha-amino-3-hydroxy-5-methyl-isoxazole-4-propionate) receptors, a subtype of ionotropic glutamate receptors, are expressed at the postsynaptic membrane of neurons where they mediate rapid excitatory synaptic transmission. Native AMPA receptors are hetero-oligomers composed of four subunits (GluR1-4). Each subunit is a large, complex transmembrane protein comprised of the amino terminal domain (ATD), the ligand-binding core (LBC), the membrane segments (3 transmembrane and 1 re-entrant pore loop), and a cytoplasmic tail. A crystal structure of the ligand-binding core (LBC) of the GluR2 flop (o) receptor has been solved with and without glutamate, AMPA, kainate, quisqualate, and other agonists. From comparative studies of the apo and holo forms of the LBC, specific inferences about the relationship between ligand-binding and channel gating have been proposed.

The LBC is comprised of domain 1 (D1) and domain 2 (D2) and can be thought of as a "clamshell" because upon ligand-binding, a rotation of D2 towards D1 occurs. This conformational transition results in residues from D2 moving >7 Å closer to D1 when, for example, glutamate occupies the binding cleft. When the LBC forms crystallized dimers, the hinges form the dimer interface; as a result, the movement of D2 from one subunit towards D1 of the same subunit concomitantly may be seen as its movement away from D2 of the other subunit. Thus, cleft closure of dimers of the LBC, results in the atomic distance between D2's of two subunits to increase, while the distance between D1 and D2 decreases. Although the ligand-binding constants of the LBC recapitulate those of the intact receptor, the soluble LBC is substantially different than the intact structure. Specifically, a GlyThr linker connects the two domains, whereas in a functional channel the two domains are connected via membrane domains. The GT linker thus leaves the LBC untethered, and it could be argued that movements seen in the crystal structure may not represent comparable movements in the intact receptor.

However, an elegant study of various partial agonists strongly supports a model that directly relates LBC cleft-closure with agonist efficacy. Agonists that allow full cleft closure (such as AMPA and quisqualate) allow large currents, consistent with a large open probability, whereas agonists that through steric clashes at the cleft do not permit full cleft closure permit smaller currents, consistent with a relatively lower open probability. The closing of the clamshell thus appears to correlate with an increase in intra-dimer separation distance in D2 that may translate to an opening of the pore (Jin et al., 2003). More recently, fluorescence resonance energy transfer (FRET) has been used to measure cleft closure of a soluble LBC, thereby alleviating concerns that cleft-closure was an artifact of crystallization (Ramanoudjame et al., 2006). This study measured state-dependent conformational changes with glutamate and the partial agonist kainate and concurred that the degree of cleft closure, as measured by a FRET interaction, correlated to the degree of channel activation.

The present study uses a functional approach to determine the importance of conformational changes of the LBC. Here, two different length homobifunctional crosslinkers ($BM[PEO]_3$ (1,11-bis-maleimidotriethyleneglycol) and $BM[PEO]_2$ (1,8-bis-maleimidotriethyleneglycol) are used to inhibit cleft closure of the LBC of intact GluR2o. The longer crosslinker ($BM[PEO]_3$, 17.8 Å spacer arm) significantly reduced current amplitude more than the shorter crosslinker ($BM[PEO]_2$, 14.7Å spacer arm). Crosslinked GluR2o channels were potentiated by a positive allosteric modulator that slows both desensitization and deactivation (CX546), but still had significantly smaller current amplitudes than channels that were not crosslinked. These studies offer new evidence that the extent of LBC domain closure in intact receptors translates to the probability of channel opening.

MATERIALS AND METHODS

Constructs. GluR2 flop (o) was provided by Dr. Peter Seeburg (Max Planck Institute for Medical Research, Heidelberg, Germany). These studies used the inwardly rectifying pore mutant GluR2 ($R_{607}Q$) to increase channel conductance. The channel was inserted into a pGEM expression vector. All point mutations were done using QuikChange II XL Site-Directed Mutagenesis Kit or the QuikChange Multi Kit (Stratagene, La Jolla, CA). DNA mutations were confirmed by sequencing (Macromolecular Resources, Fort Collins, CO).

Oocyte Expression. Capped mRNA was synthesized in vitro from linearized AMPA receptor cDNA T7 polymerase (mMessage Machine; Ambion, Austin, TX). Oocytes were surgically obtained from adult *Xenopus laevis* (Nasco, Fort Atkinson, WI) anesthetized by immersion in 3% Tricaine (Sigma, St. Louis, MO) for 15 min and then placed on an ice bed. Animal care and surgical procedures conformed to institutional Animal Care and Use Committee standards and practices and were carried out in accordance with the National Institutes of Health's *Guide for the*

Care and Use of Laboratory Animals. Harvested ovarian lobes were cut into small pieces and incubated with 1.5 mg/ml collagenase A (Roche Diagnostics, Indianapolis, IN) in calcium-free buffer (82.5 mM NaCl, 2 mM KCl, 1 mM $MgCl_2$, and 5 mM HEPES, pH 7.5) for 90 min at room temperature on a Nutator (Clay Adams, Parsippany, NJ). After thorough washing [88 mM NaCl, 1 mM KCl, 2.4 mM NaHCO3, 0.3 mM $Ca(NO3)_2$, 0.41 mM $CaCl_2$, 0.82 mM $MgSO_4$, and 15 mM HEPES, pH 7.6], selected eggs were stored at 18°C and injected within 24 hrs. RNA (46 nl) at 0.5 to 1.0 $\mu g/\mu l$ was injected into the oocyte cytoplasm with the use of a Drummond positive-displacement injector using micropipettes pulled to a diameter of <10 μm.

Crosslinking. After injection of cRNA, the Xenopus Oocytes were incubated for 3 days between 18-20°C. Homobifunctional crosslinkers $BM[PEO]_3$ (1,11-bis-Maleimidotriethyleneglycol) and $BM[PEO]_2$ (1,8-bis-Maleimidotriethyleneglycol) were purchased from Pierce Biotechnology (Rockford, IL). These constructs have increased water solubility and react predominantly with –SH (sulfhydryl) groups at pH 6.5-7.5 and form stable thioether linkages. $BM[PEO]_3$ was easily dissolved in Bath's solution at 37°C for <10 min, while $[PEO]_2$ required more rigorous mixing. Dissolving $BM[PEO]_2$ initially with DMSO greatly increased solubility and comprised no more than 2% of the total solution. The final pH of the crosslinking solution was between 7.3 to 7.45 and added to the oocytes for 45 min at 18-20°C. All crosslinking solutions were made fresh and added to the oocytes within 10 min of being made to prevent robust hydrolysis of the maleimide group. 50 mM cysteine (Sigma, Saint Louis, Missouri) was added for 10 min at room temperature to quench the reaction. All electrophysiology was done within 3 hrs after crosslinking.

Oocyte Electrophysiology. Experiments on oocytes were performed under two-electrode voltage clamp (Axoclamp 2A or GeneClamp 500B; Axon Instruments, Union City, CA) at a holding potential of -60 mV in a continuously perfused chamber of approximately 5 μl volume. The extracellular solution was calcium-free [88 mM NaCl, 1 mM KCl, 2.4 mM $NaHCO_3$, 0.3 mM

$Ba(NO3)_2$, 0.41 mM $BaCl_2$, 0.82 mM $MgSO_4$, and 15 mM HEPES, pH 7.6], to which was added glutamate (300 μM), or 300 μM glutamate and 500 μM CX546. Both drugs were purchased from Sigma/RBI (Natick, MA). Solution exchange was controlled via an electronic BPS-8 valve control system (ALA Scientific, Westbury, NY) and electronic valves (The Lee Co., Westbrook, CT). Drugs were applied for 60 s. Currents were measured at steady-state levels at the end of each application of drug. Electrodes of 0.1 to 3 M resistance were filled with 1 M CsCl and 5 mM EGTA. Current responses were filtered at 100 Hz (Cygnus Technology, Delaware Water Gap, PA) and acquired by a Power Macintosh 7600/132 computer with an ITC-16 (InstruTECH Corporation, Port Washington, NY) interface under control of the program Synapse (Synergistic Research Systems, Silver Spring, MD).

Statistical significance was determined with an unpaired Student's t-test. Data are reported as mean ± SEM

RESULTS AND DISCUSSION

The generation of functional mutants for crosslinking.

A functional GluR2o cysteine-"null" mutant was made, to allow us to insert reactive cysteine residues at critical positions in D1 or D2 of the LBC cleft. The cysteine-null channel lacked the first 380 amino acids (the ATD) of the mature protein similar to GluR4-ATD (Pasternack et al., 2002) in order to delete 5 endogenous cysteine residues. There are 7 remaining cysteine residues in this channel but only one is accessible. The 1FTJ crystal structure illustrates that only C_{56} is accessible (Sun et al., 2002b). This cysteine was converted to a valine ($C_{436}V$ of the mature channel). The null-cysteine receptor was functional, and served as the template for the synthesis of the cleft mutations. Using the 1FTJ (GluR2o with glutamate) and 1FTO (GluR2o without glutamate) crystal structures as a model, several residues that could be designated "cleft"

residues with appropriate distances for crosslinking were mutated to cysteine. These residues were $A_{476}C$, $D_{477}C$, and $T_{478}C$ in D1 and $E_{699}C$ and $S_{701}C$ in D2. $T_{478}C$ was the only non-functional mutant, and was not considered further. Functional, double mutant pairs, introducing cysteines in both domains, that were studied include: $E_{699}C$ with $A_{476}C$, $E_{699}C$ with $D_{477}C$, and $S_{701}C$ with $A_{476}C$ (**Figure 3.1**). $S_{701}C$ with $D_{477}C$ was not functional and is not considered further.

$BM[PEO]_3$ reduces current amplitude more than $BM[PEO]_2$.

The strategy of the present study was to compare the current amplitudes of GluR2o in the absence and presence of different crosslinkers that would react with both introduced cysteines at the cleft, and by virtue of their differing spacer arm lengths would thereby permit either less or more cleft closure. The hypothesis being tested predicts that the longer crosslinker would result in smaller current amplitudes, while the shorter crosslinker would allow the cleft to close more tightly by a couple angstroms, thus resulting in larger current amplitudes. We focused on the cysteine-null double-mutant with $A_{476}C$ in D1 with $S_{701}C$ in D2 (**Figure 3.1b**). An example current recording with and without modulator is shown in **Figure 3.2**. Crystal structure data predicts that these two residues (the A and the S) are initially 24.29 Å apart in the apo (open) state and 16.44 Å apart in the glutamate bound state while the cysteine mutants are 15.83 Å apart in the glutamate bound state (**Figure 3.1c**) and should be in the appropriate range for a 17.8 Å crosslinker to bind across the cleft (**Figure 3.1c**). The non-permeable crosslinkers $BM[PEO]_3$ (with an 11-atom spacer arm) and $BM[PEO]_2$ (with an 8-atom spacer arm) are 17.8 and 14.7Å, respectively.

The mean current amplitude of GluR2o ($A_{476}C$ + $S_{701}C$) evoked by 300 μM L-glutamate without crosslinker was 145 ± 28 nA (n = 9) (**Figure 3.3a**). After treatment of oocytes expressing the same channel with 300 μM $BM[PEO]_3$, the mean glutamate-evoked response was 39 ± 7 nA (n = 8, p = .003). In contrast, treatment with 200μM $BM[PEO]_2$ had less of an effect on mean current amplitude, reducing it to 71 ± 20 nA (n = 5, p =.11 compared to no crosslinker).

Similarly, treatment with 400 μM $BM[PEO]_2$ reduced mean current amplitude to 83 ± 35 nA (n=7, p=.21 compared to no crosslinker). Thus, crosslinking the inter-cleft cysteines with the longer spacer arm (less cleft closure) resulted in reduced mean current, most probably reflecting a reduction in open channel probability.

CX546 potentiates current amplitude with crosslinkers.

CX546 is a congener of aniracetam and CX614, which have been proposed to enhance AMPA receptor activity through a direct action that stabilizes the closed-cleft conformation. Thus, it was possible that the crosslinked channels would occlude modulation by CX546, since they also presumably stabilize the closed-cleft conformation. Therefore, the effect of CX546 on the activity of GluR2o ($A_{476}C$ + $S_{701}C$) was studied in the presence of the two crosslinkers (**Figure 3.3b**). As expected, CX546 potentiated the amplitude of non-crosslinked channels (8.8-fold) to 1062 ± 126 nA (n = 9). 300 μM $BM[PEO]_3$ with CX546 potentiated amplitude 12.6-fold to 491 ± 86 nA (n=8). Thus, potentiation with modulator is greater than control (p=.007) whereas current amplitude is less than control (p=.003). The shorter crosslinker $BM[PEO]_2$ at 200 μM with CX546 potentiated amplitude 11.5-fold to 701 ± 116 nA (n=5); potentiation with modulator is greater than control (p = .20) whereas current amplitude is less than control (p=.10). The same crosslinker at 400 μM increased current amplitude 15.3-fold to 609 ± 117 nA (n=7); thus, current amplitude is less than control, (p=.03) and potentiation with modulator is greater than control (p=.16).

Another intriguing result that still needs to be further explored is that crosslinked channels have the potential to be opened by application of only CX546 if the channels have previously been exposed to glutamate (data not shown). CX546 (in the absence of agonist) was in all cases unable to open channels without prior application of glutamate while 2/9 recordings showed the phenomenon of CX546-evoked channel opening after prior glutamate exposure. This finding is consistent with glutamate being able to access the LBC and having an increased affinity

once bound. This may be a result of the crosslinker stabilizing the closed cleft and inhibiting glutamate unbinding.

SUMMARY

This study provides evidence that the degree of LBC domain closure in a functional ion channel correlates to an increase in current amplitude, consistent with previous studies on the isolated LBC. The results suggest that the homobifunctional crosslinker $BM[PEO]_3$ hinders domain closure more than $BM[PEO]_2$ and is consistent with the model that the degree of cleft closure is related to the size of current amplitude. It remains unclear whether channels crosslinked with $BM[PEO]_3$ actually conduct current or whether the recorded current comes from a population of channels that were not crosslinked, either due to protein turnover or two $BM[PEO]_3$ molecules binding to D1 and D2 individually without crosslinking. The 200-400 μM range of crosslinker appears to be saturating as $BM[PEO]_2$ gave similar results at both concentrations. Increasing the concentration further may promote more than one $BM[PEO]_3$ binding per subunit. An interesting finding is that channels crosslinked with $BM[PEO]_3$ were more efficaciously modulated by CX546. Thus, rather than occluding the effect of this positive allosteric modulator, fixing the cleft in a closed conformation enhanced modulation. This result may suggest that CX546 acts not on cleft stability, perhaps modulating gating itself. This finding also suggests that most of the channels in this system may actually be crosslinked and can pass current with unique properties in the presence of CX546.

FIGURE LEGENDS

Fig 3.1. Chemical modification of residues A476 and S701 forces a fixed intercleft domain closure distance. (a) Schematic representation of a dimer of the ligand-binding core (LBC) of GluR2o. Protomer B (blue) and Protomer A (red) are shown in ribbon representation. The apo state is represented on the left, and the glutamate-bound state is shown on the right. Upon ligand binding, Domain 2 moves towards Domain 1 of the same protomer, decreasing the intercleft distance and increasing the inter-dimer distance proximal to the pore. The extent of ligand-induced movement of Domain 2 is hypothesized to be directly related to the efficacy of gating. (b) Visualization of the LBC cleft residues that were mutated to cysteine, on the crystal structure of the apo GluR2o S1S2 LBC (1FTO.PDB). (c) Localization of residues that were mutated to cysteines in the "null" cysteine GluR2o construct (red balls). The cysteine pair studied here is $A_{476}C + S_{701}C$, the residues to which the maleimide groups of the $BM[POE]_3$ crosslinker are bound to.

Fig 3.2. The cysteine-"null", intercleft cysteine-pair mutant is functional. The expression of GluR2o DATD+($C_{87}V$)+($A_{476}C$)+($S_{701}C$) cRNA in Xenopus oocytes was tested using two-electrode voltage clamp electrophysiology. Current responses were evoked by a 30 s pulse of 300 μM L-glutamate. In addition, current responses were potentiated after pre-treatment and co-application with 100 μM cyclothiazide (CTZ), a positive allosteric modulator that impedes receptor desensitization of GluR2o. Thus, the "null" background mutant pair was completely functional.

Fig 3.3. Crosslinking the cleft between Domain 1 and Domain two impairs current amplitude in the predicted distance-dependent manner. (a) Mean current amplitude in response to 300 μM L-glutamate of GluR2o DATD+($C_{87}V$)+($A_{476}C$)+($S_{701}C$) without (Control) or

with crosslinking agents $BM[PEO]_2$ and $BM[PEO]_3$. Mean current amplitude diminishes with increased spacer arm distance. (b) Mean current amplitude in response to 300 μM L-glutamate with 500 μM CX546 without (+CX546) or with crosslinking agents $BM[PEO]_2$ and $BM[PEO]_3$. As seen in (a), the mean current amplitude diminishes with increased spacer arm distance. Note, however, that CX546 still potentiates receptors crosslinked by both agents, suggesting that the crosslinking does not impede modulation of deactivation and/or desensitization.

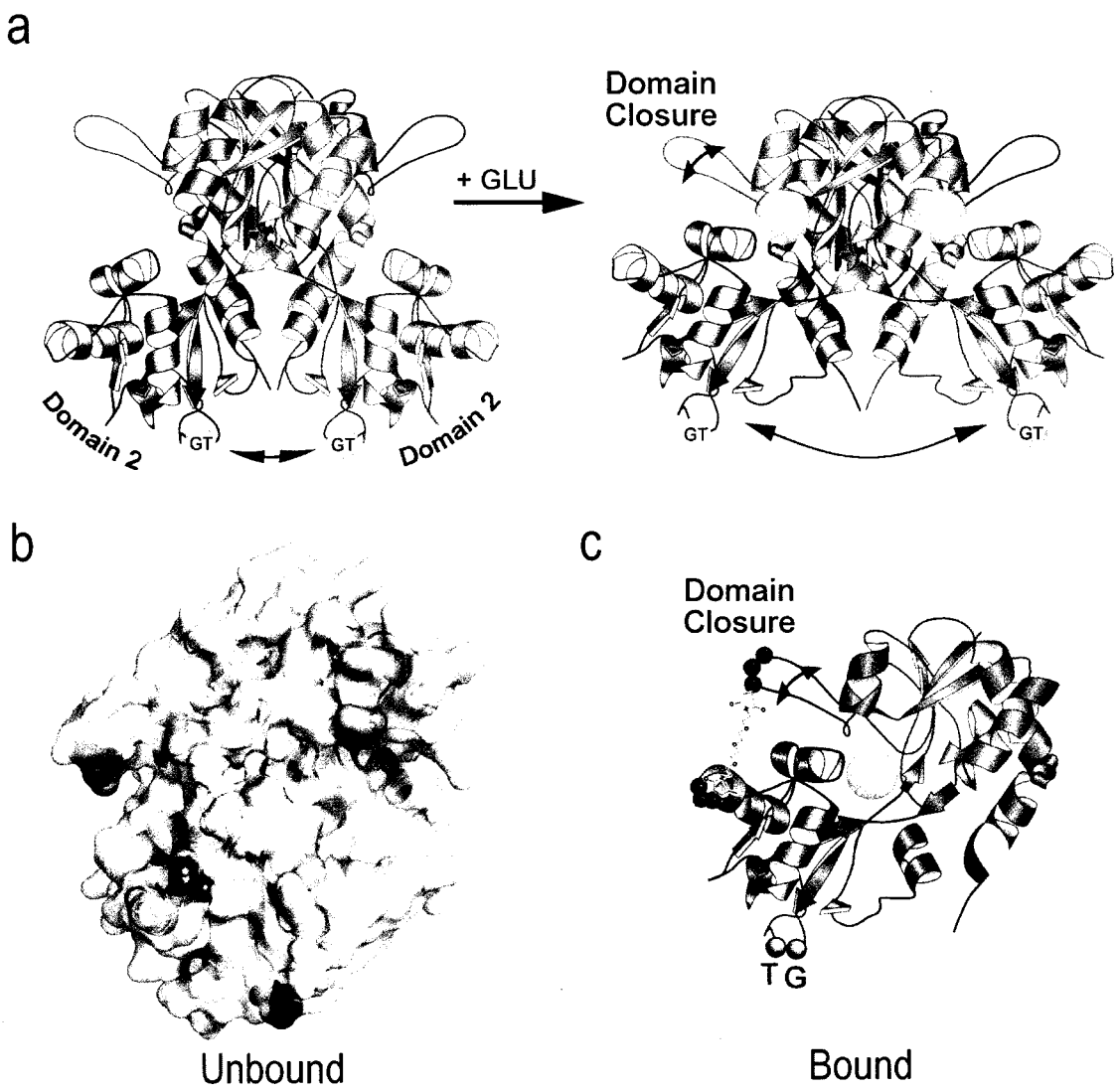

Figure 3.1

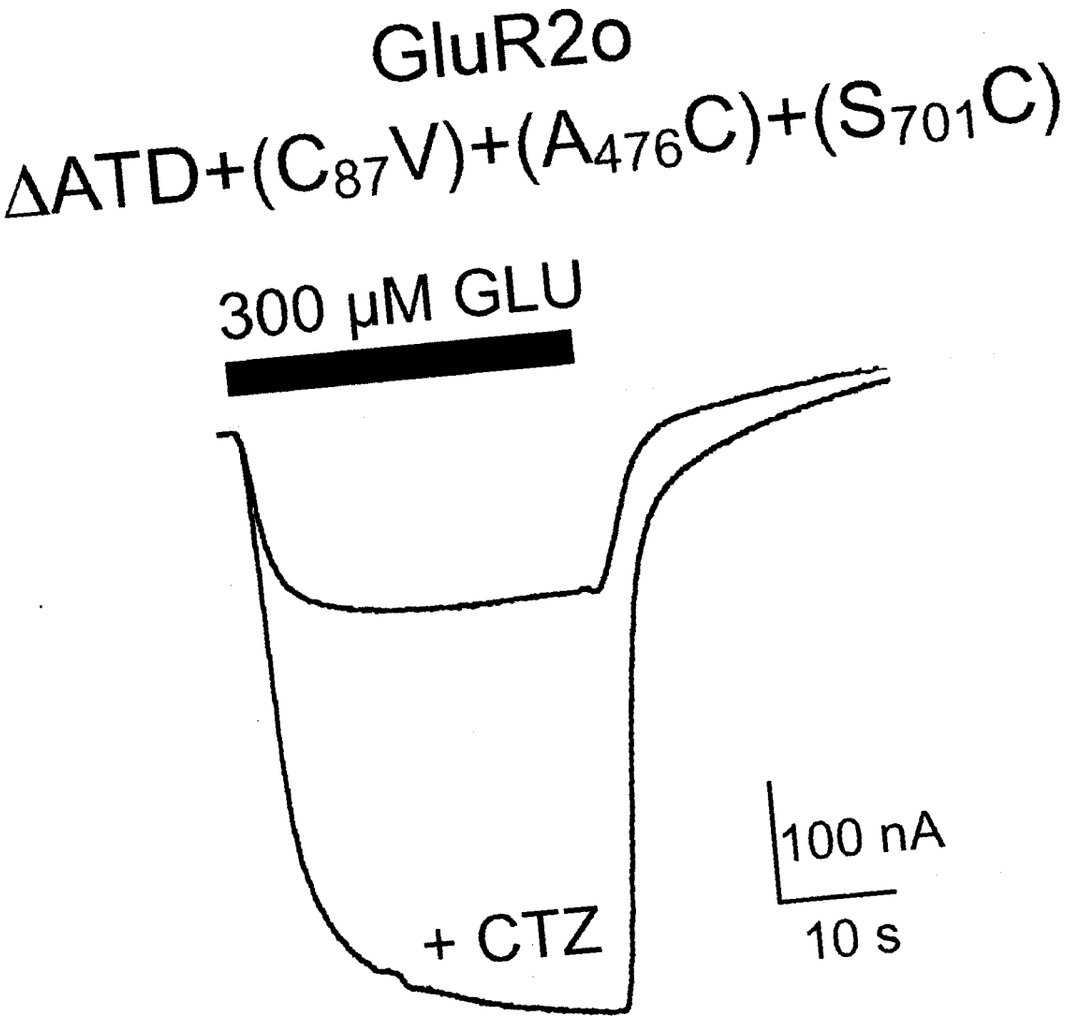

Figure 3.2

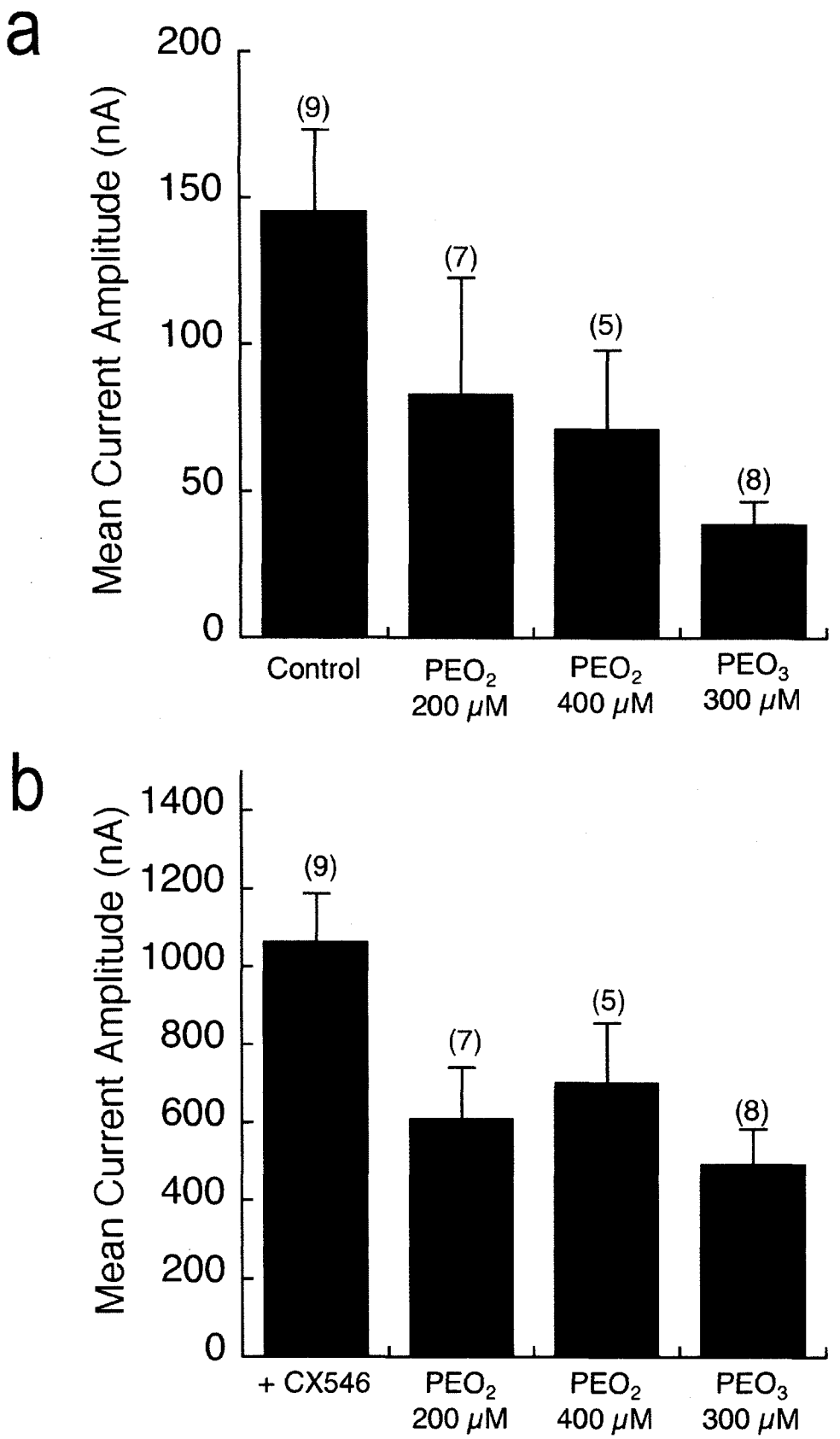

Figure 3.3

Chapter IV: Discussion and Future Directions

This work used Human Embryonic Kidney cells (HEK293) cells to study stargazin association with AMPA receptors. Although these cells are extremely easy to work with and transfect they lack many of the proteins potentially involved in AMPA receptor trafficking. These cells do, however, have an unexpected relationship to neurons and contain many different types of mRNA normally only expressed in neuronal cells (Shaw et al., 2002). Interestingly, HEK cells can make excitatory synapses in co-culture with rat cerebellar granule cells when only neuroligin and glutamate receptors are transfected. Neuroligins are brain-specific cell adhesion membrane proteins (Ichtchenko et al., 1996; Song et al., 1999) and localize postsynaptically at excitatory synapses.

To truly understand how LTP and synaptic plasticity are regulated in neurons one would need to use a system in which all endogenous proteins are present. However, there are still many unanswered questions that can be solved with heterologous expression in HEK cells. The following discussion will be my interpretation of the major results presented in my paper (chapter 2). I will also suggest future experiments to answer some remaining questions of interest.

Stargazin-mediated modulation of desensitization and deactivation

Although deactivation and desensitization of AMPA receptors determine the time course of synaptic transmission, the importance of stargazin's ability to modulate AMPA receptor kinetics remains unclear and could potentially be a byproduct of the more important ability of

stargazin to get AMPA receptors out of the ER. The work presented allows for the possibility that over-expression of stargazin used in previous studies as well as our own does not mimic physiological conditions. The ability of stargazin to increase surface expression of fluorescently tagged AMPA receptors was variable but showed a dose-dependent increase in frequency over a 16-fold range of stargazin concentration. The effects of stargazin-mediated modulation of desensitization and trafficking in neurons may be less drastic without this excess. At the very least, stargazin appears to modulate desensitization to a greater extent than deactivation as 4/4 GluR1i constructs tested slowed desensitization significantly without slowing deactivation. There was, however, a trend in increasing the modulation of desensitization and a significant difference in modulation of deactivation between cells showing enhanced surface expression and cells that didn't. This result could mean that cells with significantly enhanced surface expression have multiple stargazin molecules bound at the surface membrane and exert an additive effect on deactivation and desensitization.

The Mechanism of Stargazin-mediated AMPA receptor trafficking

It would appear that stargazin does not increase surface expression by preventing endocytosis (Vandenberghe et al., 2005a) or enhancing AMPA receptor recycling and exocytosis from endosomes. Agonist-induced AMPA receptor endocytosis has been shown to cause dissociation between the two proteins, with stargazin remaining at the surface membrane (Tomita et al., 2004). It is unclear how the stargazin protein gets removed from the surface membrane. Excess stargazin at the surface membrane would presumably cause a greater overall modulation of AMPA receptor kinetics by binding to newly exocytosed receptors. This may be one aspect of LTP and synapse maintenance independent of AMPA receptor trafficking. The results shown in chapter 2 are consistent with the hypothesis that the major role of stargazin is to get AMPA receptors out of the ER to both synaptic and extrasynaptic sites in neurons.

My results suggest that a major limiting factor for enhancing AMPA receptor ER export is the availability of stargazin. This is consistent with the γ-8 KO mouse study that showed a reduction in hippocampal LTP by 75% (Rouach et al., 2005). In HEK cells, stargazin gets readily transported out of the ER to the surface membrane and even if there is potential for an interaction with an AMPA receptor, the proteins may not find each other. Confocal imaging using a fluorescently tagged stargazin protein shows that stargazin is almost exclusively located at the surface membrane in HEK cells with almost no cytosolic expression. My results also suggest that stargazin may form multimers that are unable to interact with AMPA receptors. One intriguing possibility is that synaptic activity may increase stargazin expression and could be one mechanism of LTP.

Perhaps in neurons there is a protein or proteins not present in HEK cells that would help sequester stargazin in the ER. Fluorescently tagged stargazin expressed in neurons does not have the same surface expression pattern as in HEK cells (Chetkovich et al., 2002) and supports this hypothesis. Also, co-transfection of non-truncated fluorescent stargazin in COS-7 cells with PSD-95 produces a more punctate surface expression pattern not seen in my experiments. It is unknown if this is due to cell type differences or co-expression with PSD-95.

If stargazin were partially sequestered in the ER of neurons, this would increase the availability of stargazin and enhance interaction with AMPA receptors in the ER. This scenario may mimic the stargazin dose-response curve of AMPA receptor surface expression observed in my studies. Whereas a single stargazin molecule may help AMPA receptors exit from the ER, multiple stargazin proteins binding to receptors may enhance exit even more. I found that an over-expression of AMPA receptors relative to stargazin was able to hinder stargazin's ability to reach the surface membrane. This suggests that stargazin can be sequestered by AMPA receptors in the ER and that 1 stargazin molecule per tetramer does not effectively traffic the receptor. I

propose that multiple stargazin molecules can bind to AMPA receptor tetramers in the ER and enhance trafficking by blocking more ER retention sites.

It is unclear if stargazin binds only at the dimer interface of AMPA receptor tetramers or if there are four independent binding sites on each subunit. Although figure 2.7 suggests the existence of four independent binding sites, my experimental method does not rule out the possibility that stargazin can bind to a dimer interface in the ER comprised of one short and one long fluorescent subunit. One way to address this would be to try and retain stargazin in the cytosol by over-expressing heteromers of short and long subunits. It has previously been shown that AMPA receptor subunits preferentially form heteromers than homomers (Mansour et al., 2001; Brorson and Suzuki, 2004). An interesting experiment would be to from heteromers between short GluR1i and long GluR2o subunits and determine if an over-expression of these constructs is capable of reducing stargazin surface expression as was previously shown for long homomers but not short. A negative result would suggest that stargazin binds at the dimer interface of AMPA receptors, while a positive result would suggest that stargazin binds independently to each subunit.

The absence of functional AMPA receptors in the rat cerebellum of the stargazer mouse should be noted especially since heterologous expression of all AMPA receptor subunits in the absence of stargazin results in functional receptors. This suggests that there may be additional proteins in neurons not in HEK cells that prevent AMPA receptors from reaching the surface membrane.

The AMPA receptor domain(s) necessary for stargazin-mediated trafficking:

Exploration of the role of the AMPA receptor cytoplasmic tail

My original hypothesis was that stargazin enhanced surface expression of AMPA receptors by blocking an ER retention signal located within the first 14 amino acids of the

proximal cytoplasmic tail, presumably residues 8-14. These residues differ significantly from GluR6 which does not interact with stargazin (Chen et al., 2003).

While the first 10 amino acids of the proximal cytoplasmic tail of GluR2 have been deemed an ER retention site (Greger et al., 2002), the first 14 amino acids of each AMPA receptor subunit are highly conserved and there may exist a common ER retention signal among them. Even the kainate receptor GluR6 has 6/7 of the first amino acids of the cytoplasmic tail conserved with AMPA receptors. Presumably a deletion of this putative ER retention site (amino acids 1-10) would enhance AMPA receptor surface expression. Previous work, however, indicates that AMPA receptor interaction with protein 4.1N, which binds at least partially to residues 7-12 in GluR4, is required for robust surface expression in HEK cells. The mutation of 3 residues in GluR4 reduced surface expression by ~75% (Coleman et al., 2003). Interestingly, protein 4.1 was required for normal levels of surface expression for GluR1 and GluR4 in HEK cells but GluR2 was not and did not interact with protein 4.1.

Surprisingly, when a GluR1i mutant was constructed with a cytoplasmic tail swap of the first 7 amino acids of GluR6 this channel still had robust surface expression enhancement when co-transfected with stargazin. Presumably then stargazin does not interact with the AMPA receptor cytoplasmic tail and can take the place of protein 4.1. In addition, I found that stargazin could slightly enhance surface expression of GluR1 and GluR4 channels with only the GluPhe residues (the first two amino acids of the cytoplasmic tail). Although stargazin increased surface expression of the GluR4 channel, it could not recover the surface expression levels to GluR4 with a full-length tail with or without stargazin. It is unclear, however, why the deletion of all but the first two amino acids of the cytoplasmic tail virtually ablated all surface expression in our studies and one reported previously (Coleman et al., 2003).

That stargazin could not fully rescue GluR4 surface expression in HEK cells could indicate that the initial amino acids of the AMPA receptor tail are not an ER retention signal but play a greater role in ER exit. An alternative explanation is that only amino acids 1-2 of the

cytoplasmic tail, for example, represent an ER retention signal and the remaining proximal tail of AMPA receptors inhibits this signal.

Stargazin does not bind to specific residues on the AMPA receptor cytoplasmic tail but its action on trafficking requires access to an intracellular site

The finding that the cytoplasmic tail of AMPA receptors is not necessary for stargazin-mediated trafficking seemed inconsistent with the finding that YFP attachment to GluR1 and GluR2 channels directly after the conserved cytoplasmic tail inhibited stargazin-mediated AMPA receptor surface expression. In addition to the tail deletion, specific mutations were made to test if certain residues in the conserved GluR1 cytoplasmic tail different from GluR6 may be required for trafficking. All constructs tested were trafficked by stargazin. This led me to insert a 38 amino acid spacer sequence between residue 15 of the GluR1i cytoplasmic tail and the fluorophore. This transformed the previously un-trafficable construct into one that could be trafficked by stargazin.

My experiments suggest that the failure of channels to be trafficked by stargazin is due to an inability of the two to assemble in the ER (see Table 3 in chapter 2). Since the AMPA receptor cytoplasmic tail is not necessary for assembly with stargazin, two likely possibilities remain. The first is that a bulky fluorophore attached to the cytoplasmic tail of AMPA receptors blocks one or more specific intracellular interactions. The second is that the affinity of the two proteins is lowered but there is no specific intracellular site of interaction. Evidence against the latter comes from data that shows that the stargazin cytoplasmic tail is essential for stargazin-mediated trafficking and shows a graded response with tail length (Turetsky et al., 2005).

Future Directions

I provide evidence that an intracellular interaction with stargazin is essential for AMPA receptor ER exit. The residues necessary for this interaction, however, remain unknown, although the AMPA receptor cytoplasmic tail is not required. Results from my paper suggest that the

affinity between these two proteins can be reduced by a fluorophore insertion close to TM3. The ability of stargazin to bind to $R1_{15}$YFP at the plasma membrane but not significantly in the ER suggests the existence of at least two independent binding sites.

To determine if there is an extracellular or transmembrane interaction site, which is presumed, GluR1/GluR6 chimeras can be made. My adivisor Dr. Partin has already created multiple functional chimeras. Since GluR6 does not associate with stargazin, the site of interaction could be narrowed down using this method.

Despite the potential for multiple independent binding sites, an intracellular interaction between AMPA receptors and stargazin seems to be necessary and sufficient for AMPA receptor trafficking (Tomita et al., 2005b). It has been suggested that the stargazin cytoplasmic tail acts by blocking AMPA receptor ER retention signals but stargazin could also act by taking the place of other chaperones such as BiP, which may cover up ER exit signals or anchor the receptor in the ER. In addition or instead of blocking ER retention signals, stargazin may potentially provide an ER exit signal to the AMPA receptor complex and/or help in stabilizing AMPA receptor folding.

Consistent with stargazin blocking one or multiple AMPA receptor ER retention signals, I found that ER retained wild type GluR2 homomers can be trafficked by stargazin to the surface membrane similar to the pore mutant R607Q. The inability of wild type GluR2 to reach the surface membrane is due to the R607 residue being an ER retention signal (Greger et al., 2002). This is evidence that stargazin may block this specific ER retention signal and may do so by associating near the intracellular side of the pore.

My studies show that AMPA receptor surface expression in HEK cells can be increased by a stargazin protein with no more than 70 amino acids of its cytoplasmic tail. Many of these residues are positively charged. The intracellular region of AMPA receptors after TM1 and before the pore loop is highly negatively charged and differs from GluR6. There is a high negative charge density over 5 amino acids for GluR1, 2 and 4 (--N--) and over 6 amino acids for GluR3 (-

-NN--), N = neutral residue. Interestingly GluR3 was shown to be less effectively trafficked compared to the other AMPA receptor subunits (Turetsky et al., 2005).

Although this region seemed the most promising, the interaction between AMPA receptors and stargazin may be hydrophobic and not electrostatic in nature. I made two constructs in GluR1i; one of these neutralizes the two charges to the left of the neutral residue and the other neutralizes the two charges to the right of the neutral residue. I found that both constructs can be trafficked by stargazin and thus the charges here are not necessary. Preliminary patch clamp recordings from these two constructs yield ~10x increase in current amplitude with stargazin compared to without, which is greater than the ~6x increase in current amplitude from wt channels. Confocal microscopy also suggests that trafficking is better in these constructs but a more careful analysis and repeat of these experiments is still required to be sure.

Other potential factors for stargazin-mediated AMPA receptor trafficking that may not include ER retention sites have been suggested. The C-terminus of stargazin shows a strong interaction with microtubule-associated protein light chain 2 (LC2) and may be involved in trafficking AMPA receptors to the surface membrane (Ives et al., 2004). This interaction may also play a role in altering the cytosolic distribution in neurons and also HEK cells with other related microtubule proteins. Stargazin may also enhance AMPA receptor binding to glutamate in the ER. It has previously been shown that trafficking of glutamate receptors from the ER involves ligand binding as a control mechanism (Mah et al., 2005). Other non-functional glutamate receptor mutants have been shown previously to be retained in the ER (Fleck et al., 2003). An interesting experiment would be to determine if stargazin could traffic AMPA receptors that cannot bind to glutamate.

A positive result would leave open the possibility that stargazin may traffic AMPA receptors not by blocking any specific ER retention signal but instead by pulling AMPA receptors to the surface membrane by virtue of association. Stargazin does not have to block an AMPA

receptor ER exit site but instead could provide an ER exit site to the complex that would aid in transport to the cis-Golgi.

An important experiment is to determine if the cytoplasmic tail of stargazin is enough to traffic AMPA receptors to the surface membrane. The creation of this cytosolic protein would enable us to rule out that other stargazin domains aren't necessary to help in AMPA receptor folding and that stargazin does not traffic receptors by pulling them to the membrane.

To help rule out that the stargazin cytoplasmic tail does not act by providing an ER exit site to an AMPA receptor complex, a fluorescent stargazin protein without the cytoplasmic tail could be made. Stargazin with a tail length of ~70 amino acids made surface expression rings in ~82% of HEK cells. If the more severely truncated protein had reduced surface expression, this is evidence that the tail may contain an ER exit site. If there remains equal stargazin surface expression, this would more strongly suggest that the stargazin tail blocks an AMPA receptor ER retention site.

If stargazin acts solely by blocking an ER retention site or sites, presumably these sites could be mutated and receptor current amplitudes and surface expression would be increased even in the absence of stargazin. The ability of stargazin to mediate AMPA receptor trafficking in a graded manner depending on the size of its cytoplasmic tail (with more trafficking the channel the most) (70), suggests that stargazin may act by blocking multiple ER retention signals. Perhaps mutating residues in the AMPA receptor is not the best strategy since stargazin may not associate with the specific residues involved in ER retention. Stargazin may also associate at multiple sites.

A remaining question in AMPA receptor trafficking that is independent of stargazin is why do channels lacking cytoplasmic tails have virtually no surface expression? Channels with a 7 amino acid tail readily reach the surface membrane while channels with only a two amino acid tail do not. Many proximal cytoplasmic tail residues have been mutated in my studies and do not hinder trafficking. My hypothesis is that the first several amino acids represent part of an ER retention sequence that may include part of TM3. Mutating several residues in the proximal

AMPA receptor cytoplasmic tail (residues 4-6) resulted in ~2% of fluorescent cells showing surface expression rings without stargazin, which was well below the number of cells that would form rings with stargazin-mediated trafficking. Although there is significant homology between AMPA receptors and GluR6 in the initial 7 residues of the cytoplasmic tail, this region may be a site that stargazin blocks but does not specifically bind to. To address this question, the initial EF residues of the cytoplasmic tail will need to be mutated. If surface expression were enhanced in the absence of stargazin this would indicate that this region is an ER retention signal. Co-transfection of stargazin can be used to determine if stargazin exerts its effects by blocking this site or is additive.

REFERENCES

Arai AC, Suzuki E (2005) THE C-TERMINUS OF THE AMPA RECEPTOR PLAYS DIFFERENT ROLES IN MEDIATING STARGAZIN'S EFFECTS ON RECEPTOR KINETICS VERSUS RECEPTOR TRAFFICKING. Abstract Viewer/Itinerary Planner Washington, DC: Society for Neuroscience, 2005 Online Program No. 949.8.

Armstrong N, Gouaux E (2000) Mechanisms for activation and antagonism of an AMPA-sensitive glutamate receptor: crystal structures of the GluR2 ligand binding core. Neuron 28:165-181.

Armstrong N, Sun Y, Chen GQ, Gouaux E (1998) Structure of a glutamate-receptor ligand-binding core in complex with kainate. Nature 395:913-917.

Ayalon G, Stern-Bach Y (2001) Functional assembly of AMPA and kainate receptors is mediated by several discrete protein-protein interactions. Neuron 31:103-113.

Barry MF, Ziff EB (2002) Receptor trafficking and the plasticity of excitatory synapses. Current Opinions in Neurobiology 12:279-286.

Black JL, 3rd (2003) The voltage-gated calcium channel gamma subunits: a review of the literature. J Bioenerg Biomembr 35:649-660.

Bredt DS, Nicoll RA (2003) AMPA receptor trafficking at excitatory synapses. Neuron 40:361-379.

Brorson JR, Suzuki T (2004) Selective expression of heteromeric AMPA receptors driven by flip-flop differences. Journal of Neuroscience 24:3461-3470.

Chang EH, Savage MJ, Flood DG, Thomas JM, Levy RB, Mahadomrongkul V, Shirao T, Aoki C, Huerta PT (2006) AMPA receptor downscaling at the onset of Alzheimer's disease pathology in double knockin mice. Proc Natl Acad Sci U S A 103:3410-3415.

Chen L, El-Husseini A, Tomita S, Bredt DS, Nicoll RA (2003) Stargazin differentially controls the trafficking of alpha-amino-3-hydroxyl-5-methyl-4-isoxazolepropionate and kainate receptors. Mol Pharmacol 64:703-706.

Chen L, Chetkovich DM, Petralia RS, Sweeney NT, Kawasaki Y, Wenthold RJ, Bredt DS, Nicoll RA (2000) Stargazin regulates synaptic targeting of AMPA receptors by two distinct mechanisms. Nature 408:936-943.

Chetkovich DM, Chen L, Stocker TJ, Nicoll RA, Bredt DS (2002) Phosphorylation of the postsynaptic density-95 (PSD-95)/discs large/zona occludens-1 binding site of stargazin regulates binding to PSD-95 and synaptic targeting of AMPA receptors. J Neurosci 22:5791-5796.

Coleman SK, Cai C, Mottershead DG, Haapalahti JP, Keinanen K (2003) Surface expression of GluR-D AMPA receptor is dependent on an interaction between its C-terminal domain and a 4.1 protein. J Neurosci 23:798-806.

Corboy MJ, Thomas PJ, Wigley WC (2005) Aggresome formation. Methods in Molecular Biology 301:305-327.

Damke H, Baba T, Warnock DE, Schmid SL (1994) Induction of mutant dynamin specifically blocks endocytic coated vesicle formation. J Cell Biol 127:915-934.

Daw MI, Chittajallu R, Bortolotto ZA, Dev KK, Duprat F, Henley JM, Collingridge GL, Isaac JT (2000) PDZ proteins interacting with C-terminal GluR2/3 are involved in a PKC-dependent regulation of AMPA receptors at hippocampal synapses. Neuron 28:873-886.

Dingledine R, Borges K, Bowie D, Traynelis SF (1999) The glutamate receptor ion channels. Pharmacology Reviews 51:7-61.

Doyle DA, Morais Cabral J, Pfuetzner RA, Kuo A, Gulbis JM, Cohen SL, Chait BT, MacKinnon R (1998) The structure of the potassium channel: molecular basis of K+ conduction and selectivity. Science 280:69-77.

Ehlers MD (2000) Reinsertion or degradation of AMPA receptors determined by activity-dependent endocytic sorting. Neuron 28:511-525.

Esteban JA (2003) AMPA receptor trafficking: a road map for synaptic plasticity. Mol Interv 3:375-385.

Fleck MW, Cornell E, Mah SJ (2003) Amino-acid residues involved in glutamate receptor 6 kainate receptor gating and desensitization. J Neurosci 23:1219-1227.

Fukata Y, Tzingounis AV, Trinidad JC, Fukata M, Burlingame AL, Nicoll RA, Bredt DS (2005) Molecular constituents of neuronal AMPA receptors. J Cell Biol 169:399-404.

Garcia EP, Mehta S, Blair LA, Wells DG, Shang J, Fukushima T, Fallon JR, Garner CC, Marshall J (1998) SAP90 binds and clusters kainate receptors causing incomplete desensitization. Neuron 21:727-739.

Gerges NZ, Backos DS, Esteban JA (2004) Local control of AMPA receptor trafficking at the postsynaptic terminal by a small GTPase of the Rab family. J Biol Chem 279:43870-43878.

Gouaux E (2003) Structure and function of AMPA receptors. Journal of Physiology (London) 554.2:249-253.

Greger IH, Khatri L, Ziff EB (2002) RNA editing at arg607 controls AMPA receptor exit from the endoplasmic reticulum. Neuron 34:759-772.

Greger IH, Khatri L, Kong X, Ziff EB (2003) AMPA receptor tetramerization is mediated by Q/R editing. Neuron 40:763-774.

Hall RA, Hansen A, Andersen PH, Soderling TR (1997) Surface expression of the AMPA receptor subunits GluR1, GluR2, and GluR4 in stably transfected baby hamster kidney cells. Journal of Neurochemistry 89:625-630.

Hanley JG, Khatri L, Hanson PI, Ziff EB (2002) NSF ATPase and alpha-/beta-SNAPs disassemble the AMPA receptor-PICK1 complex. Neuron 34:53-67.

Hayashi T, Rumbaugh G, Huganir RL (2005) Differential regulation of AMPA receptor subunit trafficking by palmitoylation of two distinct sites. Neuron 47:709-723.

Hayashi Y, Shi SH, Esteban JA, Piccini A, Poncer JC, Malinow R (2000) Driving AMPA receptors into synapses by LTP and CaMKII: requirement for GluR1 and PDZ domain interaction. Science 287:2262-2267.

Higuchi M, Single FN, Köhler M, Sommer B, Sprengel R, Seeburg PH (1993) RNA editing of AMPA receptor subunit GluR-B: a base-paired intron-exon structure determines position and efficiency. Cell 75:1361-1370.

Hume RI, Dingledine R, Heinemann SF (1991) Identification of a site in glutamate receptor subunits that controls calcium permeability. Science 253:1028-1031.

Ichtchenko K, Nguyen T, Sudhof TC (1996) Structures, alternative splicing, and neurexin binding of multiple neuroligins. J Biol Chem 271:2676-2682.

Ives JH, Fung S, Tiwari P, Payne HL, Thompson CL (2004) Microtubule-associated protein light chain 2 is a stargazin-AMPA receptor complex-interacting protein in vivo. J Biol Chem 279:31002-31009.

Jin R, Banke TG, Mayer ML, Traynelis SF, Gouaux E (2003) Structural basis for partial agonist action at ionotropic glutamate receptors. Nature Neuroscience 6:803-810.

Jin R, Clark S, Weeks AM, Judman JT, Gouaux E, Partin KM (2005) Mechanism of positive allosteric modulators acting on AMPA receptors. J Neurosci 25:9027-9036.

Jones MV, Westbrook GL (1996) The impact of receptor desensitization on fast synaptic transmission. Trends in Neurosciences 19:96-101.

Kandel ER (2001) The molecular biology of memory storage: a dialog between genes and synapses. Biosci Rep 21:565-611.

Kang M-G, Chen C-C, Wakamri M, Hara Y, Mori Y, Campbell KP (2006) A functional AMPA-receptor calcium channel complex in the postsynaptic membrane. Proc Natl Acad Sci U S A 103:5661-5666.

Kask K, Zamanillo D, Rozov A, Burnashev N, Sprengel R, Seeburg PH (1998) The AMPA receptor subunit GluR-B in its Q/R site-unedited form is not essential for brain development and function. Proc Natl Acad Sci U S A 95:13777-13782.

Kennedy MB (2000) Signal-processing machines at the postsynaptic density. Science 290:750-754.

Kim E, Sheng M (2004) PDZ domain proteins of synapses. Nature Reviews Neuroscience 5:771-781.

Klumperman J (2000) Transport between ER and Golgi. Curr Opin Cell Biol 12:445-449.

Koike M, Tsukada S, Tsuzuki K, Kijima H, Ozawa S (2000) Regulation of kinetic properties of GluR2 AMPA receptor channels by alternative splicing. J Neurosci 20:2166-2174.

Konradi C, Heckers S (2003) Molecular aspects of glutamate dysregulation: implications for schizophrenia and its treatment. Pharmacol Ther 97:153-179.

Lee SH, Liu L, Wang YT, Sheng M (2002) Clathrin adaptor AP2 and NSF interact with overlapping sites of GluR2 and play distinct roles in AMPA receptor trafficking and hippocampal LTD. Neuron 36:661-674.

Leever DL, Clark SZ, Weeks AM, Partin KM (2003) Identification of a site in GluR1 and GluR2 important for modulation of deactivation and desensitization. Molecular Pharmacology 64:5-10.

Letts VA (2005) Stargazer- A mouse to seize! Epilepsy Currents 5:161-165.

Letts VA, Felix R, Biddlecome GH, Arikkath J, Mahaffey CL, Valenzuela A, Bartlett FS, Mori Y, Campbell KP, Frankel WN (1998) The mouse stargazer gene encodes a neuronal Ca2+-channel gamma subunit. Nature Genetics 19:340-347.

Leuranguer V, Papadopoulos S, Beam KG (2006) Organization of calcium channel beta1a subunits in triad junctions in skeletal muscle. J Biol Chem 281:3521-3527.

Lin Y, Skeberdis VA, Francesconi A, Bennett MV, Zukin RS (2004) Postsynaptic density protein-95 regulates NMDA channel gating and surface expression. J Neurosci 24:10138-10148.

Liu SJ, Cull-Candy SG (2005) Subunit interaction with PICK and GRIP controls Ca2+ permeability of AMPARs at cerebellar synapses. Nat Neurosci 8:768-775.

Lynch G (2004) AMPA receptor modulators as cognitive enhancers. Curr Opin Pharmacol 4:4-11.

Ma Y, Hendershot LM (2001) The unfolding tale of the unfolded protein response. Cell 107:827-830.

Mah SJ, Cornell E, Mitchell NA, Fleck MW (2005) Glutamate receptor trafficking: endoplasmic reticulum quality control involves ligand binding and receptor function. J Neurosci 25:2215-2225.

Malenka RC (2003) Synaptic plasticity and AMPA receptor trafficking. Ann NY Acad Sci 1003:1-11.

Malinow R (2003) AMPA receptor trafficking and long-term potentiation. Philos Trans R Soc Lond B Biol Sci 358:707-714.

Malinow R, Malenka RC (2002) AMPA receptor trafficking and synaptic plasticity. Annu Rev Neurosci 25:103-126.

Malinow R, Mainen ZF, Hayashi Y (2000) LTP mechanisms: from silence to four-lane traffic. Curr Opin Neurobiol 10:352-357.

Mansour M, Nagarajan N, R.B. N, Clements J, Rosenmund C (2001) Heteromeric AMPA receptors assemble with a preferred subunit stoichiometry and spatial arrangement. Neuron 32:841-853.

Matsuda S, Kamiya Y, Yuzaki M (2005) Roles of the N-terminal domain on the function and quaternary structure of the ionotropic glutamate receptor. J Biol Chem 280:20021-20029.

Mayer ML (2005) Glutamate receptor ion channels. Current Opinions in Neurobiology 15:282-288.

Meng Y, Zhang Y, Jia Z (2003) Synaptic transmission and plasticity in the absence of AMPA glutamate receptor GluR2 and GluR3. Neuron 39:163-176.

Mosbacher J, Schoepfer R, Monyer H, Burnashev N, Seeburg P, Ruppersberg JP (1994) A molecular determinant for submillisecond desensitization in glutamate receptors. Science 266:1059-1062.

Nagarajan N, Quast C, Boxall AR, Shahid M, Rosenmund C (2001) Mechanism and impact of allosteric AMPA receptor modulation by the Ampakine® CX546. Neuropharmacology 31:650-663.

Nakagawa T, Cheng Y, Sheng M, Walz T (2006) Three-dimensional structure of an AMPA receptor without associated stargazin/TARP proteins. Biol Chem 387:179-187.

Nakagawa T, Cheng Y, Ramm E, Sheng M, Walz T (2005) Structure and different conformational states of native AMPA receptor complexes. Nature 433:545-549.

Narisawa-Saito M, Carnahan J, Araki K, Yamaguchi T, Nawa H (1999) Brain-derived neurotrophic factor regulates the expression of AMPA receptor proteins in neocortical neurons. Neuroscience 88:1009-1014.

Narisawa-Saito M, Iwakura Y, Kawamura M, Araki K, Kozaki S, Takei N, Nawa H (2002) Brain-derived neurotrophic factor regulates surface expression of alpha-amino-3-hydroxy-5-methyl-4-isoxazoleproprionic acid receptors by enhancing the N-ethylmaleimide-sensitive factor/GluR2 interaction in developing neocortical neurons. J Biol Chem 277:40901-40910.

Nicoll RA (2003) Expression mechanisms underlying long-term potentitation: a postsynaptic view. Philos Trans R Soc LondB Biol Sci 358:721-726.

Nicoll RA, Tomita S, Bredt DS (2006) Auxiliary subunits assist AMPA-type glutamate receptors. Science 311:1253-1256.

Nishimune A, Isaac JT, Molnar E, Noel J, Nash SR, Tagaya M, Collingridge GL, Nakanishi S, Henley JM (1998) NSF binding to GluR2 regulates synaptic transmission. Neuron 21:87-97.

O'Brien R, Xu D, Mi R, Tang X, Hopf C, Worley P (2002) Synaptically targeted narp plays an essential role in the aggregation of AMPA receptors at excitatory synapses in cultured spinal neurons. J Neurosci 22:4487-4498.

O'Brien RJ, Xu D, Petralia RS, Steward O, Huganir RL, Worley P (1999) Synaptic clustering of AMPA receptors by the extracellular immediate-early gene product Narp. Neuron 23:309-323.

O'Connell KM, Tamkun MM (2005) Targeting of voltage-gated potassium channel isoforms to distinct cell surface microdomains. Journal of Cell Science 118:2155-2166.

Osten P, Khatri L, Perez JL, Kohr G, Giese G, Daly C, Schulz TW, Wensky A, Lee LM, Ziff EB (2000) Mutagenesis reveals a role for ABP/GRIP binding to GluR2 in synaptic surface accumulation of the AMPA receptor. Neuron 27:313-325.

Osten P, Srivastava S, Inman GJ, Vilim FS, Khatri L, Lee LM, States BA, Einheber S, Milner TA, Hanson PI, Ziff EB (1998) The AMPA receptor GluR2 C terminus can mediate a reversible, ATP-dependent interaction with NSF and alpha- and beta-SNAPs. Neuron 21:99-110.

Palmer CL, Cotton L, Henley JM (2005) The molecular pharmacology and cell biology of alpha-amino-3-hydroxy-5-methyl-4-isoxazolepropionic acid receptors. Pharmacol Rev 57:253-277.

Partin KM, Fleck MF, Mayer ML (1996) AMPA receptor flip/flop mutants affecting deactivation, desensitization and modulation by cyclothiazide, aniracetam and thiocyanate. Journal of Neuroscience 16:6634-6647.

Passafaro M, Piech V, Sheng M (2001) Subunit-specific temporal and spatial patterns of AMPA receptor exocytosis in hippocampal neurons. Nat Neurosci 4:917-926.

Pasternack A, Coleman SK, Jouppila AK, Mottershead DG, Lindfors M, Pasternack M, Keinanen K (2002) a-amino-3-hydroxy-5-methyl-4-isoxazolepropionic acid (AMPA) receptor channels lacking the N-terminal domain. Journal of Biological Chemistry 277:49662-49667.

Piccini A, Malinow R (2002) Critical postsynaptic density 95/disc large/zonula occludens-1 interactions by glutamate receptor 1 (GluR1) and GluR2 required at different subcellular sites. J Neurosci 22:5387-5392.

Poo MM (2001) Neurotrophins as synaptic modulators. Nat Rev Neurosci 2:24-32.

Price MG, Davis CF, Deng F, Burgess DL (2005) The AMPA receptor trafficking regulator "stargazin" is related to the claudin family of proteins in its ability to mediate cell-cell adhesion. Journal of Biological Chemistry 280:19711-19720.

Priel A, Kolleker A, Ayalon G, Gillor M, Osten P, Stern-Bach Y (2005) Stargazin reduces desensitization and slows deactivation of the AMPA-type glutamate receptors. J Neurosci 25:2682-2686.

Ramanoudjame G, Du M, Mankiewicz KA, Jayaraman V (2006) Allosteric mechanism in AMPA receptors: A FRET-based investigation of conformational changes. Proc Natl Acad Sci U S A.

Raol YH, Lynch DR, Brooks-Kayal AR (2001) Role of excitatory amino acids in developmental epilepsies. Ment Retard Dev Disabil Res Rev 7:254-260.

Rosenmund C, Stern-Bach Y, Stevens CF (1998) The tetrameric structure of a glutamate receptor channel. Science 280:1596-1599.

Rouach N, Byrd K, Petralia RS, Elias GM, Adesnik H, Tomita S, Karimzadegan S, Kealey C, Bredt DS, Nicoll RA (2005) TARP gamma-8 controls hippocampal AMPA receptor number, distribution and synaptic plasticity. Nat Neurosci 8:1525-1533.

Rouch N, Byrd K, Petralia RS, Elias GM, Adesnik H, Tomita S, Karimzadegan S, Kealey C, Bredt DS, Nicoll RA (2005) TARP g-8 controls hippocampal AMPA receptor number, distribution and synaptic plasticity. Nature Neuroscience 8:1525-1533.

Sanes JR, Lichtman JW (1999) Can molecules explain long-term potentiation? Nat Neurosci 2:597-604.

Sans N, Racca C, Petralia RS, Wang YX, McCallum J, Wenthold RJ (2001) Synapse-associated protein 97 selectively associates with a subset of AMPA receptors early in their biosynthetic pathway. J Neurosci 21:7506-7516.

Shaw G, Morse S, Ararat M, Graham FL (2002) Preferential transformation of human neuronal cells by human adenoviruses and the origin of HEK 293 cells. Faseb J 16:869-871.

Shen L, Liang F, Walensky LD, Huganir RL (2000) Regulation of AMPA receptor GluR1 subunit surface expression by a 4. 1N-linked actin cytoskeletal association. J Neurosci 20:7932-7940.

Shi S, Hayashi Y, Esteban JA, Malinow R (2001) Subunit-specific rules governing AMPA receptor trafficking to synapses in hippocampal pyramidal neurons. Cell 105:331-343.

Sitia R, Braakman I (2003) Quality control in the endoplasmic reticulum protein factory. Nature 426:891-894.

Sommer B, Köhler M, Sprengel R, Seeburg PH (1991) RNA editing in brain controls a determinant of ion flow in glutamate-gated channels. Cell 67:11-19.

Sommer B, Keinänen K, Verdoorn TA, Wisden W, Burnashev N, Herb A, Köhler M, Takagi T, Sakmann B, Seeburg PH (1990) Flip and flop: a cell-specific functional switch in glutamate-operated channels of the CNS. Science 249:1580-1585.

Song I, Kamboj S, Xia J, Dong H, Liao D, Huganir RL (1998) Interaction of the N-ethylmaleimide-sensitive factor with AMPA receptors. Neuron 21:393-400.

Song JY, Ichtchenko K, Sudhof TC, Brose N (1999) Neuroligin 1 is a postsynaptic cell-adhesion molecule of excitatory synapses. Proc Natl Acad Sci U S A 96:1100-1105.

Stern-Bach Y, Bettler B, Hartley M, Sheppard PO, O'Hara PJ, Heinemann SF (1994) Agonist-selectivity of glutamate receptors is specified by two domains structurally related to bacterial amino acid binding proteins. Neuron 13:1345-1357.

Sugiyama Y, Kawabata I, Sobue K, Okabe S (2005) Determination of absolute protein numbers in single synapses by a GFP-based calibration technique. Nature Methods 2:677-684.

Sun Y, Olson R, Horning M, Armstrong N, Mayer ML, Gouaux E (2002a) Mechanism of glutamate receptor desensitization. Nature 417:245-253.

Sun Y, Olson R, Horning M, Armstrong N, Mayer M, Gouaux E (2002b) Mechanism of glutamate receptor desensitization. Nature 417:245-253.

Suzuki E, Kessler M, Arai AC (2005) C-terminal truncation affects kinetic properties of GluR1 receptors. Mol Cell Neurosci 29:1-10.

Tikhonov DB, Mellor JR, Usherwood PN, Magazanik LG (2002) Modeling of the pore domain of the GLUR1 channel: homology with K+ channel and binding of channel blockers. Biophys J 82:1884-1893.

Tomita S, Fukata M, Nicoll RA, Bredt DS (2004) Dynamic interaction of stargazin-like TARPs with cycling AMPA receptors at synapses. Science 303:1508-1511.

Tomita S, Stein V, Stocker TJ, Nicoll RA, Bredt DS (2005a) Bidirectional synaptic plasticity regulated by phosphorylation of stargazin-like TARPs. Neuron 45:269-277.

Tomita S, Chen L, Kawasaki Y, Petralia RS, Wenthold RJ, Nicoll RA, Bredt DS (2003) Functional studies and distribution define a family of transmembrane AMPA receptor regulatory proteins. J Cell Biol 161:805-816.

Tomita S, Adesnik H, Sekiguchi M, Zhang W, Wada K, Howe JR, Nicoll RA, Bredt DS (2005b) Stargazin modulates AMPA receptor gating and trafficking by distinct domains. Nature 435:1052-1058.

Turetsky D, Garringer E, Patneau DK (2005) Stargazin modulates native AMPA receptor functional properties by two distinct mechanisms. J Neurosci 25:7438-7448.

Vandenberghe W, Nicoll RA, Bredt DS (2005a) Interaction with the unfolded protein response reveals a role for stargazin in biosynthetic AMPA receptor transport. J Neurosci 25:1095-1102.

Vandenberghe W, Nicoll RA, Bredt DS (2005b) Stargazin is an AMPA receptor auxiliary subunit. Proc Natl Acad Sci U S A 102:485-490.

Walsh DM, Klyubin I, Fadeeva JV, Cullen WK, Anwyl R, Wolfe MS, Rowan MJ, Selkoe DJ (2002) Naturally secreted oligomers of amyloid beta protein potently inhibit hippocampal long-term potentiation in vivo. Nature 416:535-539.

Wenthold RJ, Petralia RS, Blahos J, Niedzielski AS (1996) Evidence for multiple AMPA receptor complexes in hippocampal CA1/CA3 neurons. Journal of Neuroscience 16:1982-1989.

Xu D, Hopf C, Reddy R, Cho RW, Guo L, Lanahan A, Petralia RS, Wenthold RJ, O'Brien RJ, Worley P (2003) Narp and NP1 form heterocomplexes that function in developmental and activity-dependent synaptic plasticity. Neuron 39:513-528.

Yachi PP, Ampudia J, Gascoigne NR, Zal T (2005) Nonstimulatory peptides contribute to antigen-induced CD8-T cell receptor interaction at the immunological synapse. Nat Immunol 6:785-792.

Yamazaki M, Ohno-Shosaku T, Fukaya M, Kano M, Watanabe M, Sakimura K (2004) A novel action of stargazin as an enhancer of AMPA receptor activity. Neuroscience Research 50:369-374.

Zamanillo D, Sprengel R, Hvalby O, Jensen V, Burnashev N, Rozov A, Kaiser KM, Koster HJ, Borchardt T, Worley P, Lubke J, Frotscher M, Kelly PH, Sommer B, Andersen P, Seeburg PH, Sakmann B (1999) Importance of AMPA receptors for hippocampal synaptic plasticity but not for spatial learning. Science 284:1805-1811.

Zhang K, Kaufman RJ (2004) Signaling the unfolded protein response from the endoplasmic reticulum. J Biol Chem 279:25935-25938.

Zhang Y, Mori M, Burgess DL, Noebels JL (2002) Mutations in high-voltage-activated calcium channel genes stimulate low-voltage-activated currents in mouse thalamic relay neurons. J Neurosci 22:6362-6371.

Zheng F, Erreger K, Low CM, Banke T, Lee CJ, Conn PJ, Traynelis SF (2001) Allosteric interaction between the amino terminal domain and the ligand binding domain of NR2A. Nature Neuroscience 4:894-901.

Zhu JJ, Esteban JA, Hayashi Y, Malinow R (2000) Postnatal synaptic potentiation: delivery of GluR4-containing AMPA receptors by spontaneous activity. Nat Neurosci 3:1098-1106.